University of Alberta

Library Release Form

Name of Author: Khosrow Naderi

Title of Thesis: Core and Pore Scale Investigations on Immiscible Displacement and Enhanced Oil/Heavy-Oil Recovery under Ultrasonic Waves

Degree: Master of Science

Year this Degree Granted: 2008

_____

Signature


بسم الله الرحمن الرحيم

University of Alberta

Core and Pore Scale Investigations on Immiscible Displacement and Enhanced Oil/Heavy-Oil Recovery under Ultrasonic Waves

by

Khosrow Naderi

A thesis submitted to the Faculty of Graduate Studies and Research
in partial fulfillment of the requirements for the degree of

Master of Science

in

Petroleum Engineering

Department of Civil and Environmental Engineering

Edmonton, Alberta
Fall 2008

University of Alberta

Faculty of Graduate Studies and Research

The undersigned certify that they have read, and recommend to the Faculty of Graduate Studies and Research for acceptance, a thesis entitled **Core and Pore Scale Investigations on Immiscible Displacement and Enhanced Oil/Heavy-Oil Recovery under Ultrasonic Waves** submitted by **Khosrow Naderi** in partial fulfillment of the requirements for the degree of **Master of Science**.

Dr. Tayfun Babadagli
(Supervisor)

Dr. Ergun Kuru

Dr. Zhenghe Xu

Dedicated with the utmost love and gratitude

to my great family – the best friends one may find

(thank God) :

Fariba

Ali

Azade

Roshanak

Navid

without them I cannot imagine what I would have achieved (if any!)

ABSTRACT

Previous theoretical and experimental works described the acoustic stimulation as a potential method for enhancement of oil recovery. Several mechanisms have been suggested to govern the process of additional oil recovery under acoustic energy; nevertheless more research is needed to understand the exact physics behind the process.

The main focus of this work is to investigate the effects of ultrasonic radiation on immiscible oil displacement in porous media at both pore and core scale and also the influence of ultrasonic energy on enhanced oil recovery. To achieve this, an experimental program investigating (a) oil recovery due to spontaneous imbibition, (b) immiscible oil displacement of oil by water in 2-D sand pack models, (c) pore scale displacement mechanism using nanotechnology-based micro-model, and (d) penetration of ultrasonic waves in different media was designed. In each series of experiments various parameters were changed to monitor their influence on the process. Those parameters include fluid properties (mainly viscosity), porous medium characteristics (mainly wettability), and ultrasonic wave properties (frequency and intensity).

The results helped clarify the effects of ultrasonic energy on oil recovery and -immiscible- displacement mechanics for different rock and fluid properties. We were also able to identify some of the governing oil recovery mechanisms caused by ultrasonic energy for different conditions and limiting factors to apply this technology. This work is hoped to be another footstep for research in this area.

Table of Contents

CHAPTER 7

List of Tables

List of Figures

Nomenclature

f:	Frequency
I:	Intensity
NUS :	Non Ultrasonic
OW :	Oil Wet
P:	Average Power
p:	Instantaneous Power
S_{wi} :	Initial Water Saturation
US :	Ultrasonic
v:	Instantaneous Voltage
V_m:	Maximum Voltage
WW :	Water Wet

CHAPTER 1

INTRODUCTION

Oil is still playing the most prominent role in providing energy for the thirsty industrial world and the prospect of near future does not show any major resource to take its place. High demand for oil and rising trend of oil prices have urged oil companies to search for newer and more efficient ways of oil production.

Natural driving forces responsible for primary recovery such as reservoir pressure and gravity forces usually produce a small fraction of original oil in place, especially in reservoirs with unfavorable conditions such as low oil gravity and oil-wet rocks. After secondary recovery, e.g. waterflooding, there could still be a large amount of oil remaining in such reservoirs. Various methods of enhanced oil recovery have been introduced to maximize oil production. They may not be suitable for every type of reservoirs either due to economical or technical limitations. Therefore, many different unconventional techniques have been proposed and even tested in the field conditions.

Use of acoustic energy to stimulate oil reservoirs is a potential method which, at the first glance, might seem a mechanical stimulation. This, however, needs profound research to reveal the physics of the process and mechanisms involved in oil recovery under acoustic energy. Looking at previous works in this area, we designed

and performed a number of experimental works to obtain a better insight into the subject particularly on the effects of ultrasonic waves on oil displacement and recovery.

There are some advantages of using elastic sound waves to improve oil recovery. For example, it is environmentally friendly and, from the recovery point of view, it is an efficient way to distribute the energy in all directions in a medium due to its spherical transmission. Its major limitation, on the other hand, appears to be the rapid attenuation of high frequency waves through porous media because of shorter wavelengths. The impact of high frequency waves is expected to be more critical at pore scale. The mechanisms of stimulation in porous media by elastic waves are not well understood yet. This requires more physical experimentation especially at core/pore scale.

1.1 Statement of the Problem

Introduction of ultrasonic energy (high frequency sound waves) as a stimulation method dates back to early 60's. Studies done over this period of time are still limited to disclose the physics that governs the process to improve oil recovery, especially from liquid-liquid and solid-liquid interaction under ultrasonic radiation point of view.

Understanding the governing mechanisms is important for field applications. The proposed mechanisms related to capillary forces are peristaltic movement due to the pore walls deformation imposed by mechanical vibration, capillary forces reduction due to weakening of surface films at pore boundaries, coalescence of oil drops due to the Bjerknes forces, oscillatory movement of oil drops trapped by capillary forces,

forces from bubble cavitation and sonocapillary effect which is the increase of depth of fluid penetration into pores in an ultrasonic field (Malykh et al. 2003).

Mechanical vibrations generated by ultrasonic radiation influence interfacial forces and increase the relative permeability of the phases. At high intensities ultrasonic waves can also decrease the wetting films adherence to the matrix. Moreover, the heat generated due to vibration generated by ultrasonic waves reduces viscosity, density and surface tension. In the presence of surfactants, ultrasonic energy helps emulsification of oil. The vibration may lead to deformation of pore walls which will increase permeability and the porosity of rock. This vibration can also help removing the fines, clays and asphaltenes from pores.

These mechanisms depend on both medium (rock and fluid) and wave properties. Parameters such as rock elasticity, porosity, fluid viscosity, surface tension, wave frequency and intensity determine the viability of the mechanisms. For example, wave penetration and its ability to make pore walls deformation are highly dependent on its frequency and power (intensity). Experimental works at core and pore scale are still needed to investigate the influence of ultrasonic waves on these parameters in the context of incremental oil recovery. It is also critical to identify under what circumstances (or for which type of reservoirs) this technique becomes more suitable.

1.2 Methodology

To investigate the effects of ultrasonic radiation on oil recovery and immiscible displacement of oil in porous media, we designed four series of experiments each focusing on a different aspect.

First, we performed capillary imbibition experiments (core experiments) to study the effect of ultrasound on oil and heavy oil recovery by imbibition/drainage process. We changed a number of parameters such as wettability, viscosity, initial water saturation, wave intensity, and frequency. In each case, the mechanics of the recovery process was identified. The experiments were static so that the process was driven purely by capillary forces without contribution of any viscous forces. This way, we were able to identify the effect of ultrasonic energy on the surface/interfacial forces.

Secondly, sand pack models were employed for 2-D visualization experiments. In these experiments, the emphasis was on the liquid-liquid interface during immiscible displacement of oil by water. In addition to qualitative investigations, we also performed quantitative analysis on the generated patterns of water using fractal geometry. In these experiments, we examined the process for different conditions such as presence of water saturation, wettability, and oil viscosities.

As a third attempt, to have a better insight into the displacement process at pore scale, we built a homogenous micro-model and run a series of experiments. We specifically tested the effect of injection rate to identify which parameters, i.e., capillary or viscous, are more influenced by ultrasonic energy.

An important point to apply ultrasonic radiation to a field or use it as a well stimulation tool is its penetration depth. Therefore, we performed a series of experiments to investigate the penetration of ultrasonic waves inside air, water and a slurry mixture of sand and water. A few imbibition experiments were also run to clarify the effect of distance from source on the intensity of ultrasound waves and their ability to influence the oil recovery by spontaneous imbibition process.

The experimental program was designed in such a way that we can identify the effect of different parameters of porous medium, contained fluid and ultrasonic wave properties on various processes including spontaneous imbibition/drainage and immiscible displacement.

Fig 1.1 shows a diagram of our experimental program. The parameters investigated by each group of experiments are listed and the connection between different sets of experiments is shown.

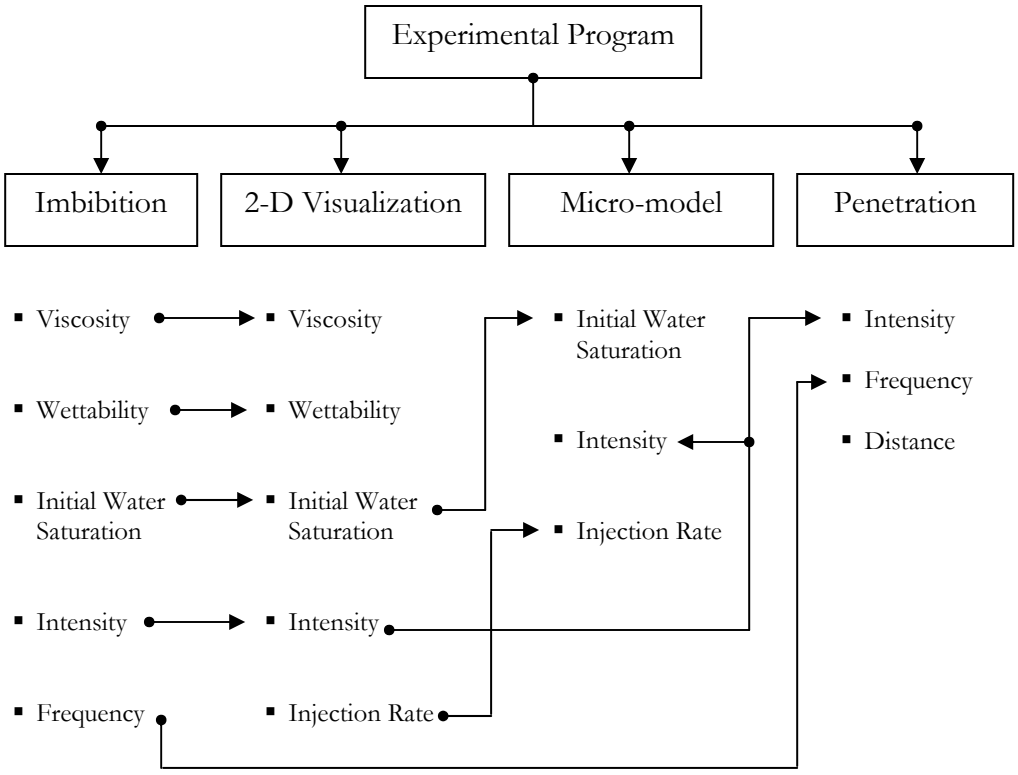

Fig.1-1: Experimental program.

CHAPTER 2

LITERATURE REVIEW

The idea of using elastic waves to improve oil recovery dates back to the 1950s. The very first research study in this area was reported in 1965 to the best of our knowledge. Duhon and Campbell (1965) conducted waterflooding tests on cores under ultrasonic energy with frequencies of 1, 3.1, and 5.5 MHz. The injection point was at the center of a sandstone core in which the ultrasonic probe was also introduced. A receiving probe was placed at the end of the core. Their experiments showed that the ultrasonic energy improved the oil recovery and displacement efficiency in the cores. They also observed that by increasing frequency, the cavitation and recovery decreases.

In the next three decades, the attention was devoted to elastic wave stimulation on oil recovery by seismic waves which have smaller frequencies than ultrasound waves. Beresnev and Johnson (1994) compiled and well documented all these efforts and provided a comprehensive review of methods using elastic wave stimulation of oil production, including both ultrasonic and seismic methods. What they concluded after this review was that the elastic wave and seismic excitations to porous media affect permeability and production rate in most cases.

They also listed laboratory cases that focused on the influence of seismic and ultrasound waves on the different characteristics of fluids, porous structure, and oil

recovery. Among them there were a few ultrasonic cases. Nosov (1965) observed a decrease in the viscosity of polystyrene solution under sound waves. Chen (1969) and Fairbanks and Chen (1971) reported increase in oil percolation rate through porous medium. Chen (1969) also showed that the effect of heat generated by ultrasonic radiation was minimal on the observed oil recovery increase. Johnston (1971) studied the influence of ultrasound on decreasing polymer viscosity. Cherskiy et al. (1977) described a sharp increase in permeability of core samples saturated with fresh water in the presence of acoustic field. Neretin and Yudin (1981) observed an increase in rate of oil displacement by water through loose sand under ultrasound. Pogosyan et al. (1989) showed that gravitational separation of water and kerosene accelerates due to acoustic field.

In addition to laboratory research, Beresnev and Johnson (1994) then pointed out four case studies of downhole reservoir ultrasonic stimulation. Morris (1974) used a very high frequency device in a field in Texas and observed an increase in oil production. Kuznetsov and Efimova (1983) and Simkin et al. (1990) reported a similar response to ultrasonic excitation tests in Siberia. Shaw Resources Services Inc. (1992) applied ultrasonic radiation in two field tests in California which stimulated oil production remarkably.

Ganiev at al. (1989) proposed that ultrasound would deform the pore walls and alter the radius of the pore. This vibration causes fluctuations in capillary pressure and expansion of surface films. Traveling waves along pore walls may cause a "peristaltic transport" of fluid displacement. This can be a possible explanation for permeability changes observed by Cherskiy et al. (1977).

More recently, Aarts and Ooms (1998) showed that mechanism of peristaltic transport works only at ultrasonic frequencies, and also the intensity of the ultrasonic field should be more than a specific amount. With these conditions, the effect will occur only near well bore due to the high attenuation of ultrasound.

Later, Aarts et al. (1999) showed that ultrasonic radiation deforms the pore walls and enhances the fluid velocity in porous media. They used a rubber stopper as the porous medium and water as the fluid and a 20 kHz ultrasonic source. They analyzed the "peristaltic transportation" mathematically. Their both numerical and experimental results showed that, by increasing ultrasonic power, the velocity of fluid inside the porous media increases. They suggested that ultrasonic energy may facilitate well acidizing. In their work the liquid phase was water and they used artificial porous medium which was not a representative of natural porous media.

Gadiev (1977) radiated ultrasound to oil saturated unconsolidated sand packs and observed considerable increase in both cumulative oil production and production rate. He assumed that this effect was due to a phenomenon called "sono-capillary effect", in which the depth of fluid penetration into pores is raised due to the pressure created from cavitation which collapses bubbles. This effect has been studied by a number of authors later (Hilpert et al. 2000; Rozina 2003; Rozina and Rosin 2003; Malykh et al. 2003; Dezhkunov and Leighton 2004) as reported by Hamida and Babadagli (2007c).

Nikolaevskii (1989, 1992) reviewed the possibility of mechanical (acoustic and seismic) stimulation of oil reservoir. The positive effect of vibration on oil recovery was demonstrated and it was attributed to the restoration of permeability as a result of drop

clusterization. A mathematical model was also proposed to illustrate the dominant vibration frequency. Such model is based on the nonlinear effect associated with viscoelastic resonance. Elastic wave fields may reduce the capillary forces by vibrating, and consequently, breaking surface films adsorbed to pore walls. Ultrasonic vibrations may mobilize oil droplets into pores, or may result in coalescence due to the Bjerknes forces.

Dunin and Nikolaevskii (2005) and Nikolaevskii and Stepanova (2005) proposed a theory about the ultrasonic waves generation as result of nonlinear effects associated with seismic and low frequency acoustic waves in porous media saturated with fluid. Under the conditions of long-short-wave resonance, the nonlinear generation of high ultrasonic frequencies by seismic waves is possible.

Nikolaevskiy et al. (1996) provided an explanation of a vibro-seismic recovery process describing the wave generation and propagation in porous media. They found that a characteristic frequency must be determined depending on reservoir lithology, stratification and fluid saturation. Such frequency could alter oil and water production characteristics and enhance oil production near the residual oil saturation.

Kuznetsov et al. (1998) studied the effect of vibration on relative permeability and waterflood displacement rates. They observed an increase in the relative permeability ratio of oil/water when vibration is applied. Later, Kuznetsov et al. (2002) reported incremental oil recovery from vibration stimulated wells in Russia, and pointed out that decreased water cut was caused by increase in the relative permeability of oil and decrease in water/oil interfacial tension.

Simkin and Surguchev (1991) and Simkin (1993) observed an increase in oil droplet size when continuous ultrasound was applied. This coalescence induced ultrasonically occurred due to the primary Bjerknes forces which are the mutual reaction between pulsating bodies in liquid (Blake 1949). Such coalescence may assist accelerating gravity phase separation within porous media, and improve the relative permeability of oil. The Bjerknes forces acting between particles can be attractive or repulsive depending on the droplet's location relative to the wave field. Hence, its oscillating phase will be attractive if oscillations are in phase and repulsive if out of phase (Bjerknes 1906; Blake 1949; Mettin et al. 1997). The magnitude of such force depends on the density of the continuous phase, and the radius of the droplet.

Schoeppel and Howard (1966) tested various samples of oil-water emulsions with ultrasound, and observed a great increase in coalescence. Both short- and long-duration ultrasonic irradiation were effective in producing coagulation and the rate of separation increased up to 700-fold over natural settling rates.

Graham (1997, 1999) and Graham and Higdon (2000a, 2000b) numerically studied the motion of fluid droplets in harmonically forced capillary tubes and observed a significant enhancement in mobility for large droplets with diameters greater than the diameter of the capillary, especially when oscillatory forcing is strong, and the drop capillary number is low. Such enhancement is dependent on frequency, amplitude and waveform, and is associated with increased droplet deformation.

Tamura et al. (2005) performed a series of experiments showing that liquids may adhere to flat ultrasonically driven surfaces. The shape of the droplet depends on

the amplitude of vibration. They developed a simple model to predict drop shapes. The predicted drop dimensions matched closely with the experimental observations.

A series of pendant drop experiments was performed by Hamida and Babadagli (2008a). From these experiments they concluded that the ultrasound affects the dripping rate of water through a capillary into various oleic phases. This dripping rate reaches a maximum at a characteristic intensity depending on oil viscosity and interfacial tension.

In addition to that, they conducted different types of experiments involving ultrasonic effects on capillary imbibition recovery of oil and also on immiscible and miscible displacement in porous media. (Hamida and Babadagli 2005a, 2005b, 2005c, 2006, 2007a, 2007b, 2007c, 2008a, 2008b; Hamida 2006)

They performed imbibition experiments to test the ultrasonic effects on imbibition by capillary forces. They used an ultrasonic bath operating at the frequency of 40 kHz and generated power up to 2 kW. The cores were epoxy coated to create different matrix boundary conditions, i.e., one and all sides open to flow. Different fluid pairs were used in the experiments and they performed all experiments with and without ultrasonic radiation to compare the results. They observed that ultrasonic waves may enhance capillary imbibition oil recovery depending on the fluid and matrix-fracture interaction type, i.e. co- or counter-current (Hamida and Babadagli 2005a).

In a series of subsequent works, Hamida and Babadagli (2005b, 2007b, and 2007c) studied the capillary interaction between matrix and fracture under different ultrasonic intensities for different fluid types. They used an ultrasonic source with frequency of 20 kHz and power of 25 and 45 W/cm^2. Experiments showed that

rheological properties of polymers may be altered and the surfactant solubility may be increased under ultrasonic energy.

They also investigated the ultrasound effects at the interface of fluids during immiscible and miscible displacement in porous media (Hamida and Babadagli 2005c, 2007a, 2008b). They performed both capillary imbibition and Hele-Shaw experiments using ultrasonic bath with a frequency of 40 kHz and power of 35W/cm^2 and also an ultrasound source whose horn transmitted ultrasound energy with a frequency of 20 kHz and power up to 250 W/cm^2. On the displacement pattern images obtained through the Hele-Shaw experiments, they performed fractal analysis to analyze them quantitatively. They concluded that ultrasonic waves alter the shape of the interface between two immiscible fluids and reduces the interfacial tension. The ultrasonic waves also enhanced the molecular diffusion at low injection rates during miscible displacement.

An important factor controlling the feasibility of acoustic waves' stimulation in wells is its depth of penetration through porous media. The basics of the theory of elastic wave propagation in fluid saturated porous media were started by works of Frenkel (1944) and Biot (1956a, 1956b, and 1962). Biot developed a comprehensive analytical model to describe the propagation of stress waves in poroelastic solids containing a viscous and compressible fluid. He found that there are two compressional waves namely the slow (P2-wave) and the fast wave (P1-wave). Attenuation occurs mainly with slow wave due to the dissipative forces generated by pore fluid viscosity.

A great deal of work has been carried out based on Biot's theory following his pioneering papers. For example, a mathematical model was developed by Norris (1989) which described the propagation of low-amplitude waves in saturated sediments. Zimmermann and Stern (1994) presented several closed-form analytical solutions of the Biot's equations, such as radiation from a harmonically driven plane wall. Buckingham (1997, 1999, and 2005) extended the Biot's theory for consolidated and unconsolidated porous material.

Considerable amount of work has been reported in the area of the use of ultrasonic energy on formation damage. Venkitaraman et al. (1995) studied the removal of near wellbore damage by ultrasonic radiation. They tested the removal of mud solids on a plug in a laboratory study. They used two ultrasonic sources, one could be driven at frequencies of 10 to 100 kHz and the other was fixed at 20 kHz. They concluded that acoustic streaming and cavitation yielded from ultrasonic radiation can remove the damages arising from mud particles and can also increase the permeability by a factor up to six times.

Wong et al. (2003, 2004) designed a special "Linear Cell" setup in which cylindrical core samples were placed. They used this setup to see the fines damage and mud cake removal in the wellbore by acoustic waves. They applied ultrasonic radiation with a frequency of 20 kHz with a maximum power of 2000 W. They measured permeability alteration against time. They also estimated the optimum production rate for the most effective removal by ultrasound waves. They observed that higher frequency results in better cleaning, but causes more attenuation, i.e., the wave

penetration into the rocks decreases. Thus, the optimum frequency must be chosen to balance the cleaning efficiency and wave attenuation.

Poesio et al. (2002) investigated the influence of acoustic waves on liquid flow through Berea sandstone cores and found out that pressure gradient inside the cores decreases under acoustic energy. They concluded that this is related to the reduction of fluid viscosity.

Poesio and Ooms (2004) and Poesio et al. (2004) developed a theoretical model to predict removal of small particles and fines in porous media.

Gollapudi et al. (1994) applied a thin layer of asphaltene onto glass beakers and exposed them to ultrasound inside aqueous or kerosene solutions for different time intervals and intensities. They suggested that ultrasound may assist the removal of asphaltenes from wellbores.

Abad-Guerra (1976) studied the effect of ultrasonic energy on sandstone cores initially plugged by paraffins. Large improvements in the permeability were observed due to cavitation and heating by ultrasonic field.

Gadiev (1977) stated that ultrasound can reduce the viscosity of high-polymeric liquids by up to 22%. In fact, prolonged exposure of polymer solutions to high-intensity ultrasound permanently reduces its viscosity.

The idea of using ultrasound to improve the upgrading of heavy oil and tar sands has also been tested (Sadeghi et al. 1990; Sadeghi et al. 1992; Lin and Yen 1993; Sadeghi et al. 1994; Yen and Dunn 1999; Dunn and Yen 2001; Bjorndalen and Islam 2004).

Gunal and Islam (2000) investigated crude oil rheology alterations under ultrasonic and electromagnetic radiation. They exposed samples of a given specimen to electromagnetic field with a frequency of 2000 MHz and power of 700 W and also to ultrasonic radiation with a frequency of 10 kHz and power of 250 W. They concluded that electromagnetic radiation affects crude oil rheology (such as viscosity) in presence of asphaltene but this effect disappears at high temperatures. The ultrasonic radiation did not show any permanent effect on crude oil viscosity in their experiments.

Limited amount of pore scale studies investigating the effects of ultrasonic waves on displacement mechanics were also reported. Li et al. (2005) studied the mobilization of oil ganglia in a 2D etched glass micro-model under low frequency vibrations. They observed an increase in the recovery with higher amplitude and lower frequency.

Residual oil is entrapped as ganglia in narrow pores because of resisting capillary forces. Beresnev et al. (2005) showed that vibrations help overcome this resistance. Adding vibratory forces to the external gradient makes instant unplugging of entrapped ganglia occur. Their experiments on glass micro-model along with computational simulation showed that the mobilization of residual saturation of ganglia is proportional to the amplitude and inversely proportional to the frequency.

In their penetration zone, acoustic waves can have big effects on fluid-matrix interaction and therefore hydrocarbon displacement and recovery. This effect as well as the propagation distance is highly dependent on wave frequency and intensity. High frequency ultrasonic waves put a limitation in their effective penetration radius; hence many researches focused on low frequency stimulation (seismic stimulation) (Simonov

et al. 2000; Kuznetsov et al. 2002, Kostrov and Wooden 2005) and also pressure pulsing technology (Dusseault et al. 2000, Spanos et al. 2003).

Kuznetsov et al. (2002) reviewed seismic techniques of enhanced oil recovery. They performed experiments to generate capillary pressure curves with and without vibration and observed an increase in oil/water relative permeability and also oil saturation after elastic vibration. They concluded that this increase is due to fines removal by vibration.

Spanos et al. (2003) studied the pressure pulsing as a new method for improved oil recovery. They considered different models for porous media like the Biot-Gassmann and de la Cruz-Spanos models and ran a field study on pressure pulsing. They generated pulses by a hydraulically operated tool and monitored the results and found out that the water injectivity and oil production increased after pulsation. They concluded that pressure pulsing improves oil recovery by removing barriers blocking fluid flow and also reducing the viscous fingering and hence improving waterflood.

Roberts et al. (2003) studied laboratory and field scale seismic stimulation. The stimulation was created by applying mechanical stress to rock samples which were placed inside a core holder. The mechanical stress had frequencies from DC (here means zero frequency) to 2000 Hz. In the field tests, a downhole fluid pulsation source was used to generate pulses inside the well with an amplitude of 4000-5000 psi. They observed a certain degree of change in fluid flow behavior and permeability. Wettability to the non-wetting phase also increased.

Westermark et al. (2001) applied a complex system of vibration tool in a field to monitor the effect of downhole vibration stimulation on enhanced oil recovery. They

measured permeability in different frequencies ranging from 40 Hz to 400 Hz. The test showed permeability improvement at certain intensities and up to 20% increase in oil production rate.

Zhu et al. (2005) gathered the results obtained through the applications of different types of a special tool used to create downhole vibrations with a harmonic vibration frequency of 88 shocks per minute. Each shock had 5 ton strength. The field applications were done in different oil fields in China. The results showed that sand content, water content, viscosity and density of oil decreased generally. In their report, however, only the results were presented with no information about the system used or relevant experiments.

CHAPTER 3

CORE EXPERIMENTS

A series of capillary (static) imbibition experiments were performed to investigate the effect of ultrasonic energy on oil recovery using water-wet Berea sandstone samples. Some samples were exposed to wettability alteration and rendered more oil-wet through a chemical treatment process. By definition, if a wetting fluid displaces non-wetting fluid, this process is called imbibition and if it is reverse, i.e. a non-wetting fluid displaces a wetting one, it is drainage. When more oil-wet samples which were saturated with oil, were immersed into water filled cells, the term "imbibition" was still used to describe the process. All the experiments run under static condition will be called imbibition or core experiments throughout the text.

The suction process by capillary (spontaneous) imbibition is a steady process in which the system is in mechanical equilibrium and the process is based on capillary forces which depend on rock and fluid properties, while in a forced imbibition a net force such as pressure difference or gravity drives the process. Capillary imbibition recovery is totally based on capillary forces without any inertia force. Using these experiments, one may clarify the changes in the interfacial properties under ultrasonic energy, which eventually result in incremental oil recovery.

3.1 Experimental Setup

Imbibition experiments were performed using cylindrical cores of Berea sandstone. These cores were all the same size with a length of 7 cm and diameter of 2.5 cm. All sides were open and in contact with the surrounding fluid to ensure a co-current type interaction. Those cores without initial water saturation were directly saturated by oil under vacuum. The cores with the initial water saturation were first vacuum saturated by brine in a core holder using a pump and then oil was injected to drain the water out until irreducible water saturation is reached. Mineral oils with three different viscosities: 40, 500 and 1600 cp at ambient conditions were used as the oleic phase. Next, the cores were placed into graduated imbibition cells filled with 3 wt% NaCl brine. For ultrasonic experiments these cells were put inside a bath filled with water which surrounds the cell below its neck.

An ultrasonic generator provided ultrasonic energy which was delivered to the bath through a half-immersed horn. The generator used was Sonicator® 3000 ultrasonic processor which generates and emits ultrasonic waves at the frequency of 20 kHz. The generator transforms AC line power to a 20 kHz electrical signal. There is a piezoelectric converter or transducer which converts this electrical signal to a mechanical vibration. This vibration is amplified by the horn and transmitted by its tip to surrounding area. **Fig. 3-1** shows a schematic of setup designed for imbibition experiments.

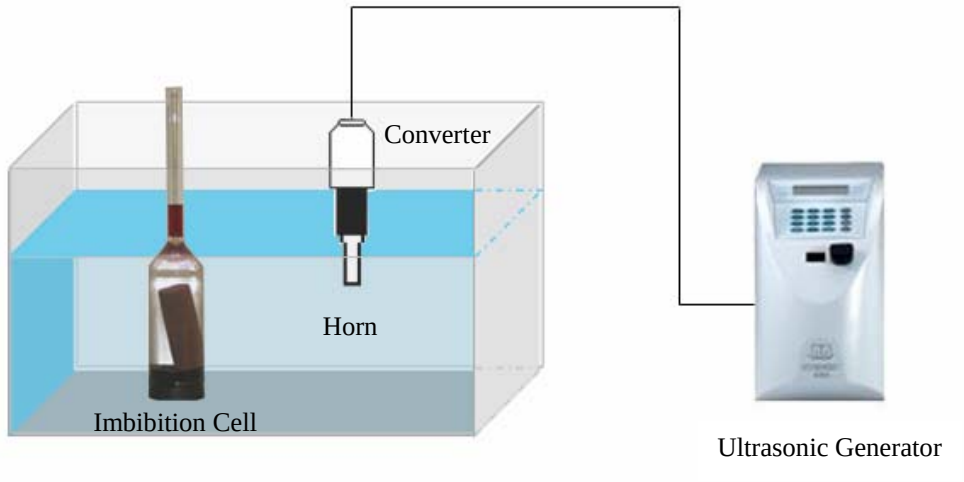

Fig. 3-1: Experimental set-up for imbibition (core) experiments.

Output power of ultrasonic generator was set to 25, 45 and 84 W/cm^2 for different cases. The frequency of ultrasonic wave generated by this generator was fixed at 20 kHz. Four experiments with low power output of 1W were also performed to observe the effect of frequency. In those experiments, another generator (Microson™ XL-2000, shown in **Fig. 3-2(a)**) was used. This device is designed for lower wave intensities and generates ultrasonic waves at the frequency of 22.5 kHz. For higher frequency tests, we used Prowave ultrasonic ceramic transducers which works at a center frequency of 40 kHz. This device is connected to a GW function generator which emits electrical signal at arbitrary frequency, amplitude and wave shape (**Fig. 3-2(b)**). The function generator was set to produce a sinusoidal signal with 10 V amplitude at frequency of 40 kHz. Having output matched impedance of 50 Ω (ohm),

the function generator transmits 1 W mean power. **Eqs. 3-1** and **3-2** are used to calculate this power.

$$v = V_m \sin(\omega t) \qquad 3\text{-}1$$

$$P = \frac{1}{T}\int_{t=0}^{t=T} p\,dt = \frac{1}{T}\int_{t=0}^{t=T} \frac{v}{R}^2\,dt = \frac{1}{T}\int_{t=0}^{t=T} \frac{V_m^2}{R}\sin^2(\omega t)dt = \frac{V_m^2}{2R} \qquad 3\text{-}2$$

where v and p are instantaneous voltage and power respectively, V_m is maximum voltage and P is average output power.

Having V_m =10 V and R =50 Ω, mean power will be: P = 1W.

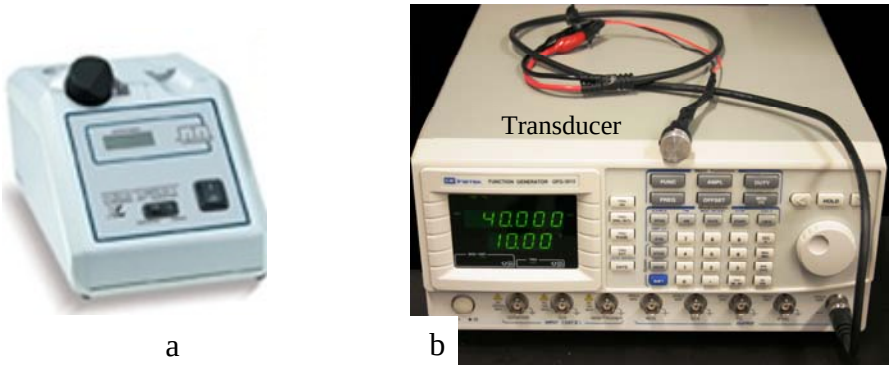

a b

Fig. 3-2: (a) Microson™ XL-2000 generator,
(b)function generator and 40 kHz ultrasonic transducer.

3.2 Procedure

For each case, two experiments were run with and without ultrasonic energy for comparison. **Table 3-1** displays the experiments conducted throughout the study. To obtain oil wet cores, dichlorooctamethyltetrasiloxane (SurfaSil™, a siliconizing fluid) was applied. This chemical was added to pentane and the mixture was injected to dry cores by vacuum saturation. Pentane evaporates under vacuum and pore walls are covered with a monolayer of SurfaSil™ which renders the core oil wet. The degree of oil wetness depends on the concentration of SurfaSil™ in the mixture. The oil wet cores were treated using very high concentration (nearly 10 vol. %) of siliconizing fluid to make them strongly oil-wet.

Table 3-1: Capillary imbibition experiments.

Experiment Number	Initial Water Saturation	Oil Viscosity (cp)	Ultrasound Intensity (W/cm^2)	Ultrasonic Frequency (kHz)	Wettability
1	0.45	35	0	20	Water Wet
2	0.45	35	25	20	Water Wet
3	0.45	35	45	20	Water Wet
4	0	500	0	20	Water Wet
5	0	500	45	20	Water Wet
6	0	500	84	20	Water Wet
7	0	1600	0	20	Water Wet
8	0	1600	45	20	Water Wet
9	0	1600	84	20	Water Wet
10	0	500	0	20	Oil Wet
11	0	500	45	20	Oil Wet
12	0	35	0	20	Oil Wet
13	0.40	35	0	20	Oil Wet
14	0	35	45	20	Oil Wet
15	0.40	35	45	20	Oil Wet
16	0	35	1 (W)	22.5	Water Wet
17	0	500	1 (W)	22.5	Water Wet
18	0	35	1 (W)	40	Water Wet
19	0	500	1 (W)	40	Water Wet

3.3 Results and Analysis

The produced oil due to imbibition accumulates in the graduated section of imbibition cells. The fraction of the produced oil to original oil in cores determines the recovery.

Fig. 3-3 shows the recovery graphs for the first three experiments which were represented by solid lines. These experiments are water wet cases with initial water saturation. For comparison we added three dotted curves which represent the identical cases but without initial water saturation reported by Hamida (2006).

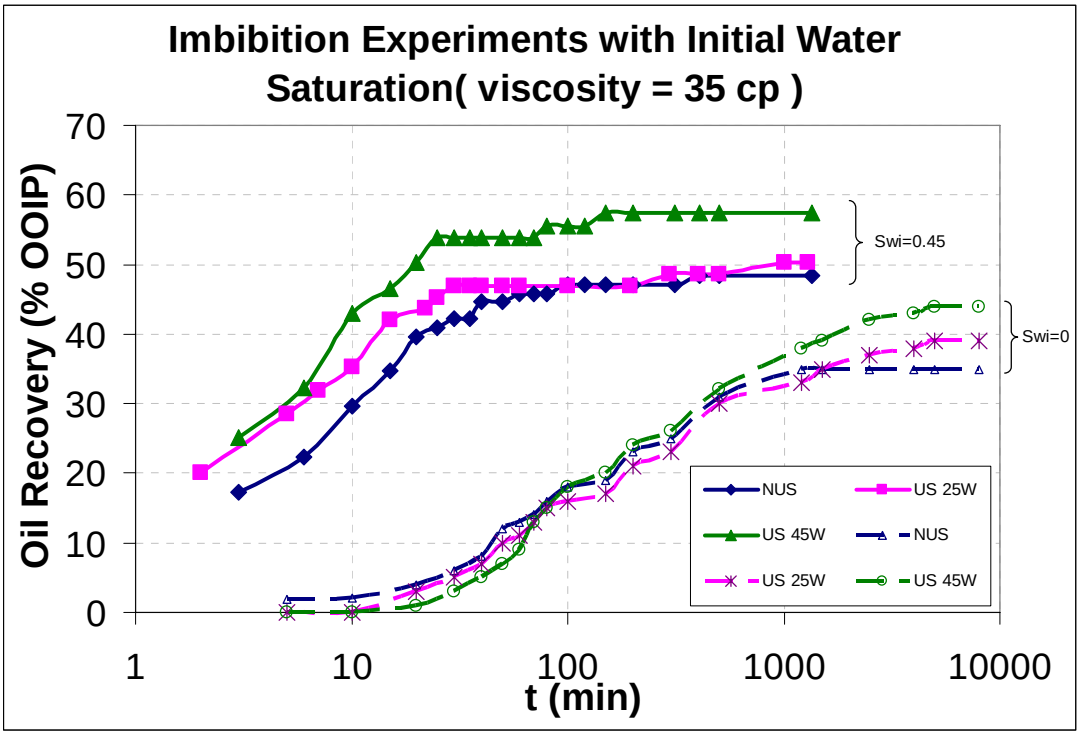

Fig. 3-3: Comparison of experiments with (solid lines - experiments #1-3) and without initial water saturation (dotted lines - from Hamida, 2006)

Two interesting observations can be made out of this graph: (1) Ultrasonic energy increases recovery especially when the output energy is 45 W/cm^2, (2) the same trend in the recovery rate and in the changes in ultimate recovery with increasing ultrasonic intensity was observed in both series of experiments, i.e., with and without initial water saturation.

Fig. 3-4 shows the recovery curves for experiments #4, #5 and #6 in which the cores were saturated with heavier oil (500 cp). The trend in both recovery rate and ultimate recovery is similar to the lower viscosity case (**Fig. 3-3**). The recovery rate is only affected at the early stages of the experiment but the ultimate recovery increased by increasing ultrasonic energy intensity.

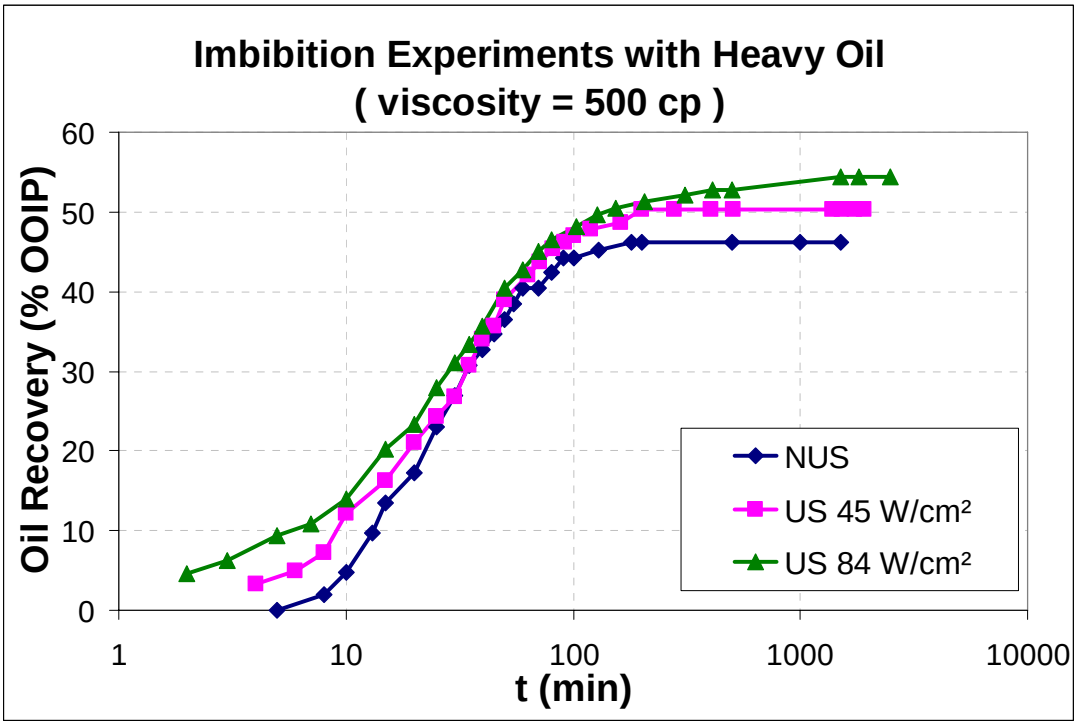

Fig. 3-4: Imbibition experiments #4-6 (water wet case).

Fig. 3-5 compares the recovery curves for much heavier oil (1600 cp) with and without ultrasonic energy (Experiments #7, #8 and #9). The change in the recovery rate and ultimate recovery due to ultrasonic energy is trivial compared to the lighter oil cases given in **Fig. 3-4**. One may conclude that when the oil viscosity increases, the effect of ultrasonic waves lessens. This is in agreement with the visual observations reported by Hamida and Babadagli (2007a). Ultrasonic experiments (#8 and #9) were repeated to check the reproducibility (Fig. 3-4). Although there exist some degree of disagreement in very early time data, the ultimate recovery is the same for all the cases. Also looking at general trend, a similar behavior was observed. The slight differences in the very early time data could be attributed to the changes in the core properties as different cores from the same block were used in each experiment.

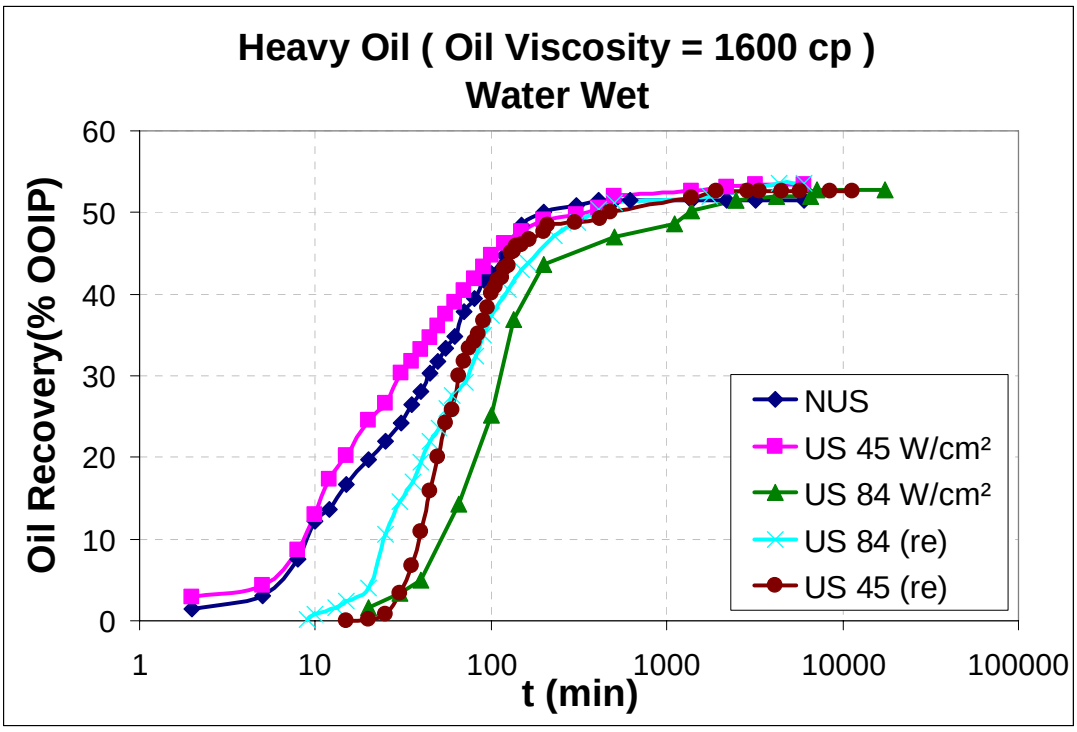

Fig. 3-5: Experiments #7-9 (water wet cores).

The recovery curves for Experiments #10 and #11 are shown in **Fig. 3-6**. In these two experiments, oil wet cores and heavy-oil with viscosity of 500 cp were used. The effect of ultrasonic energy on the recovery is much more pronounced in the oil-wet case. Due to oil wet nature of the cores, it takes much longer time in order for the recovery by capillary imbibition to start. Under no ultrasound energy, oil recovery is very minimal. While we observed about 10% increases in the recovery by applying ultrasound energy with an intensity of 45 W/cm^2 in water wet experiments, a major and considerable increase of more than 100% is seen in the oil-wet case. The significant change in the ultimate recovery can be attributed to lowered IFT and wettability alteration.

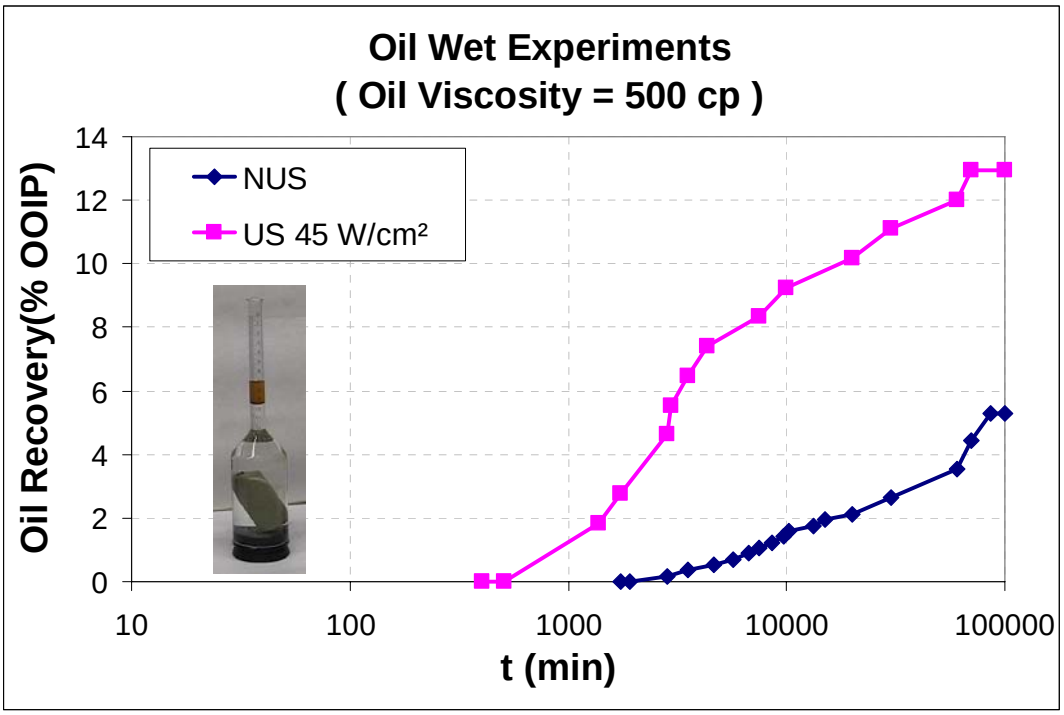

Fig. 3-6: Oil wet experiments with heavy oil (experiments #10 and #11).

Fig. 3-7 shows the recovery curves for experiments #4 to #6, #10 and #11. Oil viscosity in all cases is 500 cp. This graph is indeed a combination of **Fig. 3-4** and **Fig. 3-6** to compare the recoveries of oil wet and water wet cases better and speculate on the recovery mechanism under ultrasonic energy for two different wettabilities. The first three experiments are water wet cases and the other two are oil wet. For oil wet experiments, the effect of ultrasonic energy on the recovery is much more critical and also the production starts later in these experiments. Under no ultrasound energy, oil recovery is very minimal (~5% OOIP). Only 10% change in the ultimate recovery was observed by applying ultrasound energy with an intensity of 45 W/cm^2 in the water-wet case, whereas, with the same amount of ultrasonic intensity, oil wet cases yielded more than 100% change in the ultimate recovery. Obviously, different recovery mechanisms governed the process in water- and oil-wet cases. Favorable changes in the interfacial properties are expected in both cases as also observed by Hamida and Babadagli (2007b, 2008). The Bjerknes forces are expected to be an effective mechanism as well for the water-wet cases resulting in higher ultimate recovery under ultrasonic energy (Bjerknes 1909 and Blake 1949). That explains the difference in the ultimate recoveries that started to become obvious after 100 minutes. As the oil droplets would not be in a ganglion shape in the oil-wet case, the Bjerknes forces are not expected to be an effective mechanism. The IFT change is expected and this causes change in the wettability. The observations suggest that more attention will be given to oil-wet cases with lower viscosities as the ultrasonic effect is more pronounced in those cases.

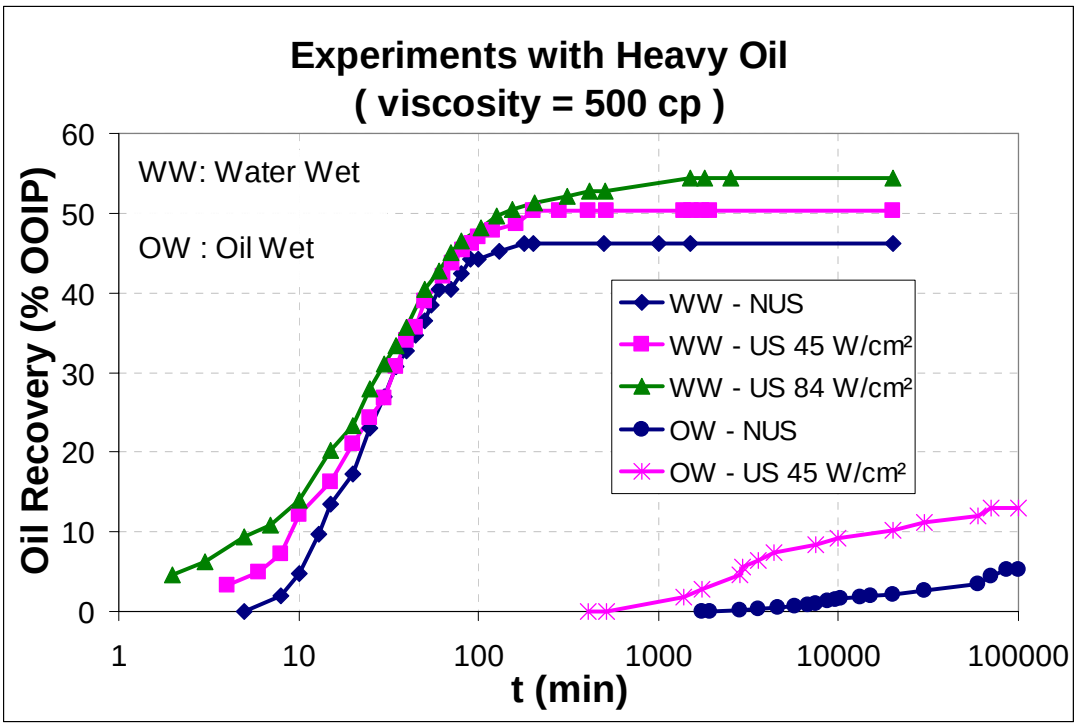

Fig. 3-7: Experiments #4-6, #10 and #11.

In addition to the previous water-wet cases, the effect of initial water was added in the new set of experiments. Peristaltic movement of water phase is expected to cause additional recovery (Ganiev et al. 1989 and Aarts et al. 1999) as the water will not be the wetting phase and be more mobile in the oil-wet case. **Fig. 3-8** shows the comparison of the recovery curves of the oil-wet cores with and without initial water saturation for the light mineral oil (35 cp) (experiments #12 #13, #14, #15). For two experiments without initial water saturation, we observe a large increase in recovery after ultrasonic radiation but this recovery improvement is even higher in the cases with initial saturation. In the oil wet medium, water has more tendency to flow because it has less affinity to the rock surface. The peristaltic movement of the initial water could facilitate faster transportation of oil resulting in more recovery. At the time of

160,000 minutes we exposed all four cases to ultrasonic energy half a day on and half a day off. As seen, the recovery of the case with initial water saturation which was not under ultrasound energy jumps up and gets close to the equivalent case which has been under stimulation since the start time (t=0). This big change verifies the effect of ultrasonic energy causing peristaltic movement of water which results in more oil production. Change in the interfacial properties (IFT, wettability) is also expected for this case.

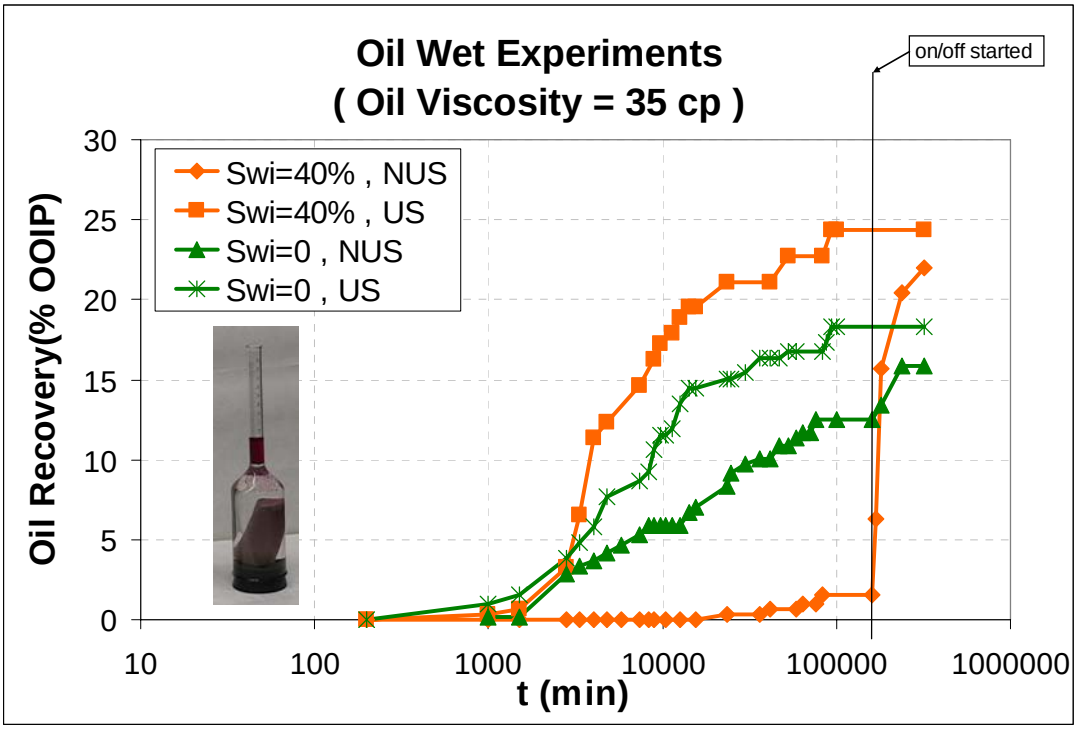

Fig. 3-8: Oil wet experiments with light mineral oil, with and without initial water saturation (experiments #12-15).

The last group of experiments was performed to observe the effect of frequency. Experiments #16 and #17 are the cases with oil viscosity of 35 and 500 cp, respectively and both were exposed to ultrasonic waves with a frequency of 22.5 kHz. Oil viscosity in experiments #18 and #19 was 35 and 500 cp, respectively and both experiments were under ultrasonic radiation of 40 kHz frequency. **Fig.3-9** shows the recovery curves of these experiments.

For reproducibility, we repeated experiments #16 and #17. This observation shows that the rate of recovery increases at higher frequencies but finally all experiments converge to a similar ultimate recovery values. Recovery for cases with higher viscosity oil is less during the experiments but ultimate recovery is almost the same for both viscosities. Repeated experiment #16 shows a similar recovery trend but its ultimate recovery is a few percent higher than experiment # 16 itself. This change might be due to a difference in core properties or experimental conditions. For experiment # 17, the recovery curve is in a very close match with its repeated equivalent.

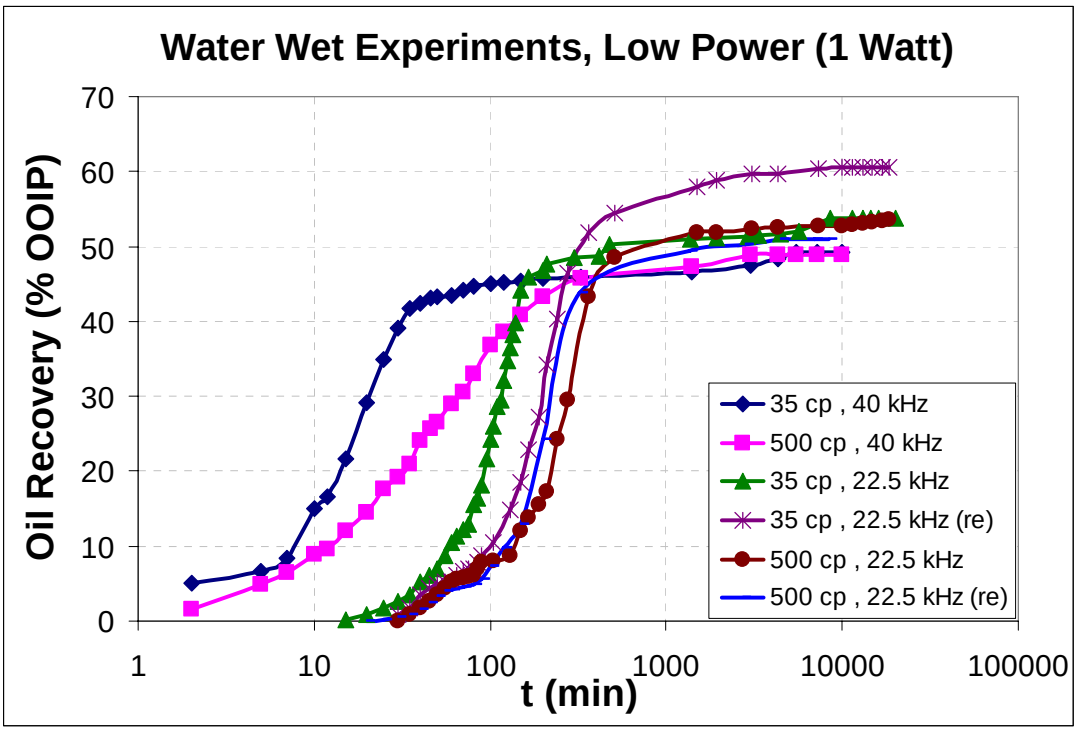

Fig.3-9: Experiments # 16-19, low power, different frequencies.

3.4 Conclusions

Imbibition experiments showed that ultrasonic radiation enhances the capillary forces and eventually increases the recovery. Similar trends of recovery were observed in water wet cases with and without initial water saturation. Comparing different oil viscosities in water wet experiments (Experiments #1-9 in **Fig.3-3 to Fig.3-5**) one may conclude that the effect of ultrasonic energy on recovery change is less for higher viscosities. The effect of ultrasonic radiation on recovery is clearly more significant in oil-wet cases. Oil-wet experiments indicated that presence of initial water saturation facilitates oil recovery under ultrasound, which is expected to be mainly due to the peristaltic movement of more mobile water.

CHAPTER 4

VISUALIZATION EXERIMENTS –

GLASS BEAD MODELS

After gaining an insight into the effects of ultrasonic waves on fully capillary driven displacement in porous media and oil recovery, dynamic experiments (waterflooding) were conducted to add the flow component into the process. Imbibition experimentation provided clarifications on how ultrasonic energy changes the interfacial properties as the process is totally controlled by capillary forces. Obviously, displacement in porous media have viscous forces component in addition to the capillary forces. The main objective is to identify the changes in the displacement process under ultrasonic energy when both viscous and capillary forces are in effect.

4.1 Experimental Setup and Procedure

2-D sand pack models made of two acrylic sheets were used in the experiments. The space between the two acrylic sheets was filled with glass beads. The beads' diameter ranges from 0.3 to 0.6 mm.

Two models with different sizes and configurations were created. The first type of model consists of two 10cm x 15cm sheets with two ports (injection and

production) installed at two ends of models. **Fig.4-1** shows a sample of this model. The second type of model was a 5-spot model in which there was an injection port at the center and four production ends at the corners. The shape was a square of 20 cm-size.

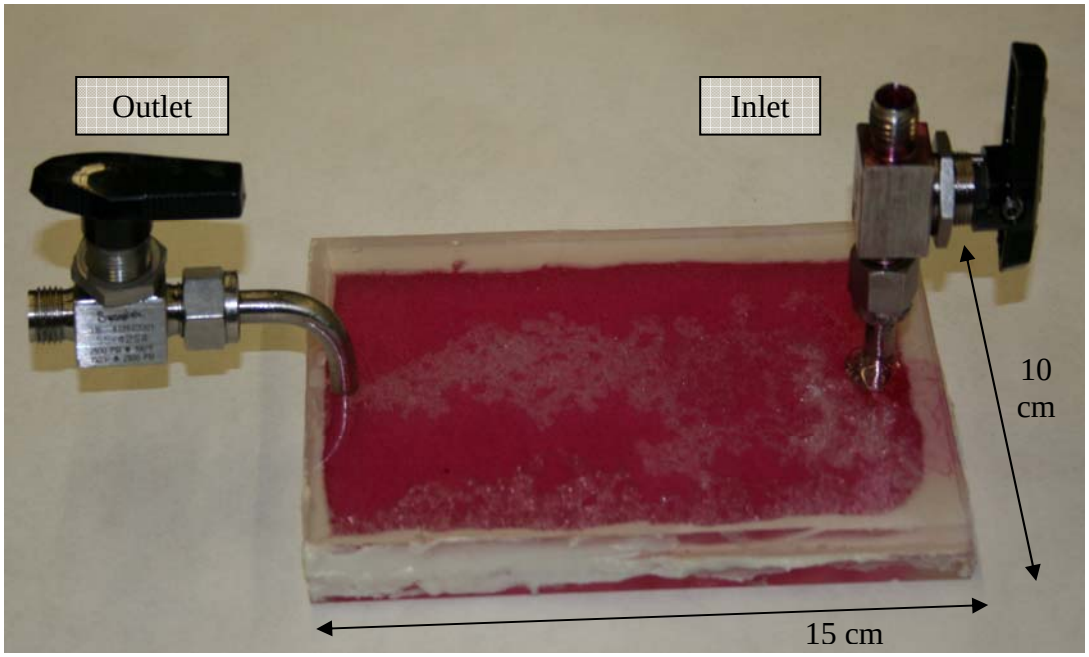

Fig.4-1: A sample of small glass beads models.

We first filled the models with a few layers of glass beads and then sealed them with epoxy and installed valves at ports. To prepare oil wet models, the glass beads were rinsed with a mixture of dichlorooctamethyltetrasiloxane (commercial name is SurfaSil™) and pentane first. After waiting for pentane to evaporate, they were used to prepare the model.

Next, models were saturated with oil under vacuum. For only two experiments, the models were saturated with brine first and then water was drained by injecting oil at a low rate until the irreducible water saturation is reached. To run the test, water was injected to displace oil inside the model. The injection rate was constant and equal to 10 ml/hr. During the experiment, images were acquired by a video camera.

To expose these models to ultrasound radiation, the models were immersed into a bath which was built by transparent acrylic sheets to be able to illuminate the models from the bottom of the bath. **Fig. 4-2** shows the setup of visualization experiments. Here, Microson™ XL-2000 was used as the ultrasonic processor. This device generates ultrasonic waves at frequency of 22.5 kHz. In the experiments, the output energy was set at 5 W.

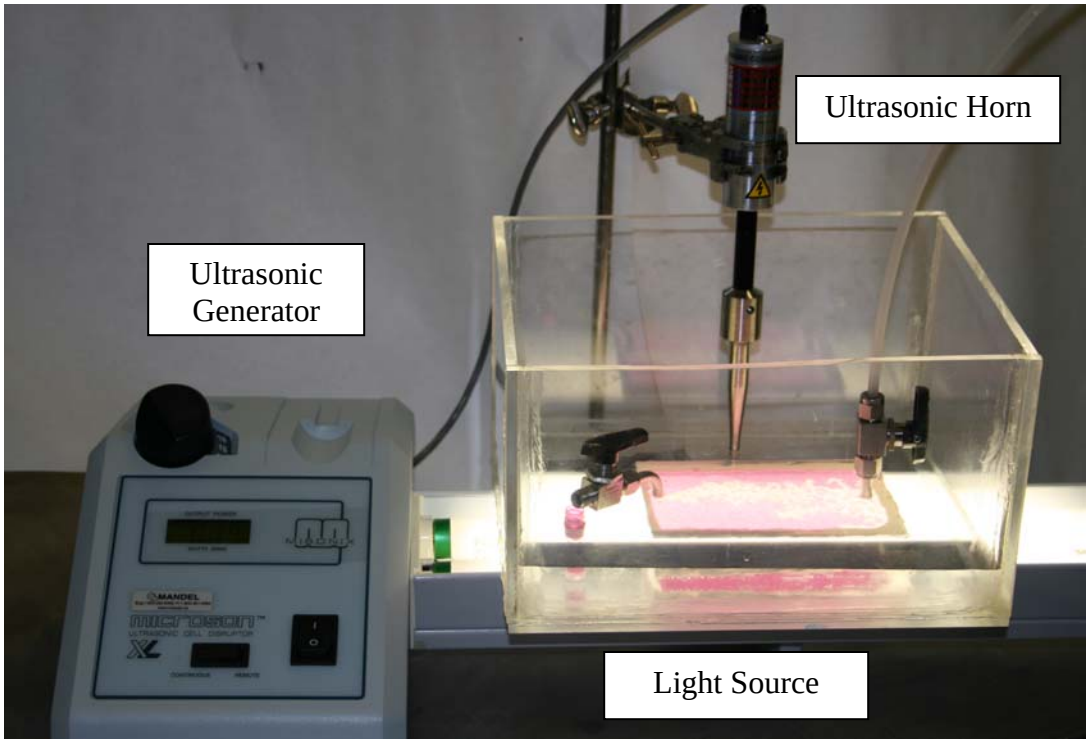

Fig.4-2: Set-up for visualization experiments.

Table 4-1 lists the experiments performed with smaller size (10x15 cm) sand pack models.

Table 4-1: Visualization experiments with small models (10x15 cm).

Experiment Number	Oil Viscosity (cp)	Ultrasound Intensity (W)	Wettability	Initial Water Saturation
1	35	0	Water Wet	No
2	35	5	Water Wet	No
3	500	0	Water Wet	No
4	500	5	Water Wet	No
5	35	0	Oil Wet	No
6	35	5	Oil Wet	No
7	500	0	Oil Wet	No
8	500	5	Oil Wet	No
9	500	0	Oil Wet	Yes
10	500	5	Oil Wet	Yes

4.2 Image Processing

The displacement patterns were evaluated qualitatively and quantitatively. For these analyses, the images were processed to improve the quality and obtain a better contrast between the displaced and displacing cases. In the quantitative analysis, the displacement patterns developed in the shape viscous fingering due to significant viscosity contrast between the displacing and displaced phases were evaluated in terms of two characteristics: (1) the fractal dimension of the pattern developed, and (2) the percent area swept by the displacing fluid.

The fractal shape of viscous fingering growth in a 2-D plane can be described by its fractal dimension which is a parameter showing the complexity of the pattern developed. A measure of this dimension using the box counting method (Liebovitch and Toth 1989) is described in **Eq. 4-1:**

$$d_B = \lim_{\varepsilon \to 0} \frac{\log N_B(\varepsilon)}{\log(\frac{1}{\varepsilon})} \qquad 4\text{-}1$$

where $N_B(\varepsilon)$ is the number of boxes of size ε that cover the set.

FracLac plug-in (Karperien 2005; the plug-in is available at http://www.geocities.com/akarpe@sbcglobal.net/box.html) of ImageJ program (Rasband (1997-2005); http://rsb.info.nih.gov/ij) was used to calculate the fractal dimension of the final patterns. In addition to that, the swept area at the mature stage of each case was also calculated. Finally, the comparisons of these characteristics were made for ultrasonic and no-ultrasonic cases.

4.3 Analysis and Results

In addition to the analysis of the displacement images taken during the experiments, the produced amounts of water and oil were also measured and analyzed. A series of the snapshots of experiment #1, which represents the water wet case saturated with light mineral oil without ultrasound, is illustrated in **Fig. 4-3**. These images show the patterns developed within 30 minutes. After 30 minutes no significant change was observed in the pattern shape after even waiting more than an hour.

In this experiment we first saturated the model with light mineral oil (35 cp) then injected water at the rate of 10 ml/hr. The results for the ultrasonic case (experiment #2) are given in **Fig. 4-4**. The displacement patterns obtained with and without ultrasonic energy differ remarkably. In the presence of ultrasound energy, the fingers are thicker and shorter while in the case of without ultrasound, the fingers are thinner and spread. This yielded a more compact cluster of the swept area.

Figs. 4-5 and **4-6** show the recovery graphs of these two experiments against time and pore volume injected, respectively. The breakthrough times are close to each other but the ultrasonic cases did not yield any recovery after breakthrough. Hence, under ultrasonic energy, when the injected phase reached the production end, it did not continue to sweep the untouched parts of the model. But in the no-ultrasonic case, we observe that there is still an increase in recovery after breakthrough. However, the swept area in the ultrasonic case is more compact and therefore, has less residual oil.

The image was processed by FracLac plug-in of ImageJ software and the results are given in **Table 4-2** for these two experiments. Although the area swept was greater in the no-ultrasound case, the displacement patterns was more compact. This is also indicated by higher fractal dimension (experiment #1).

Table 4-2: Pattern characteristics of experiments #1 and #2.

Experiment Number	Fractal Dimension	Swept Area (/total)
1	1.7396	0.4147
2	1.632	0.3523

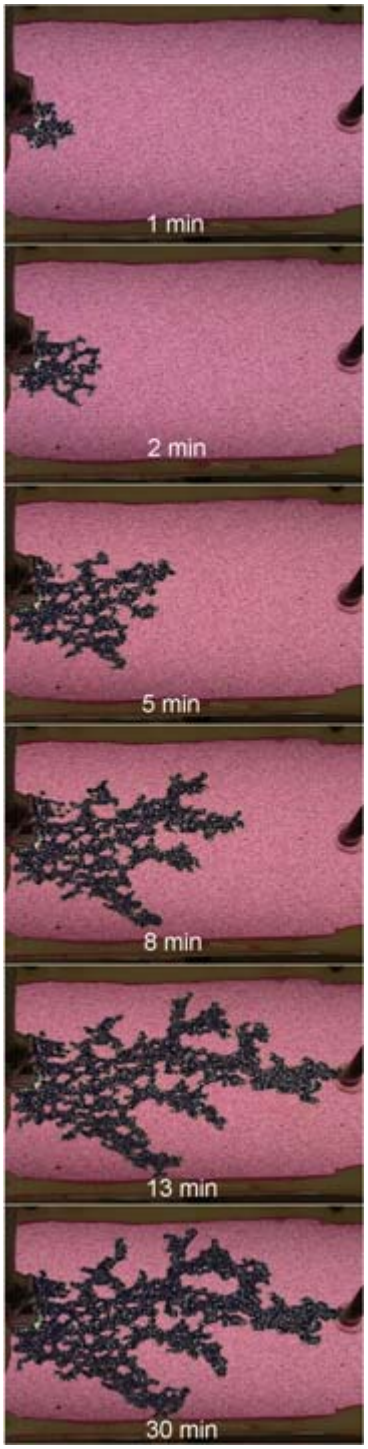

Fig. 4-3: Exp.#1, WW, Light Oil, NUS.

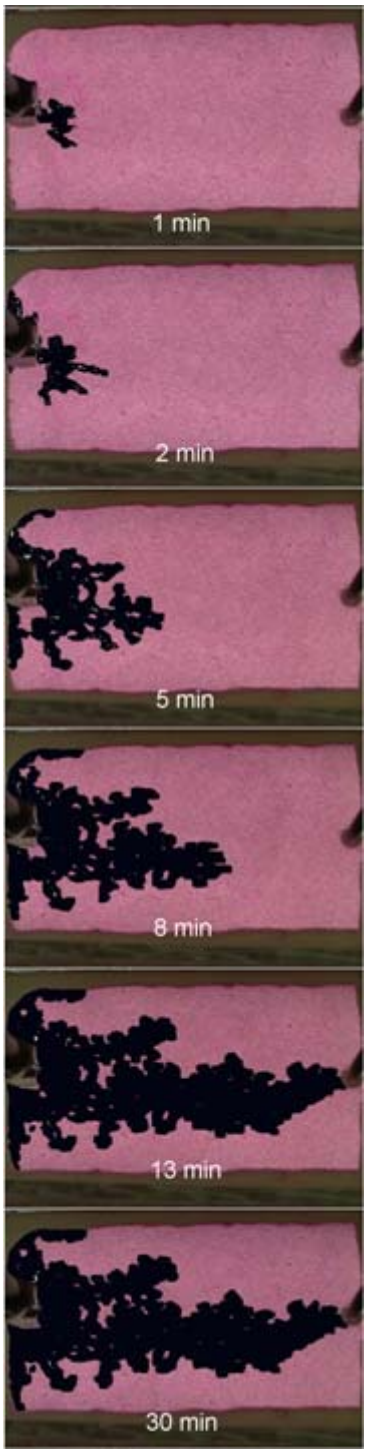

Fig. 4-4: Exp.#2, WW, Light Oil, US.

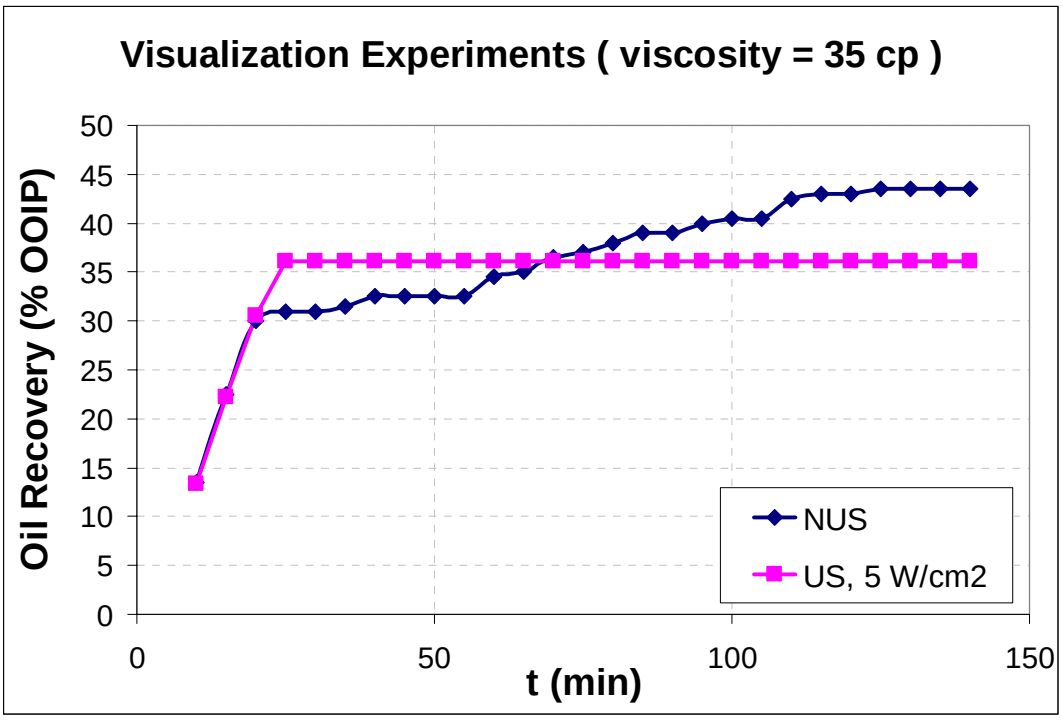

Fig. 4-5: Recovery curves of visualization experiments #1 and #2 versus time.

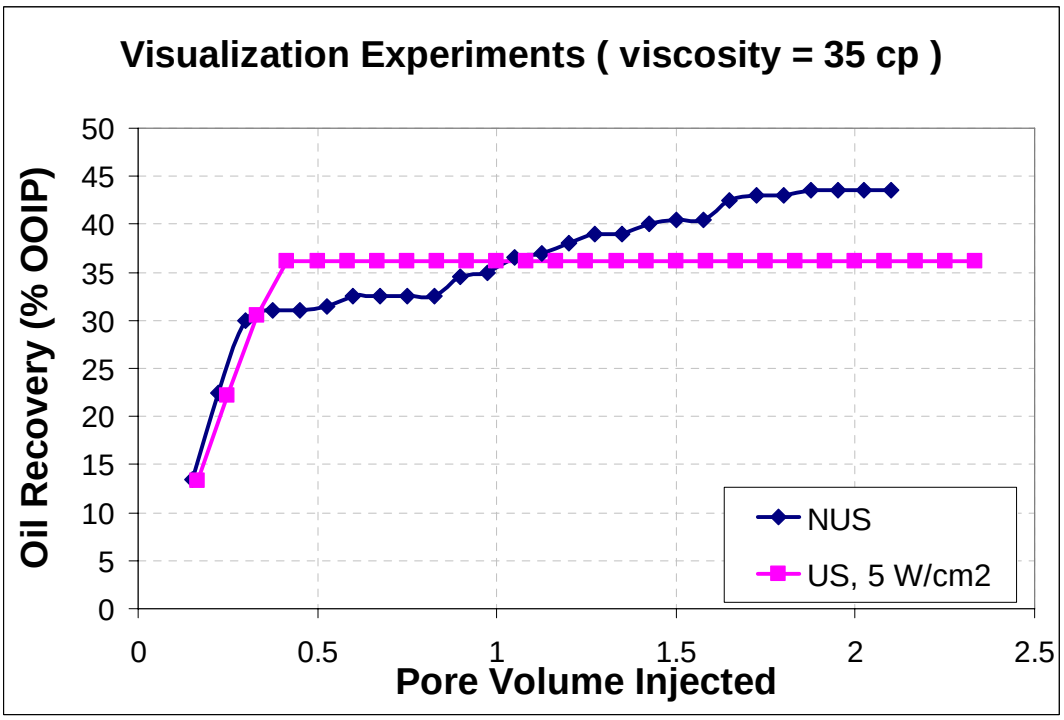

Fig. 4-6: Recovery curves of visualization experiments #1 & #2 versus injected pore volume.

Fig.4-7 shows the images of no-ultrasound experiment (experiment #3) for heavier oil (500 cp). The images of the identical case but with ultrasound (experiment #4) are given in **Fig. 4-8**. The patterns are more alike, but as similar to the previous cases, a more compact cluster with thicker and shorter fingers was obtained under ultrasound.

In **Figs. 4.9** and **4-10,** the recovery graphs of experiments #3 and #4 are given against time and injected pore volume, respectively. As in the case of light mineral oil experiments, we observed that water rapidly created a way to the producer in the ultrasound case. However, some amount of oil was produced after breakthrough unlike the previous case.

Table 4-3 shows the fractal dimension and swept area of these two experiments. Both the area swept and fractal dimensions are very similar and this is an indication of the reduced effect of ultrasound due to increasing oil viscosity. Higher ultimate recovery obtained for the ultrasonic case (**Figs. 4.9** and **4-10**), then, could be attributed to less residual oil in the swept region (more compact cluster).

Table 4-3: Pattern characteristics of experiments #3 and #4.

Experiment Number	Fractal Dimension	Swept Area (/total)
3	1.6779	0.3941
4	1.6974	0.3893

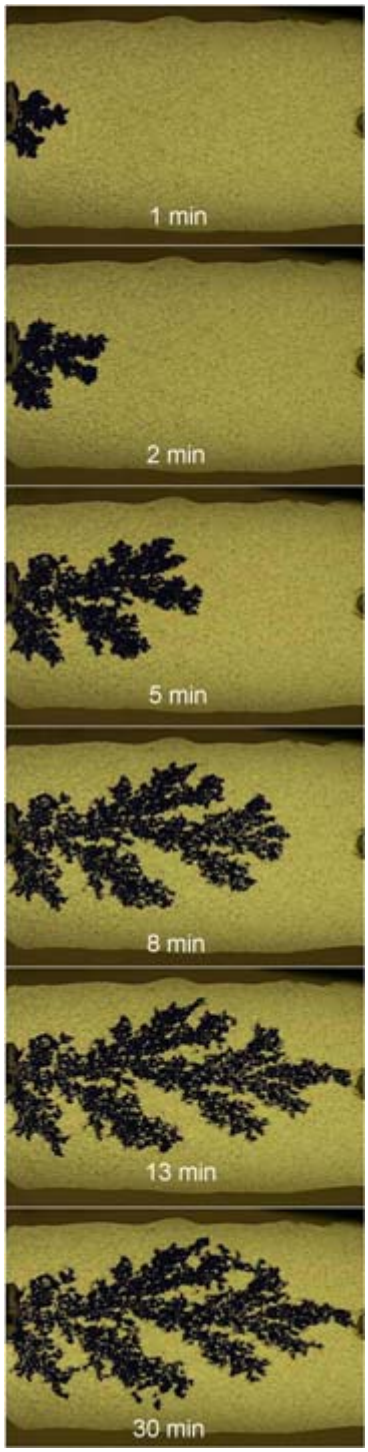

Fig. 4-7: Exp.#3, WW, Heavy Oil, NUS.

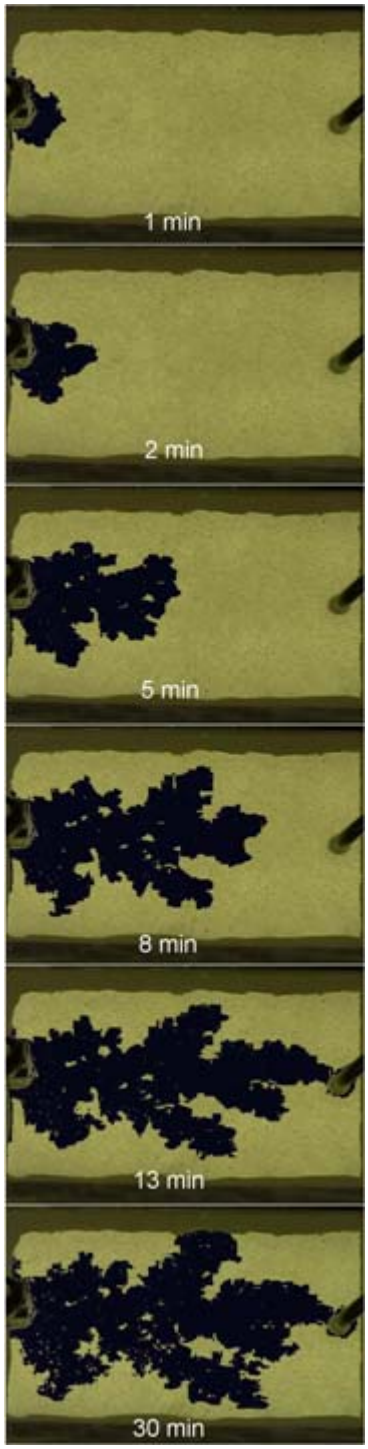

Fig. 4-8: Exp.#4,WW, Heavy Oil, US.

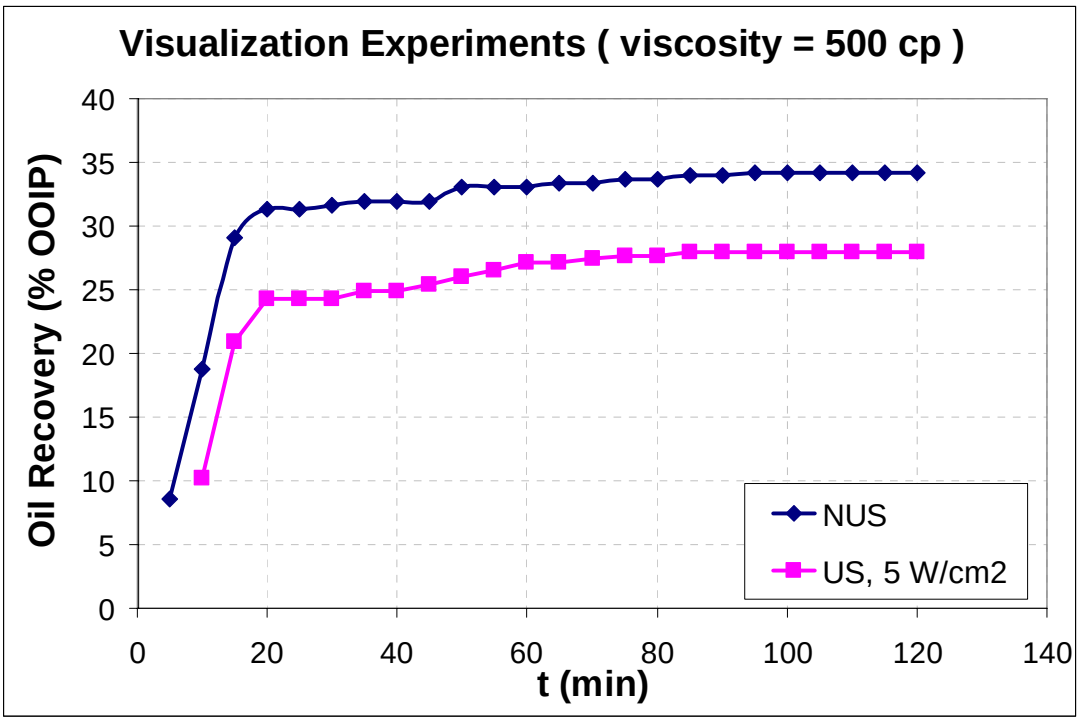

Fig. 4-9: Recovery curves of visualization experiments #3 and #4 versus time.

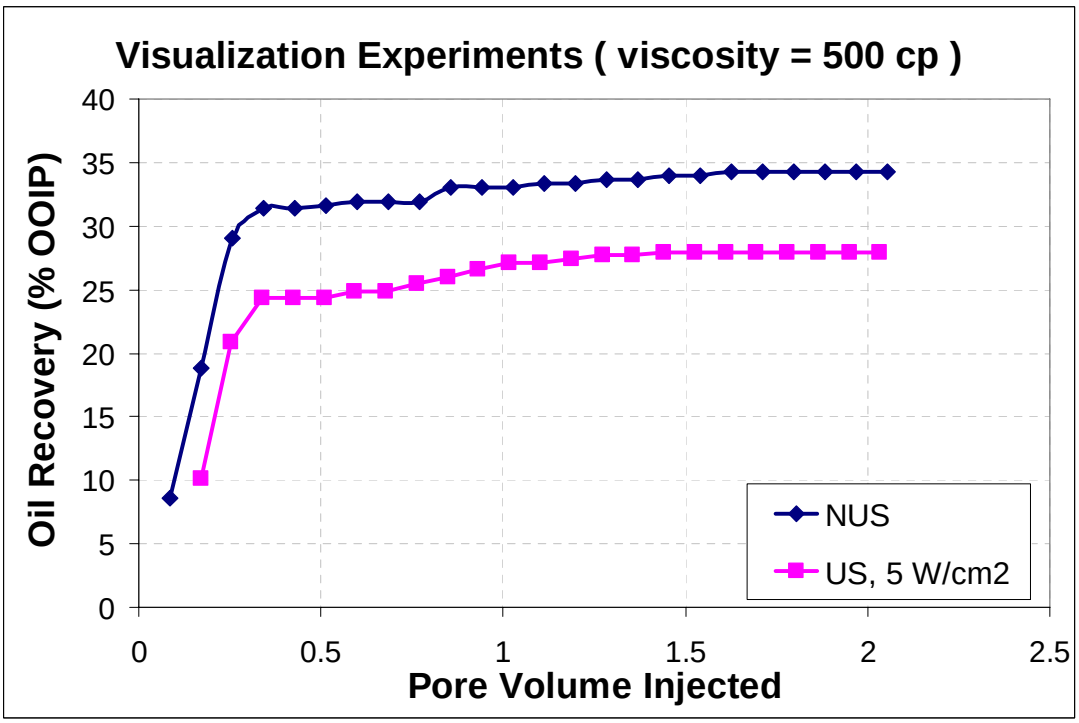

Fig. 4-10: Recovery curves of visualization experiments #3 & #4 versus injected pore volume.

Fig. 4-11 shows snapshots taken during experiment #5. This represents the oil-wet case without ultrasound. The images of the equivalent experiment with ultrasound are given in **Fig. 4-12**. None of the cases yielded a cluster and the water phase is more dispersed compared to the water-wet cases. In these experiments, water had more side fingers in the non-ultrasound experiment. In the non-ultrasound case, water spread more in the middle in different directions rather than towards the producer. Water movement toward the production end was quicker under ultrasonic radiation. The recovery curves versus time and also injected pore volume are shown in **Figs. 4-13** and **4-14**, respectively. As implied by these figures, the effect of ultrasonic waves on the recovery is more remarkable in the oil-wet case. Although the breakthrough times are closer to each other, the ultimate oil recovery is substantially higher when ultrasound was applied.

Characteristics of the displacement patterns for these cases are shown in **Table 4-4** below. No significant change in the fractal dimension of the final pattern was observed when compared the two cases. But, the ultrasound caused a better sweep as indicated by larger area swept and higher recovery.

Table 4-4: Pattern characteristics of experiments #5 and #6.

Experiment Number	Fractal Dimension	Swept Area (/total)
5	1.6305	0.3257
6	1.6574	0.3638

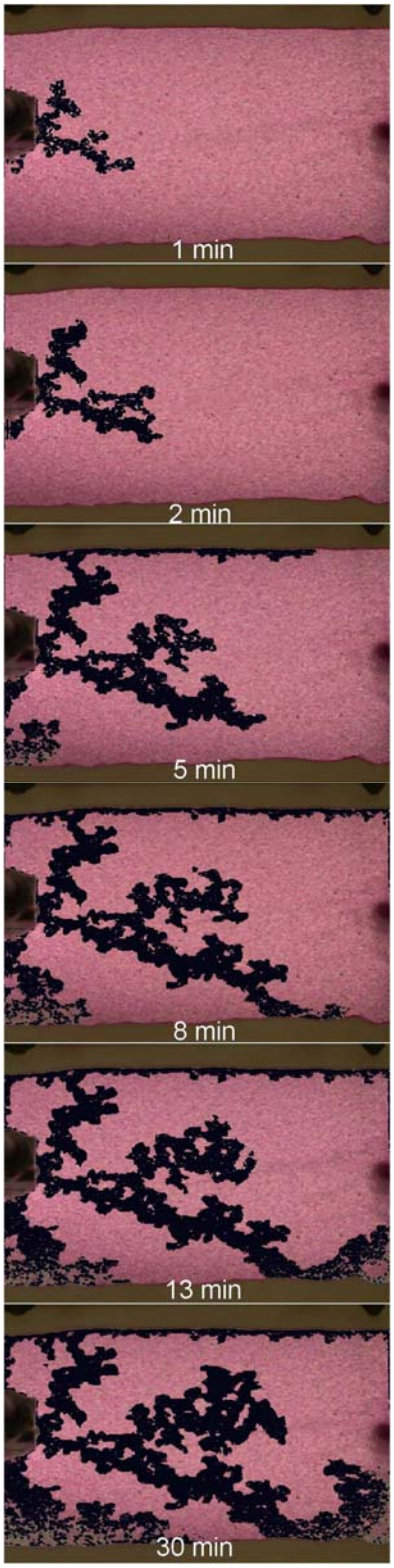

Fig. 4-11: Exp.#5, OW, Light Oil, NUS.

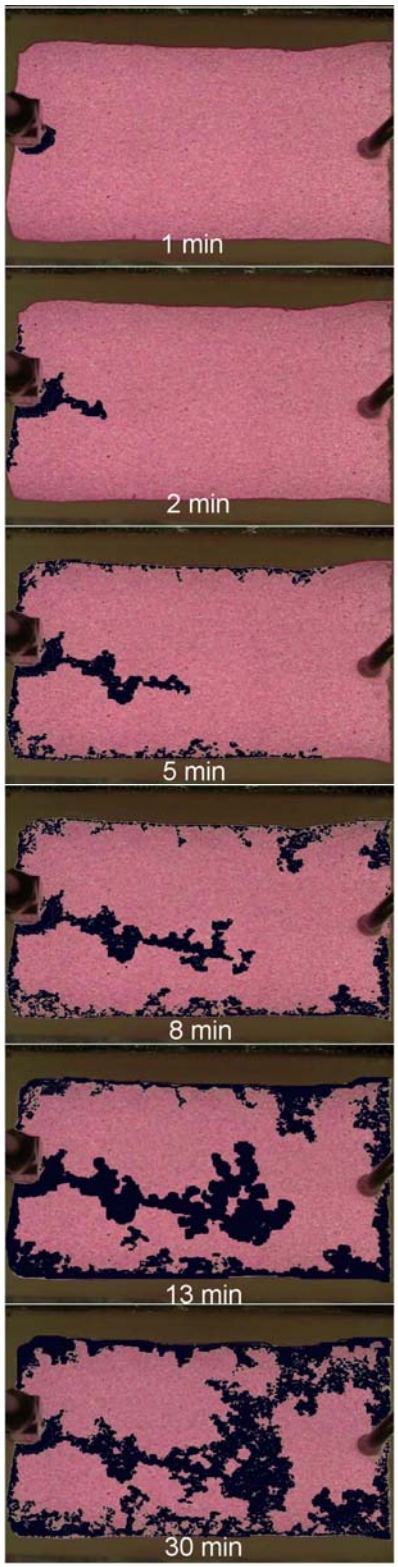

Fig. 4-12: Exp.#6, OW, Light Oil, US.

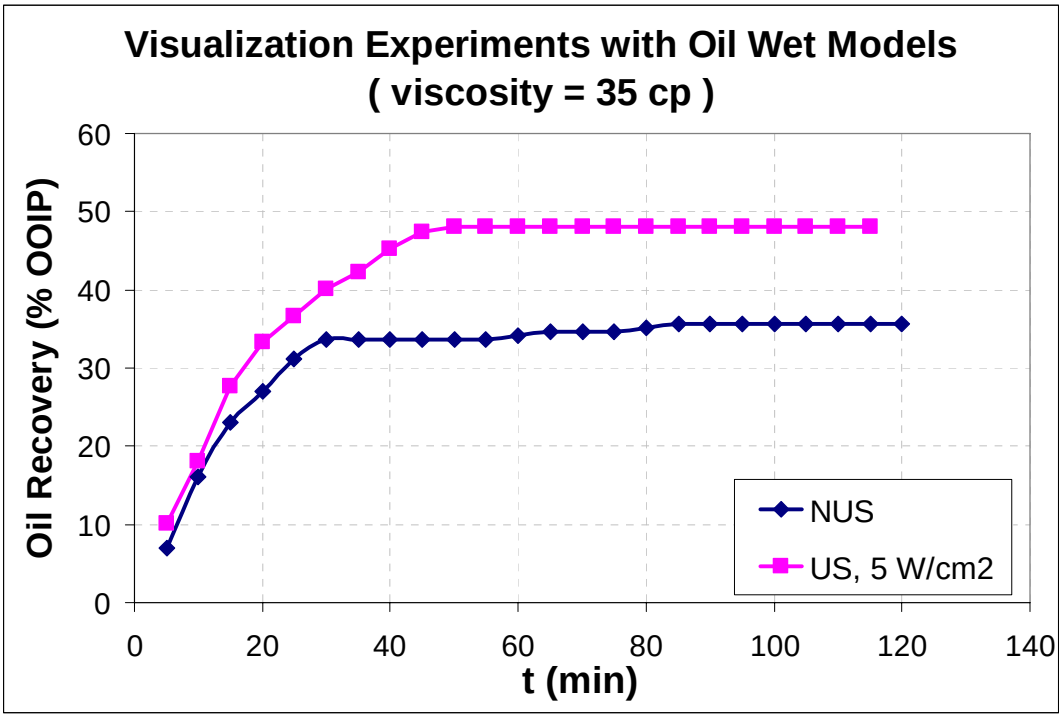

Fig. 4-13: Recovery curves of visualization experiments #5 and #6 versus time.

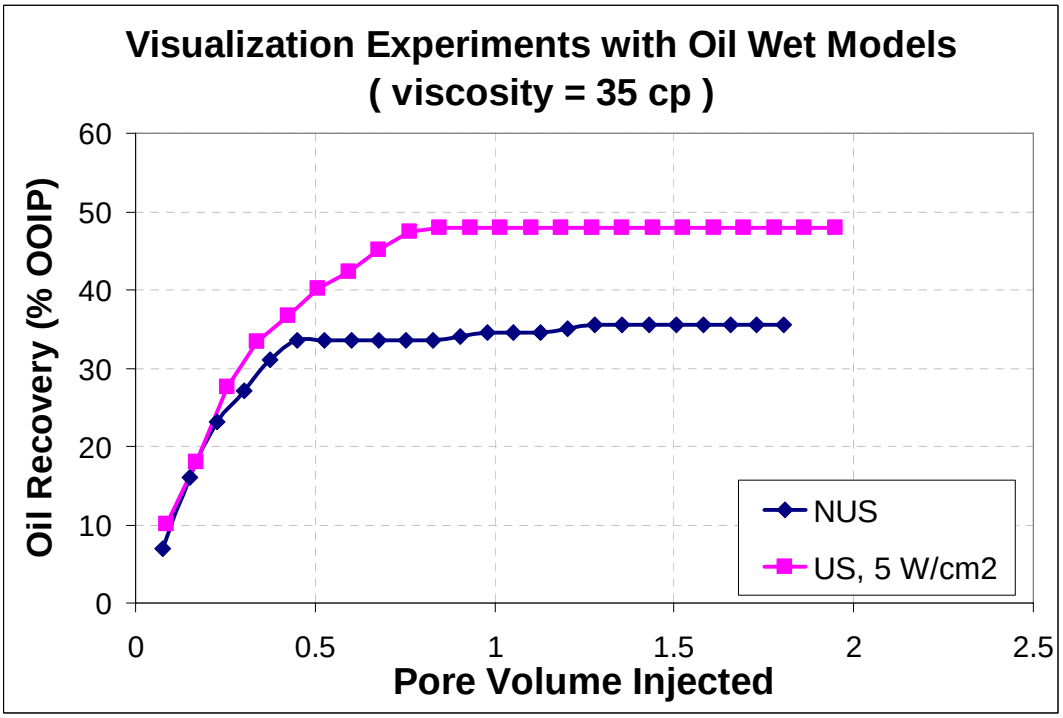

Fig. 4-14: Recovery curves of visualization experiments #5 & #6 versus injected pore volume.

Images of experiment #7 are shown in **Fig. 4-15**. In this experiment, the medium is oil wet and the viscosity of the oil which saturates the model is 500 cp. experiment #8 is the equivalent experiment with ultrasonic exposure whose images are shown in **Fig. 4-16**.

The recovery curves of experiments #7 and #8 versus time and injected pore volume are given in **Figs. 4-17** and **4-18**, respectively. In the ultrasonic case, one observes that production continues after breakthrough almost doubling the production by the non-ultrasonic case. This is opposite to the water-wet equivalent of the experiment (**Figs. 4-7 through 4-10**).

In contrast to experiments #5 and #6, no side branches were observed here. In much lower viscosity case, water had more tendency to flow through the edges due to water-wet nature of the sealing material.

The characteristics of the final pattern are listed in **Table 4-5**. The difference in the fractal dimension indicates that the ultrasonic case yielded smoother (less complex) displacement pattern (or fingers). The total area swept is, again, larger when ultrasound is applied.

Table 4-5: Pattern characteristics of experiments #7 and #8.

Experiment Number	Fractal Dimension	Swept Area (/total)
7	1.6302	0.2819
8	1.5181	0.3420

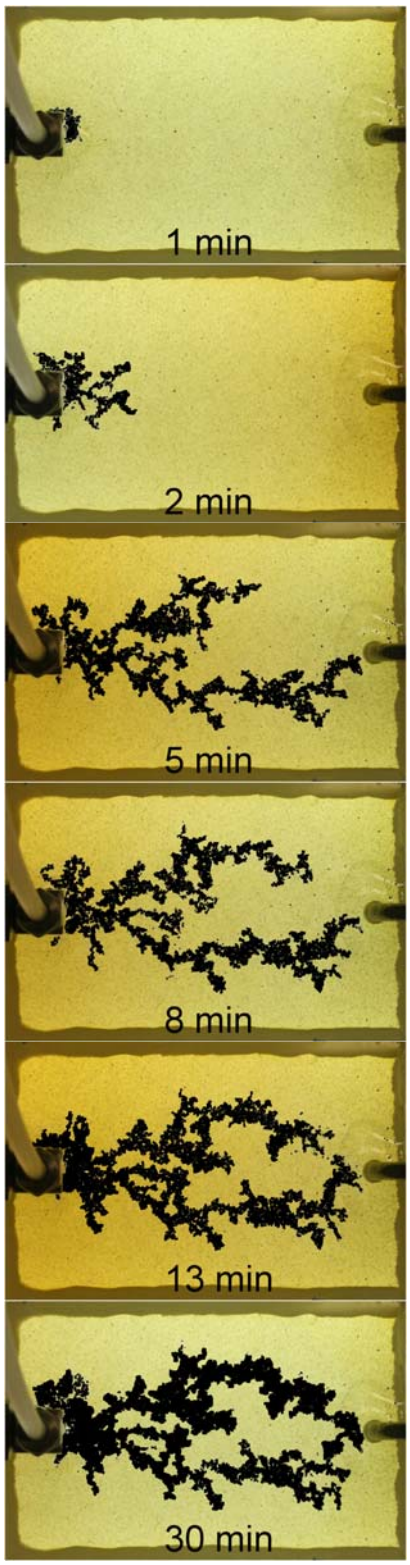

Fig. 4-15: Exp.#7, OW, Heavy Oil, NUS.

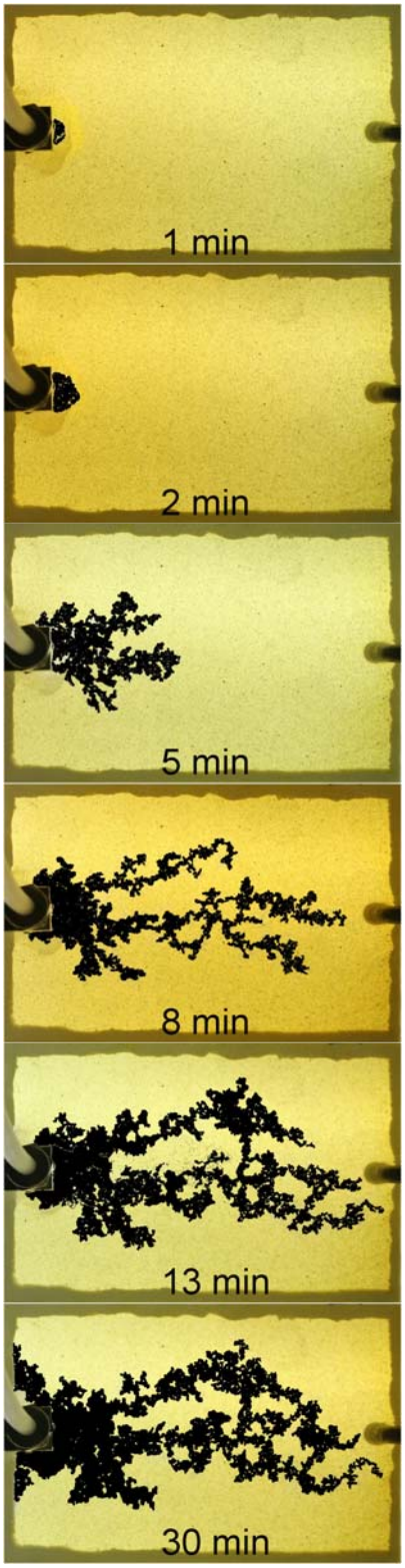

Fig. 4-16: Exp.#8, OW, Heavy Oil, US.

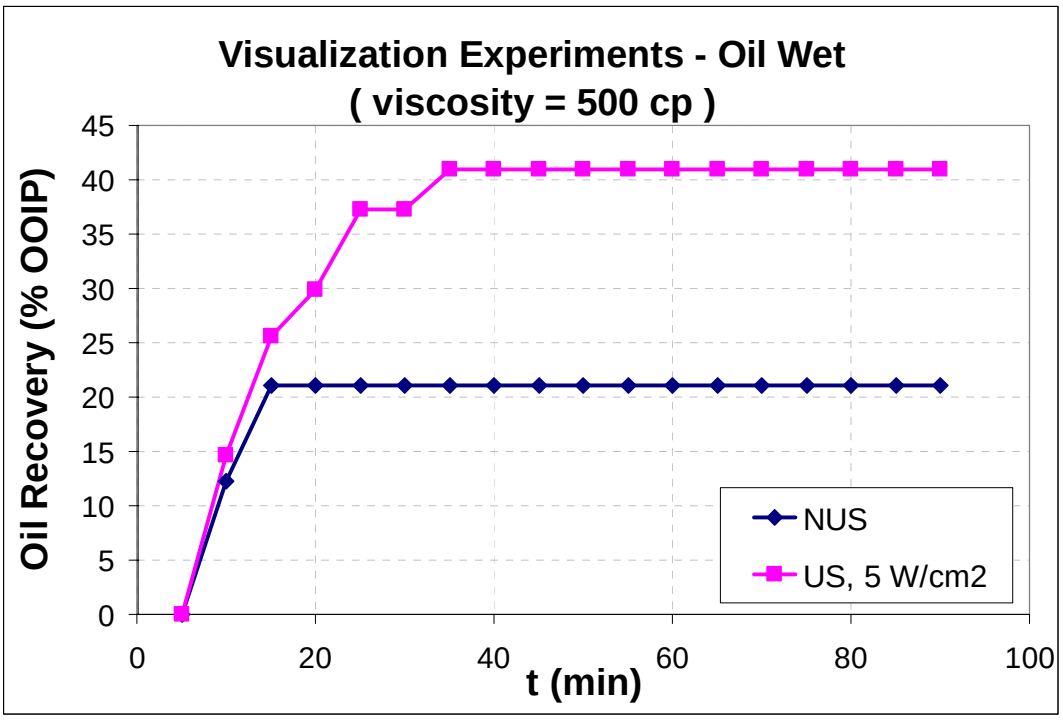

Fig. 4-17: Recovery curves of visualization experiments #7 and #8 versus time.

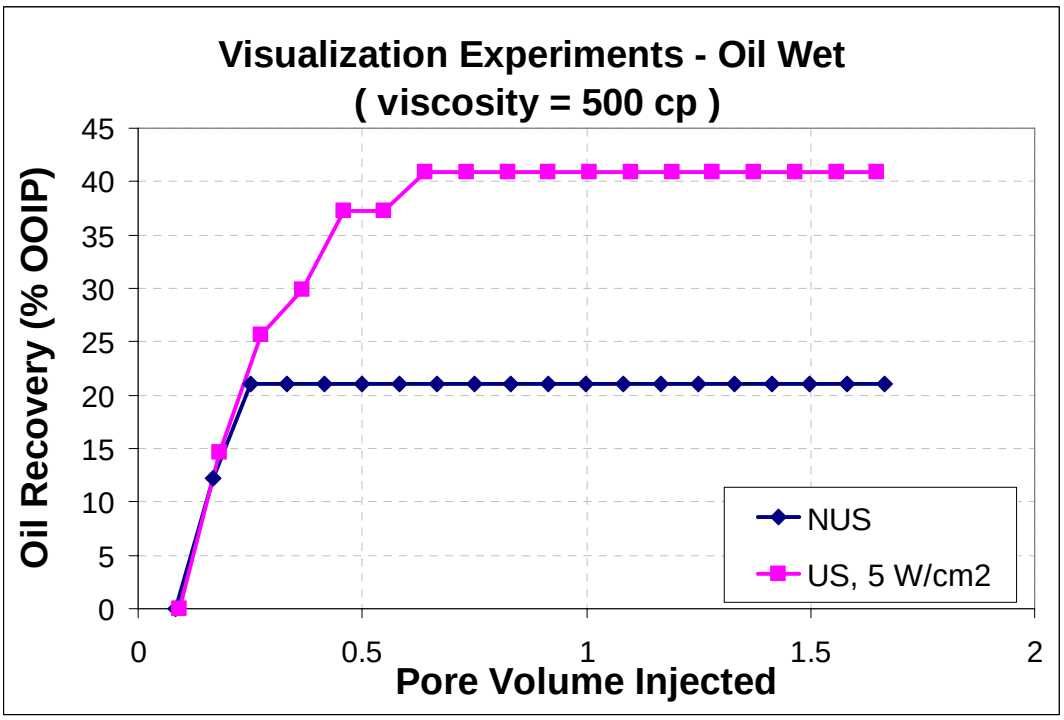

Fig. 4-18: Recovery curves of visualization experiments #7 & #8 versus injected pore volume.

Fig. 4-19 shows the images taken from experiment #9. The model in this experiment holds a small amount of initial water saturation. The medium is oil wet and 500 cp oil was used. **Fig. 4-20** is the equivalent experiment under ultrasonic energy. Although initial water amount is so low, we see that it affected the shape of the cluster significantly. Less branching to the sides is obvious. Small amount of moisture inside the model creates a path for injected water towards the outlet. In the ultrasonic case, the acoustic energy makes injected water to move more to the sides.

Figs. 4-21 and **4-22** are recovery graphs of experiments #9 and #10 versus time and injected pore volume, respectively. Breakthrough occurs a little bit later for the ultrasonic case but its final recovery is higher.

Table 4-6 contains the image processing results for these two cases. More branching in the ultrasonic case yielded higher fractal dimension but the area swept and oil recovered are still higher in the ultrasonic case.

Table 4-6: Pattern characteristics of experiments #9 and #10.

Experiment Number	Fractal Dimension	Swept Area (/total)
9	1.4873	0.1671
10	1.5122	0.1947

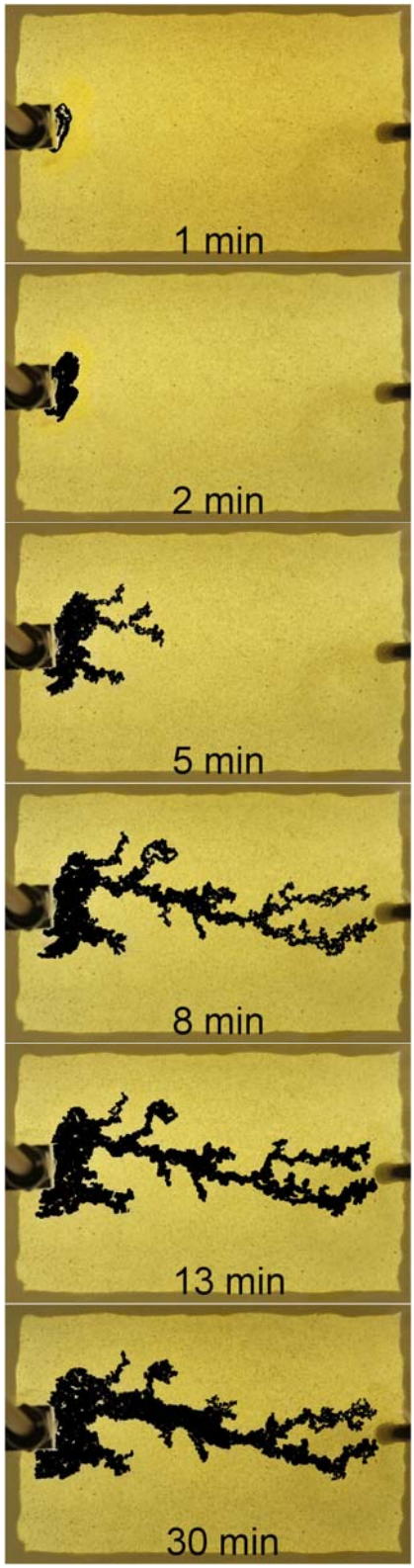

Fig. 4-19: Exp.#9, OW, S_{wi}, Heavy, NUS.

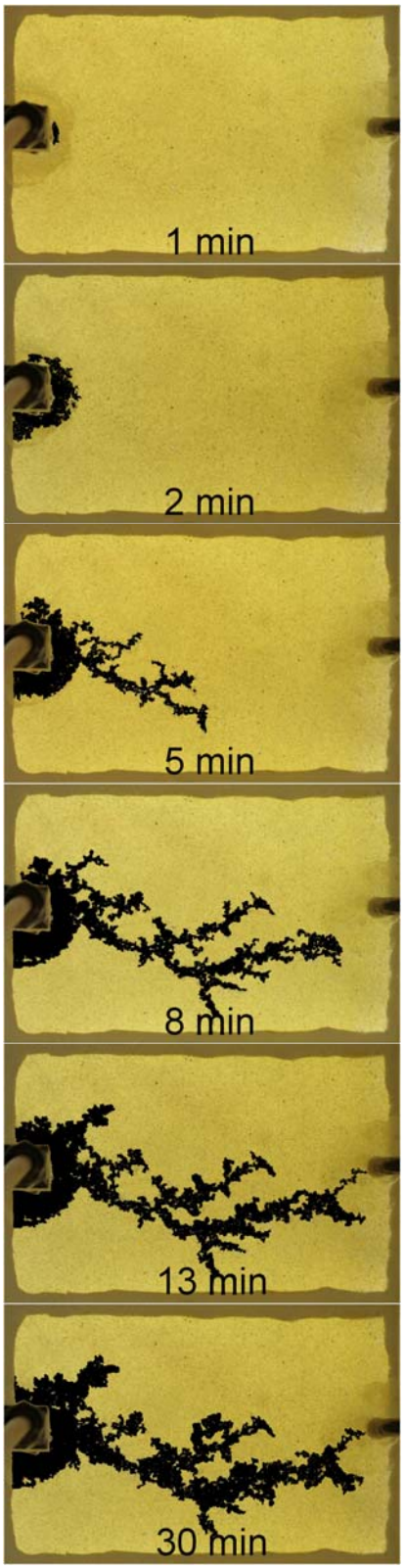

Fig. 4-20: Exp.#10, OW,S_{wi}, Heavy, US.

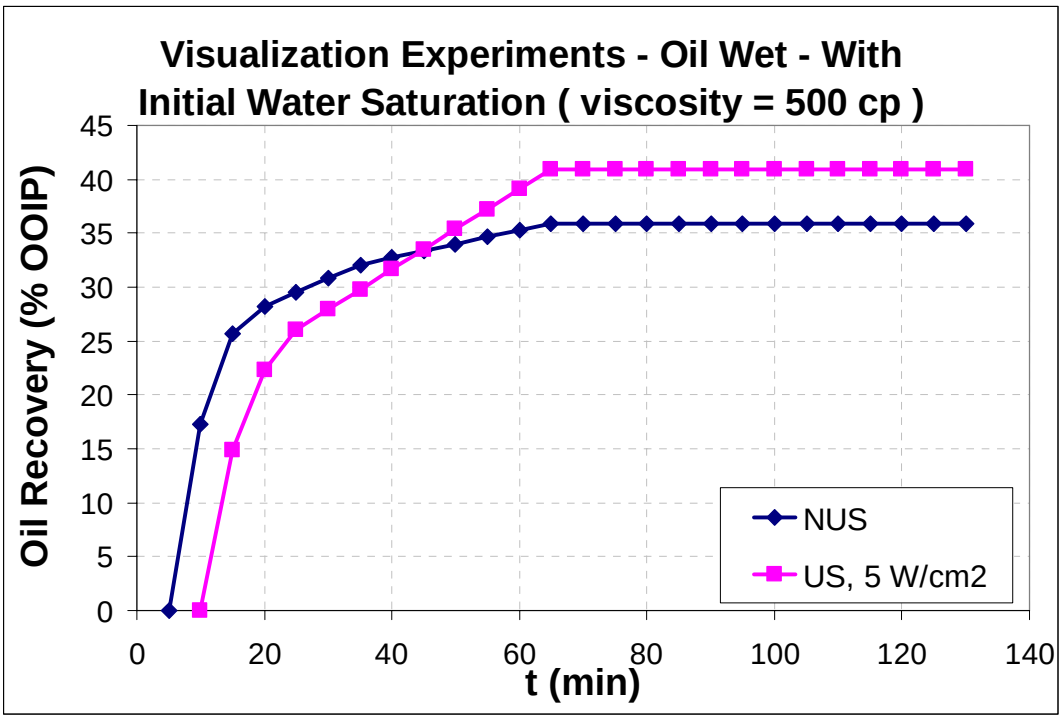

Fig. 4-21: Recovery curves of visualization experiments #9 and #10 versus time.

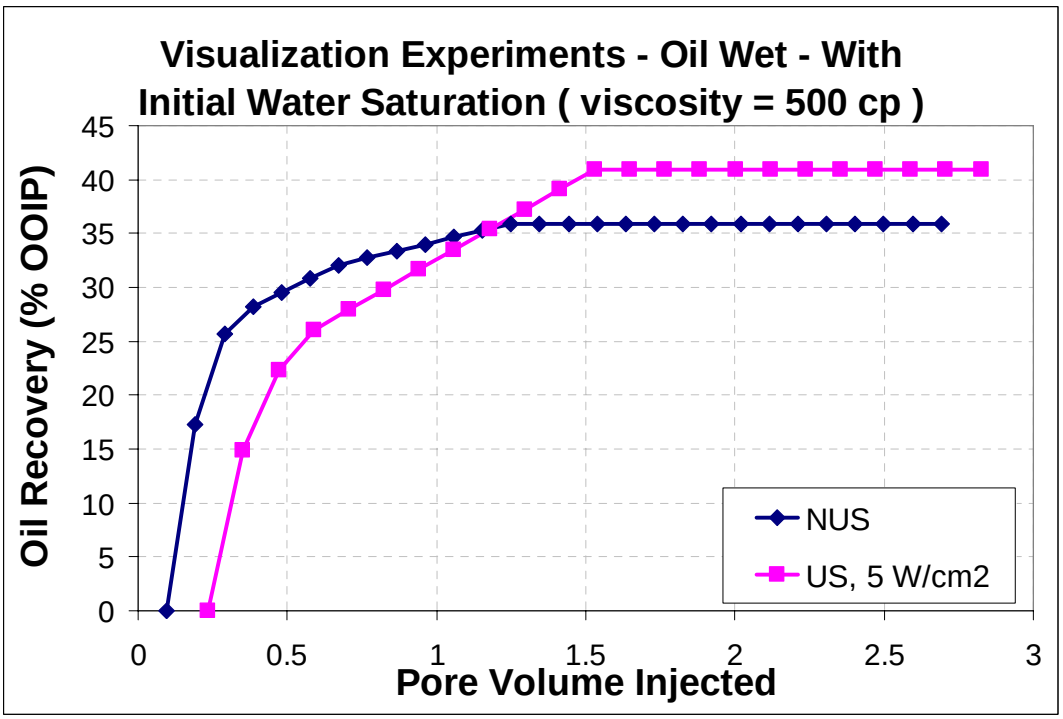

Fig. 4-22: Recovery curves of visualization experiments #9 & #10 versus injected pore volume.

4.4 Bigger 5-spot Models

As seen in **Figs. 4-11 and 4-12**, water tends to avoid dispersing throughout the porous media and tries to find the easiest path to reach the outlet in oil wet samples. Hence, there are side branches going from sides, adjacent to epoxy, towards the production point. To overcome this problem, we tried a vast number of experiments using 5-spot models where the injection point was located at the center. Each model consists of two attached square acrylic sheets with 20-cm edges holding glass beads inside. **Fig. 4-23** shows a model of this kind. There is an injection port at the center and four production ports at the corners and the model is considerably larger than the previous one-injection/one-production point models.

Note that for the ultrasound cases (**Figs. 4-28 to 4.32**); ultrasonic horn is located above the model (i.e. outside of model and at the same level inside water; not at top of model) as it is shown in **Fig. 4-23.** The same place for horn was chosen for all ultrasound cases in the small models shown in **Fig. 4-4**, **Fig. 4-8**, **Fig. 4-12**, **Fig. 4-16** and **Fig. 4-20**.

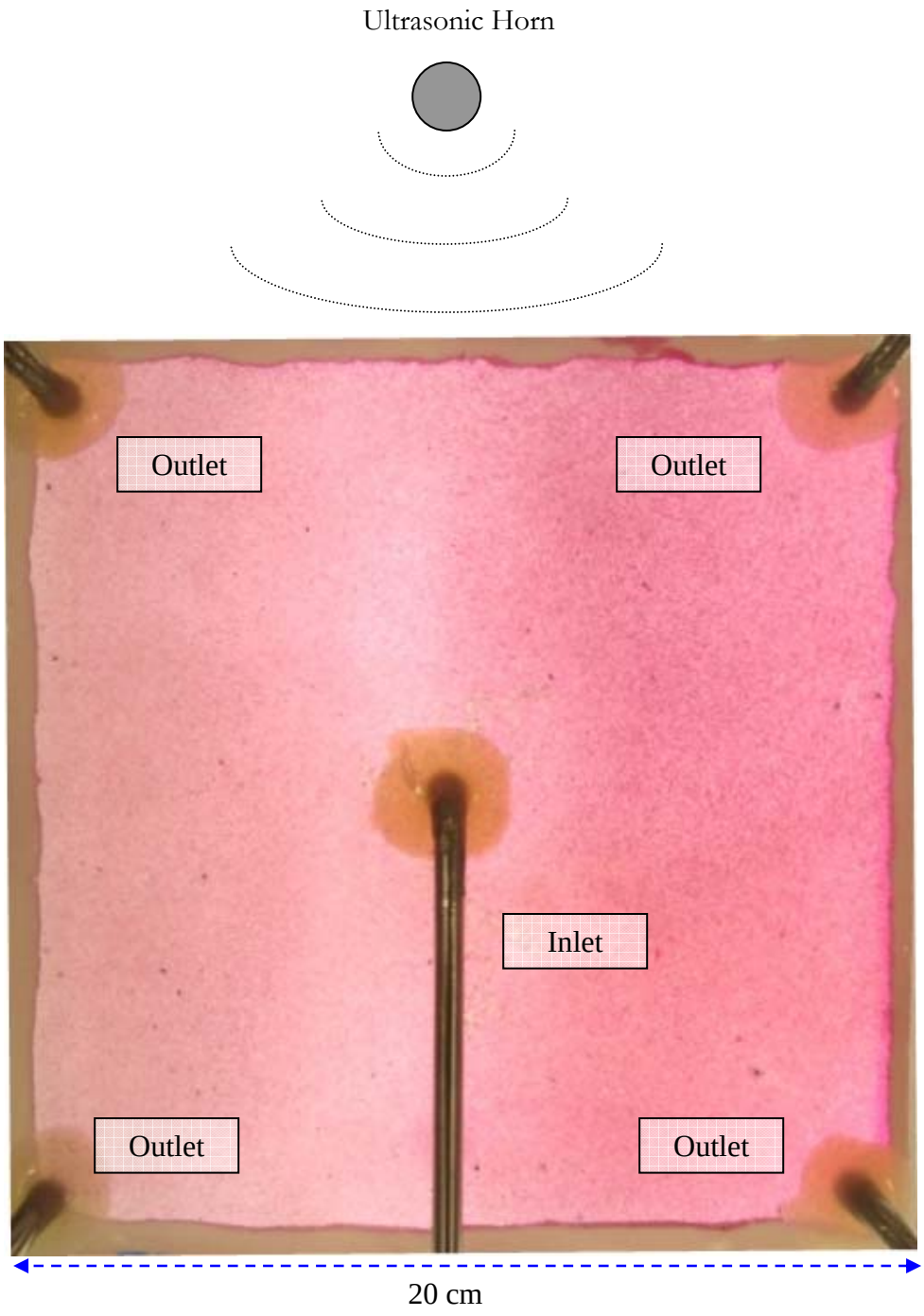

Fig.4.23: 5-spot model (top view).

All experiments with these models were oil-wet saturated with light (35 cp) mineral oil which was colored using red dye. Snapshots of twelve experiment of this type are shown in **Figs. 4-24 to 4-35.** The images shown in these figures were processed in such a way that the displacing phase (water) was represented by black color to obtain a good quality contrast. Injection rate is given in each figure caption.

Four non-ultrasonic cases were run initially at the rate of 10 ml/hr. The first three cases were conducted outside of the water bath (**Figs. 4-24, 25, and 26**). The last case was run inside the bath to compare the images with the ultrasonic case. This way, both ultrasonic and non-ultrasonic images were acquired while the model was immersed into water and any possible changes in the image during processing because of water effect were avoided. The first three cases showed a degree of branching; single (8^{th} min snapshot of **Fig. 4-24**) or multiple (20^{th} min snapshot of **Fig. 4-26**). This could be attributed to non-uniform characteristic of the sand pack. Perfect preparation of this size of sand pack model, i.e., uniform sand distribution, may not be easily possible. The very last model seen in **Fig. 4-27** turned out to be quite uniform indicated by very minimal branching.

Similarly, four ultrasonic experiments were run to check the reproducibility. The ultrasonic source was placed on top of the model that corresponds to the point just above the upper side of it. Therefore, more branching and/or progress of the front towards to the opposite side (lower side of the model) were observed (**Figs. 4-28, 29, and 30**). Based on the experience gained through these three experiments, the location of the source was changed by moving the horn back and forth. Hence, the

mechanical effect due to vibration causing energy to force the injected fluid towards to the opposite direction of the ultrasonic source was minimized (**Fig. 4-31**).

When the two equivalent cases given in **Figs. 4-27** and **4-31** were compared, more branching and tendency to flow to the production ends were observed in the ultrasonic case (**Fig. 4-31**). The area swept is larger for the ultrasonic case as well.

At a lower injection rate (5 ml/hr), totally different behavior was observed. The ultrasonic pattern is more compact (**Fig. 4-32**) compared to the higher rate case (**Fig. 4-31**). To compare the ultrasonic case with the non-ultrasonic one, three experiments were conducted as given in **Figs. 4-33, 34, and 35.** All three cases showed similar displacement patterns which were less compact and more branched out compared to the ultrasonic case (**Fig. 4-32**).

Based on these observations one can state that the effect of ultrasonic waves on the pattern of oil displacement by water injection is dependent on injection rate. At lower rates, i.e., lower capillary number, ultrasonic effect is more pronounced. This implies that the capillary forces become more dominant at lower rates and the ultrasonic energy affects the capillary characteristics. In other words, ultrasonic energy has more influence on the capillary properties rather than the viscous ones.

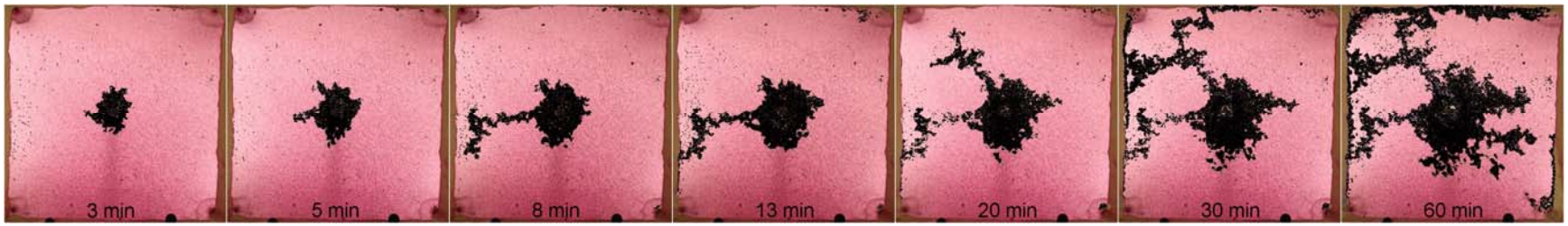

Fig.4-24: Non-Ultrasonic, Injection Rate = 10 ml/hr.

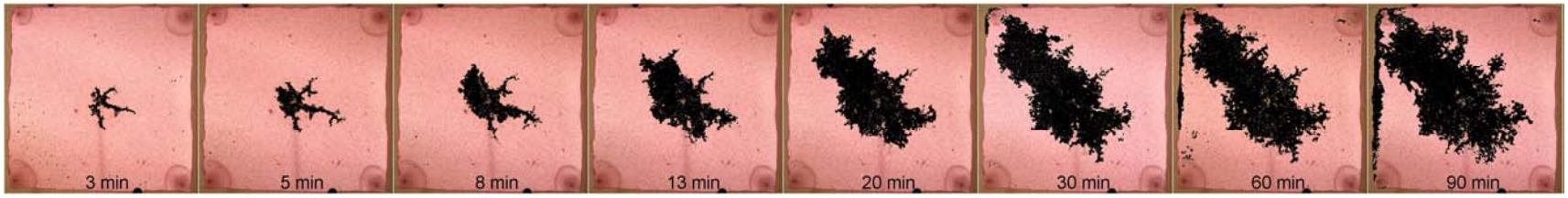

Fig.4-25: Non-Ultrasonic, Injection Rate = 10 ml/hr, (smaller valves were used in the injection system).

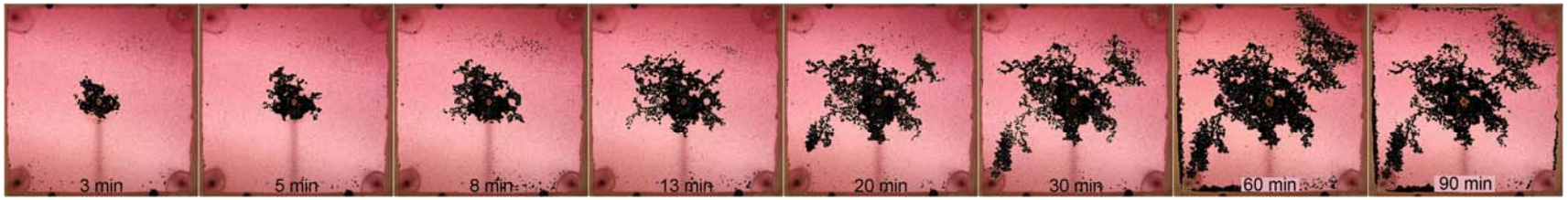

Fig.4-26: Non-Ultrasonic, Injection Rate = 10 ml/hr.

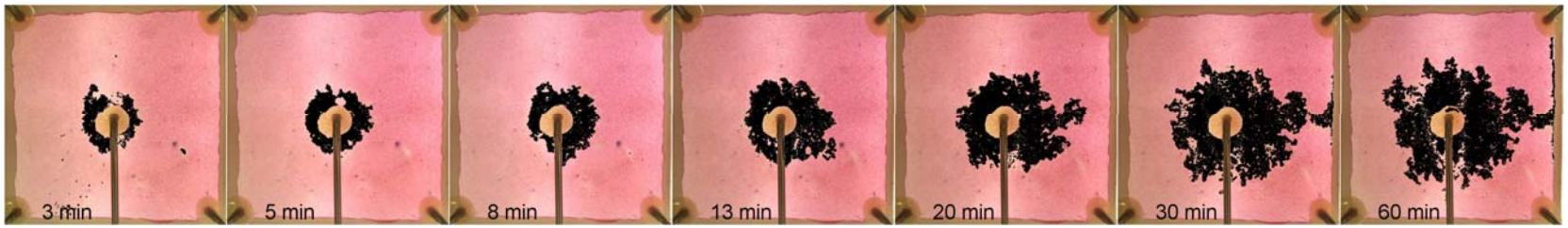

Fig.4-27: Non-Ultrasonic, Injection Rate = 10 ml/hr (experiment was conducted inside the water bath).

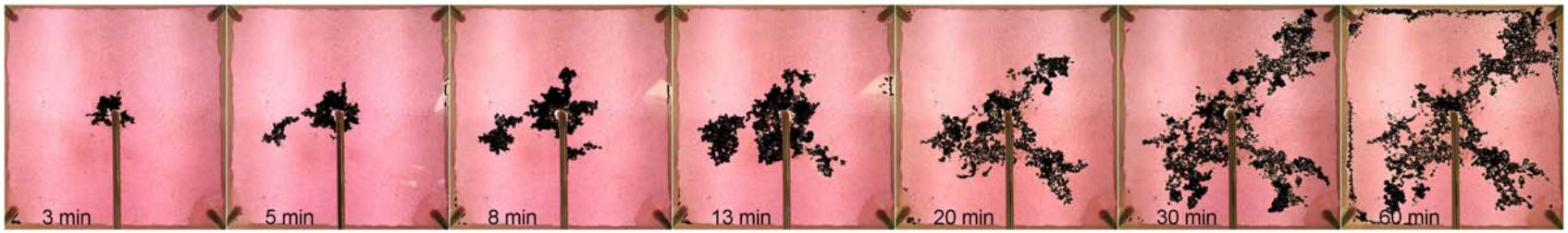

Fig.4-28: Ultrasonic, Injection Rate = 10 ml/hr.

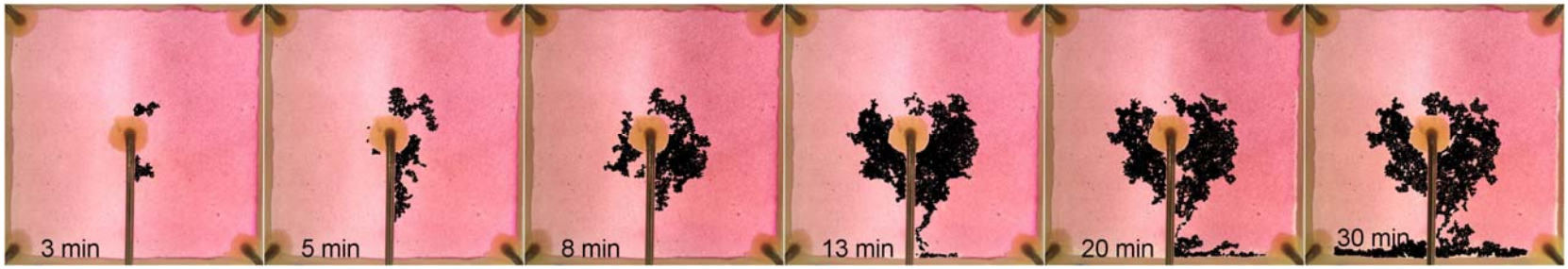

Fig.4-29: Ultrasonic, Injection Rate = 10 ml/hr.

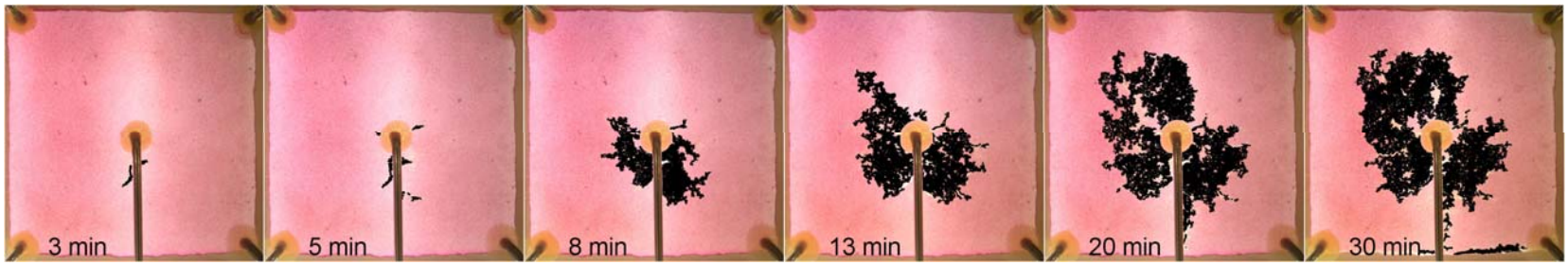

Fig.4-30: Ultrasonic, Injection Rate = 10 ml/hr.

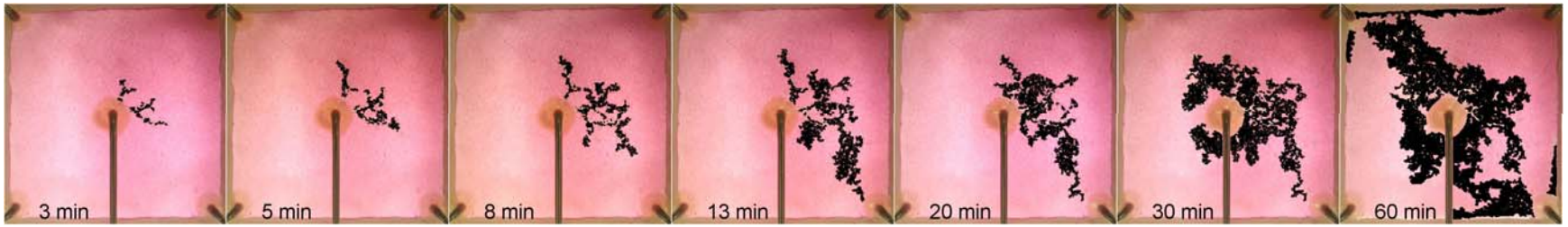

Fig.4-31: Ultrasonic, Injection Rate = 10 ml/hr.

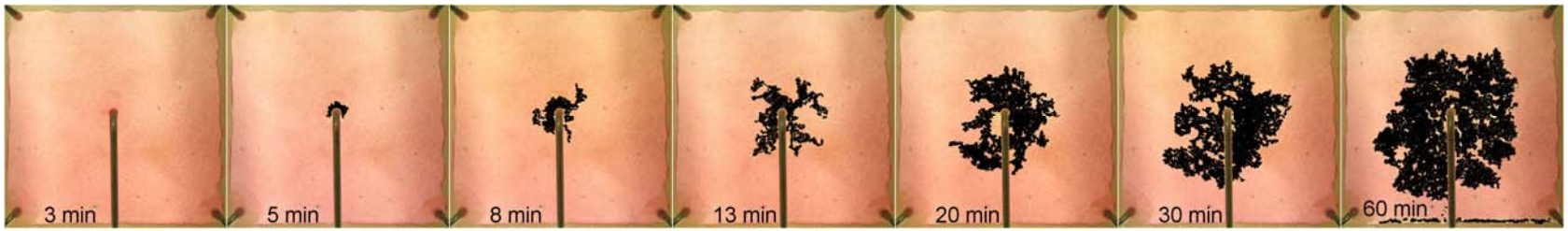

Fig.4-32: Ultrasonic, Injection Rate = 5 ml/hr.

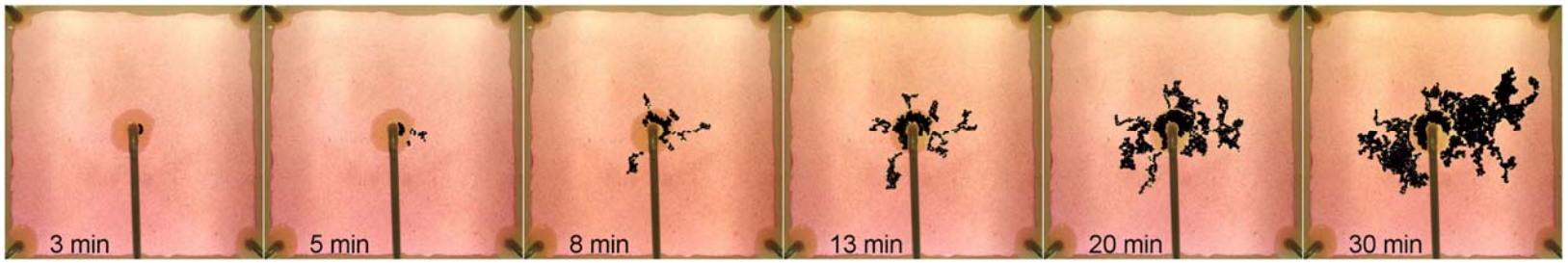

Fig.4-33: Non-Ultrasonic, Injection Rate = 5 ml/hr.

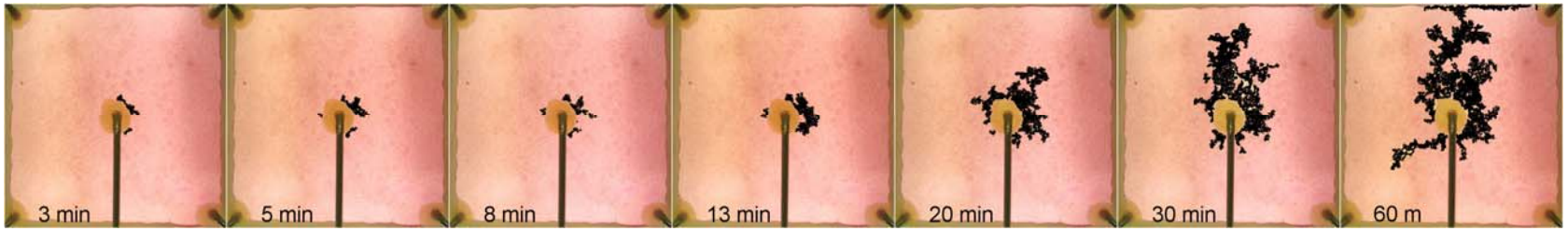

Fig.4-34: Non-Ultrasonic, Injection Rate = 5 ml/hr.

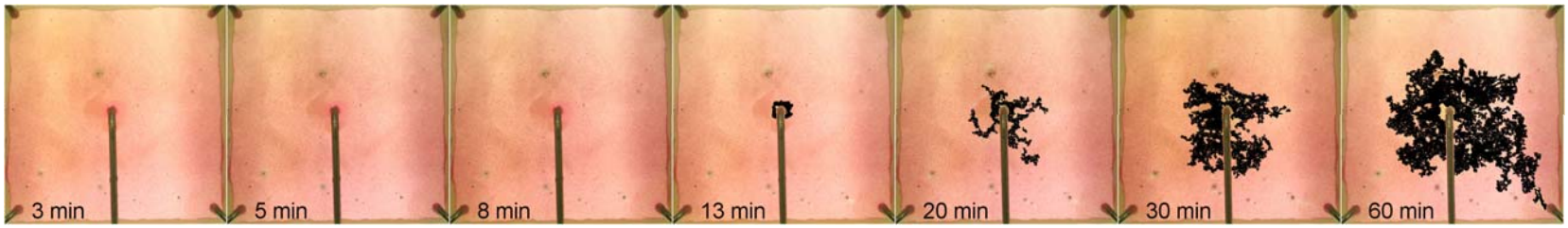

Fig.4-35: Non-Ultrasonic, Injection Rate = 5 ml/hr.

4.5 Conclusions

Visualization experiments on water-wet models showed that under ultrasonic radiation more compact clusters with shorter and thicker fingers were obtained. No oil was produced after breakthrough when ultrasound energy was applied in the water-wet/light oil case. The situation is different in case of oil-wet samples. More oil was produced after breakthrough when ultrasound was applied. For the oil wet cases, no compact clusters are formed as in the water wet cases. When an oil wet model is saturated with light mineral oil, water tends to find a preferential path and many side branches especially through the edges of the model form. However, when it comes to higher viscosities, the water branches are less free to move to all directions and get a more straight shape towards the outlet though there is still no compact cluster forming.

Initial water saturation in oil-wet models provides a small amount of liberated moisture which helps the injected water going more straight towards the end point.

The observations from 5-spot models show that, at higher rates of injection, the ultrasonic energy deforms the uniformity of the pattern which would have formed without acoustic waves. At lower rates, however, it improves the sweep efficiency resulting in more compact cluster. In other words, the effect of ultrasonic energy is more pronounced at lower rates. This is consistent with the observations reported before (Hamida 2006; Hamida and Babadagli 2005c, 2007a, 2008b).

CHAPTER 5

MICRO-MODEL VISUAL STUDIES

Visualization with 2-D glass bead models gives us a general insight into immiscible displacement of oil by water. But to understand the process at pore scale, micro-model studies are needed. For this purpose, a glass etched micro-model was built at NanoFab facilities at the University of Alberta. A series of experiments were performed on this model to capture the pore-scale physics of the displacement process under ultrasonic waves.

5.1 Micro-model Preparation

5.1.1 Fabrication

Microfluidic devices are generally two dimensional microchips enclosing small volumes and are usually used to study the fluid behavior at micro scale. In petroleum reservoir studies, micro-models are employed to represent the porous media. To produce a micro-model, one first designs the pattern and makes a photomask holding that design which is needed to etch silicon or glass. Our model is a glass etched model and its fabrication consists of a few steps as detailed below (Morin 2001; Tai 2005):

a. Photomask Design: The design is done using L-Edit software. (as will be discussed in the next section).

b. Photomask Manufacturing: A DWL 200 pattern generator creates the mask by mounting chrome on a 5" x 5" piece of glass.

c. Glass Substrate Cleaning: Glass substrate is the base of micro-model where pattern and the whole model will be etched on it. Because the work is done at nano scale, a tiny particle could cause a great damage to model so the substrate should be very clean and manufacturing process is also done in a specially designed clean room. To prevent any contamination on the substrate, it is cleaned by Piranha which is a 3:1 mixture of Sulphuric Acid (H_2SO_4) and Hydrogen Peroxide (H_2O_2)

d. Sputtering: Thin films of chrome and gold are deposited on the glass substrate through surface bombardment of the target material (chrome or gold) by energetic particles (usually ions of an inert gas like argon) in a reaction chamber.

e. Lithography: (1) First, a layer of Photoresist is applied by spinning to the model and covers the metal films, (2) then it is baked on a hot plate for evaporating the solvent (which made the photoresist liquid) and also enhancing the adhesion of resist to the wafer. Then the mask is aligned to the substrate and exposed to the ultra violet (UV) light. Clear parts on the mask (not covered by chrome) will let the UV light pass through the mask and expose the Photoresist. The UV light turns the photoactive compound to a dissolution enhancer so the exposed areas of resist on the substrate will

be removed when it is developed in sodium hydroxide solution as a developer.

f. Masking Layer Etching: The substrate is immersed in gold and chrome etchants respectively which results in wet etching of gold and chrome layers in open areas whose Photoresist is already taken off.

g. Stripping Photoresist: The remaining resist on the substrate is removed by acetone and isopropyl alcohol.

h. Glass Etching: Hydrofluoric acid (HF) solution is used to etch glass in areas uncovered with Photoresist, gold and chrome. To avoid damaging the model, backside of substrate is first covered with an adhesive plastic tape.

i. Device Substrate Stripping: The substrate is submerged into a gold etch bath, then rinsed with water and dried with nitrogen and then submerged into chrome etchant. Finally, it is cleaned in a 2:1 Piranha mixture.

j. Drilling Access Ports: Input and output ports to the microfluidic network are drilled. In our micro-model there are four ports drilled on the other glass substrate which is not etched.

k. Fusion Bonding: A Piranha cleaning is needed for both pieces of glass and then they are ready for bonding. Dry substrate is placed on a wafer mounter and a layer of tape is placed on one side of it. The device is then put inside a High Pressure Cleaning Station which washes it again to ensure it is totally clean. When both of substrates are ready, their bare surfaces are put together and after alignment bonding starts by applying a slight pressure which attaches them fairly well but to make this bonding

permanent an annealing process is needed in which the device is placed inside a Thermolyne Box Furnace. This furnace heats up the device, keeps the temperature constant and then cools it down following a controlled program. And finally makes a perfect bonding.

A schematic diagram of important steps of fabrication is shown in **Fig. 5-1**.

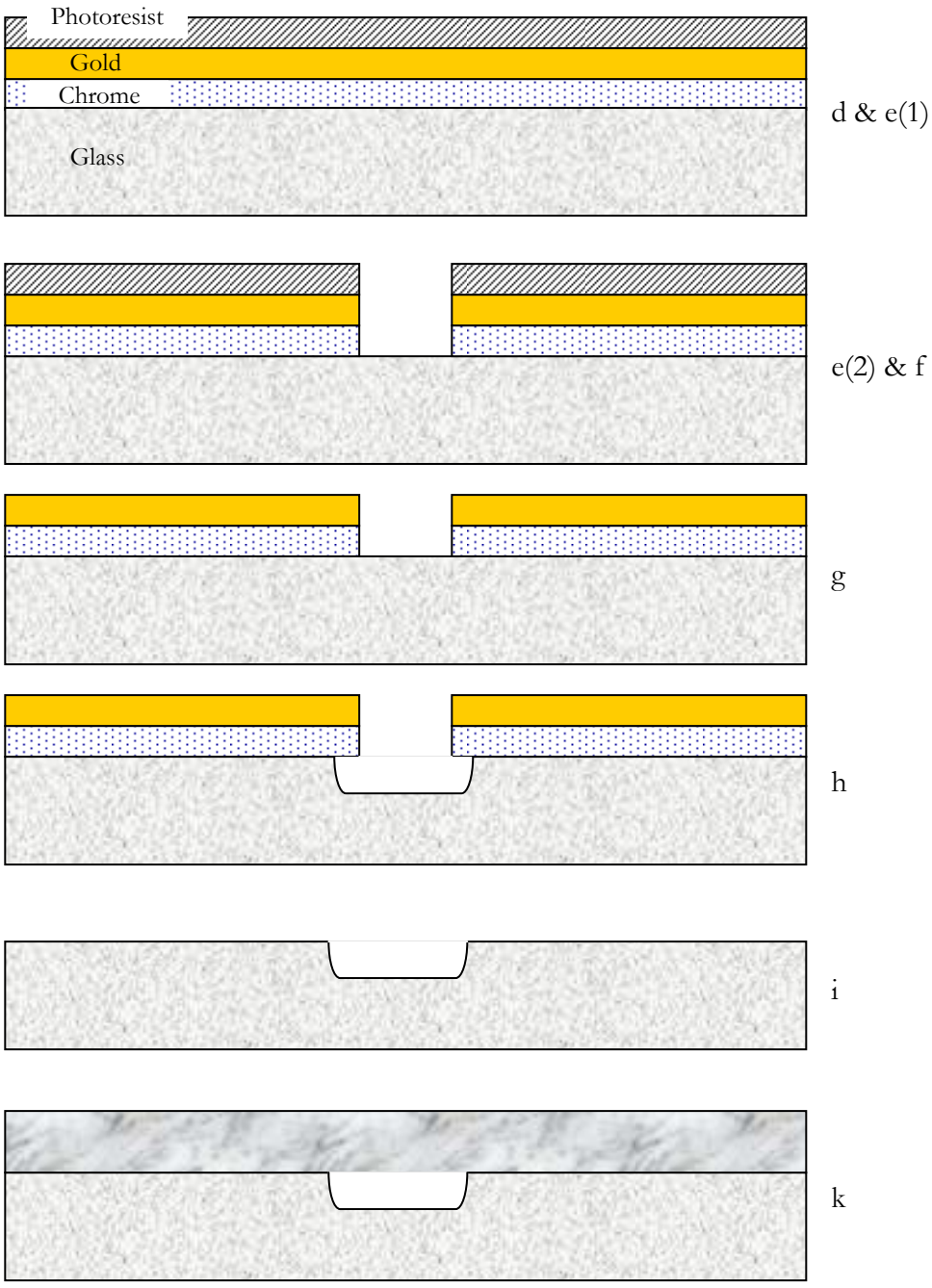

Fig. 5-1: Schematic diagram of micro-model fabrication steps.

5.1.2 Micro-model Specifications

We designed a simple homogenous model consisting of circles of around 40 micron diameter as grains and empty space among them as pores. **Fig. 5-2** shows the glass substrate of micro-model from top. **Fig. 5-3** shows the design of micro-model.

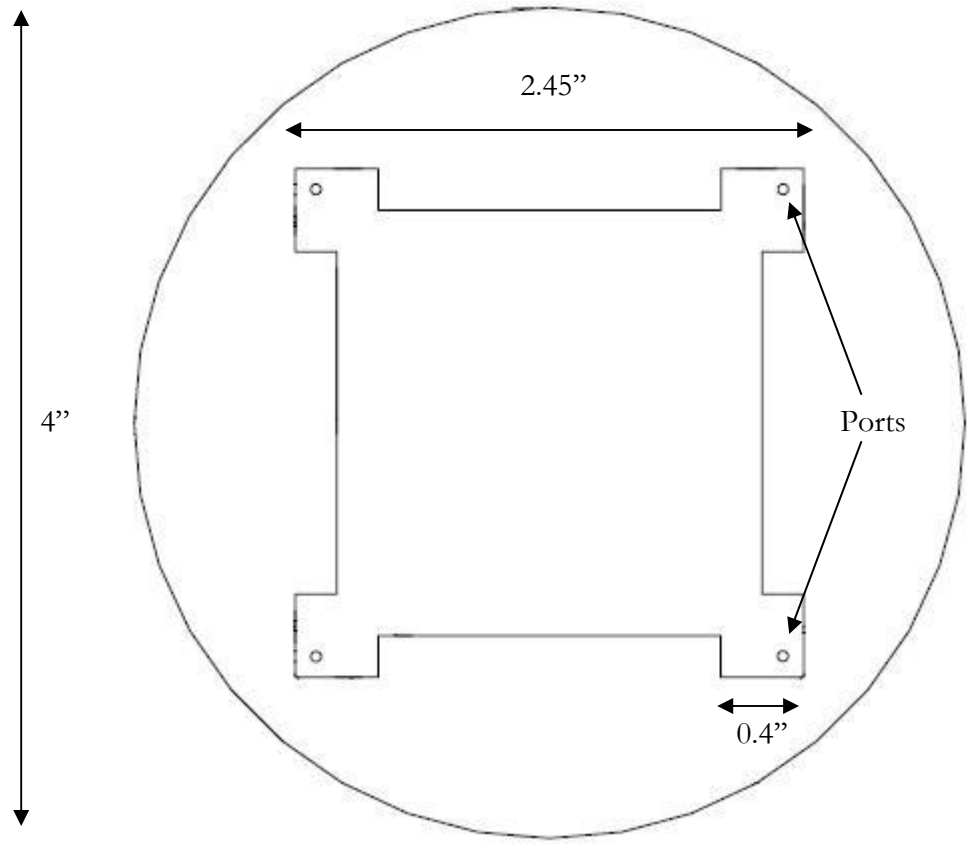

Fig. 5-2: Glass substrate for micro-model

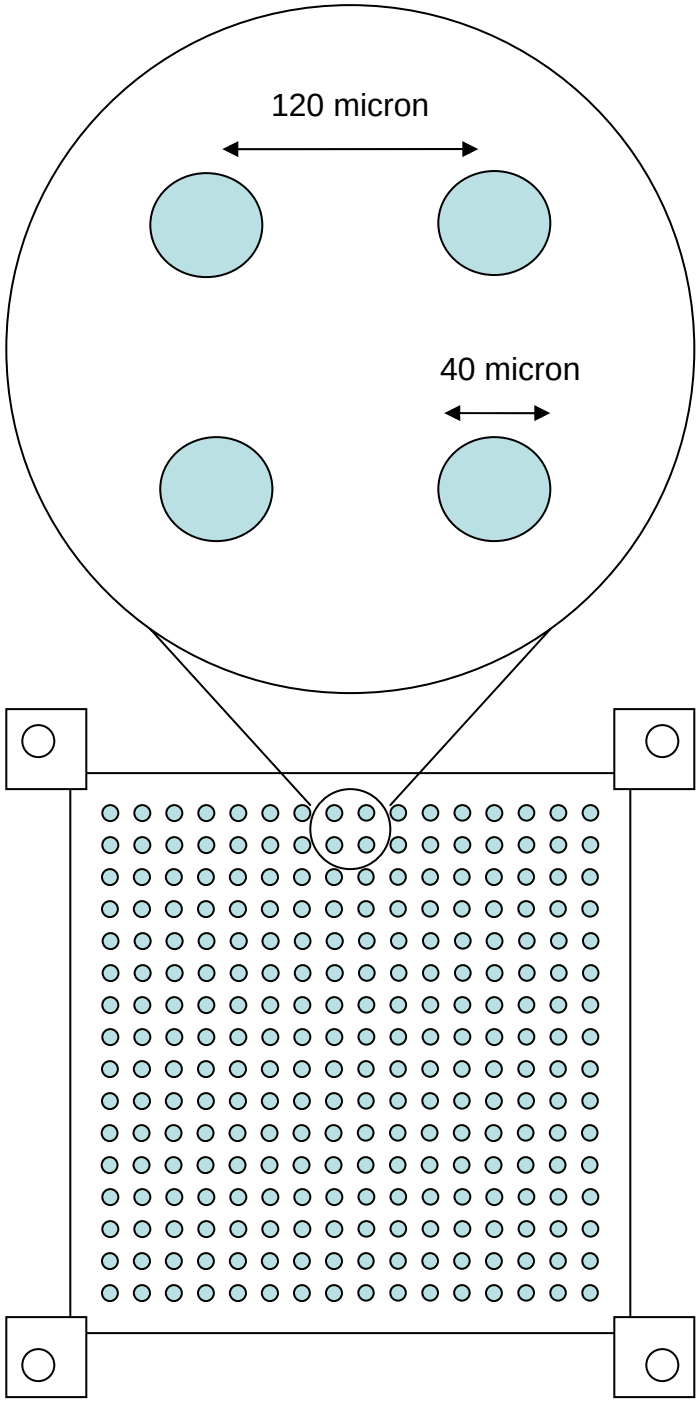

Fig. 5-3: Micro-model design (top view)

5.2 Experimental Setup

Micro-model was attached to a plastic base on which four holes were drilled. The holes were aligned on top of the micro-model ports and were sealed around with silicon. These holes were connected to four valves which control the flow in and out of the model. **Fig. 5-4** shows the micro-model after an experiment.

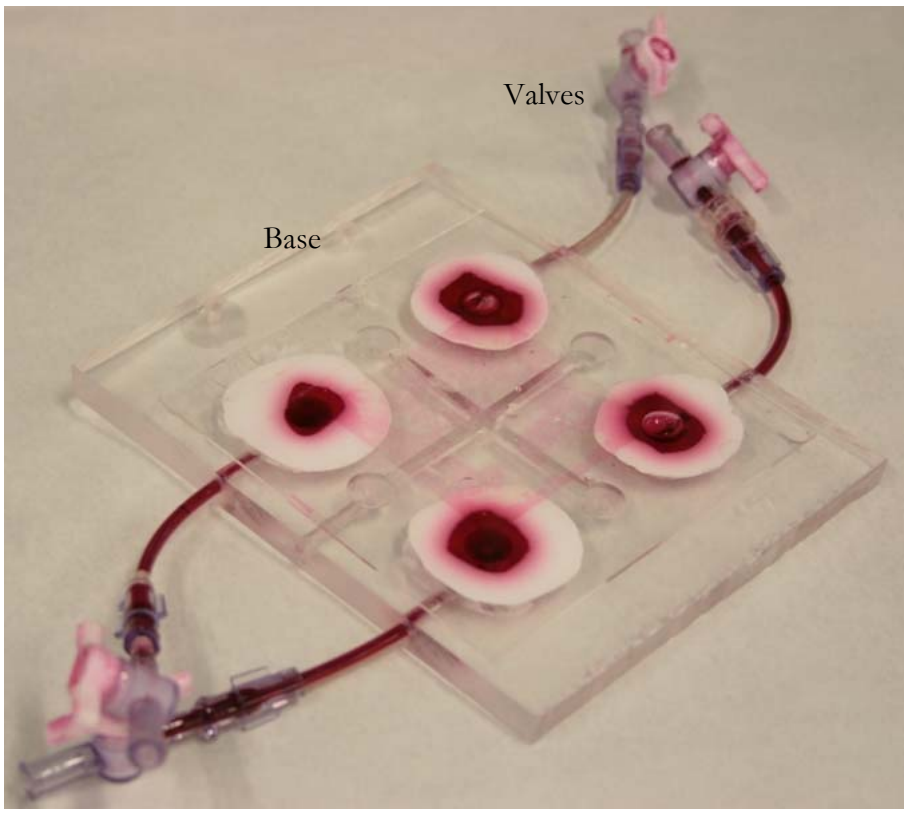

Fig. 5-4: Micro-model attached to the plastic base.

This unit was then immersed into a bath filled with water to make a suitable environment for ultrasonic application. A camera with a proper lens was focused at the pore scale. The camera mounted on the lens system sent images to a PC. For the

ultrasonic cases, Microson™ XL-2000 generator, which is able to produce ultrasonic waves at frequency of 22.5 kHz, was used. The micro-model was first saturated with water to make it wet and then vacuum-injected kerosene until it fully displaced water and saturated the model. A small amount of water saturation left inside. To inject water into the model a Kent programmable syringe pump was used. A picture of the setup is shown in **Fig. 5-5**.

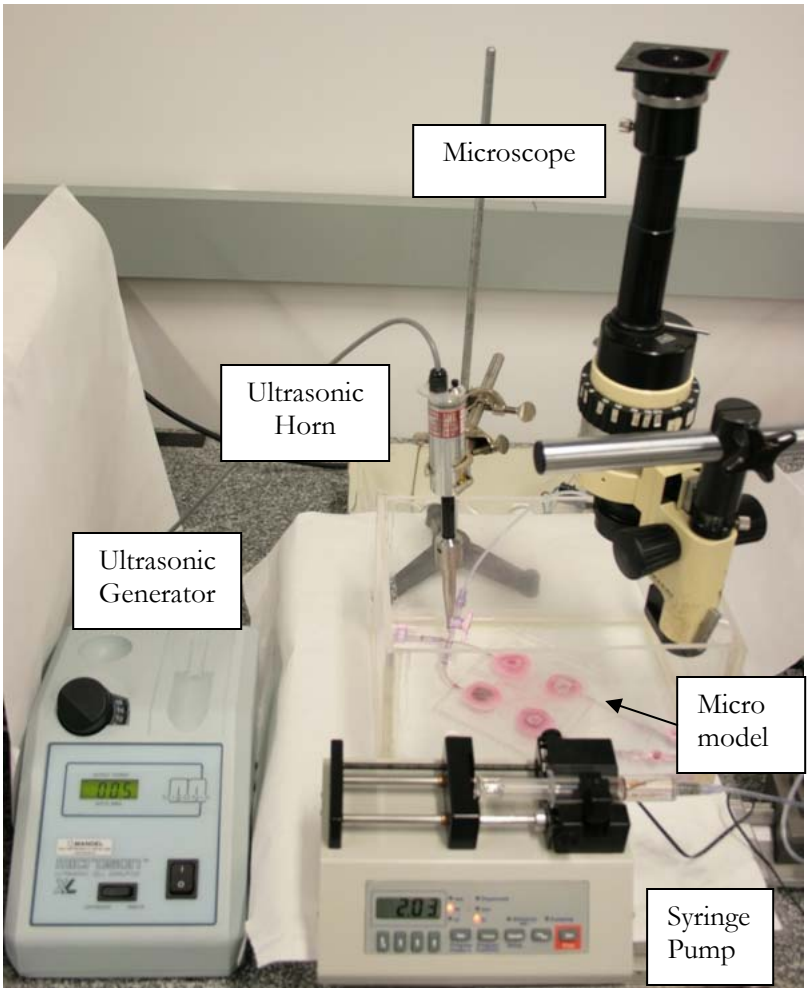

Fig. 5-5: Micro-model experimental setup.

5.3 Results

It is important to find the area to be zoomed during the experiments to capture the images describing the process. The progress of the displacement front however, cannot be easily predicted. Therefore, the focus was kept on the injection front. Experiments at different rates were conducted with and without ultrasonic exposure. A selection of acquired images is presented in this section.

Fig. 5-6 shows the snapshots of the experiment with the injection rate of 0.03 ml/hr, with and without ultrasonic radiation. The experiment was started without ultrasonic energy. Without changing the zoomed area, the ultrasonic generator was switched on at 25th minute. Hence, the patterns shown in **Fig. 5-6(c)** are the continuation of **Fig. 5-6(b)** with the only difference of ultrasonic energy existence. Red areas represent kerosene and water was indicated by white color.

Non-ultrasonic case is slow in the beginning but becomes gradually faster. Note that injection rate is constant during the experiment and the change in the area swept could be due the front movement to this direction. In fact, the front movement was not uniform in all directions. After switching the ultrasonic energy, it was observed that the water penetration was enhanced.

Although our comparison is qualitative based on a series of pictures and video clips generated from them, we also attempted to obtain a more quantitative estimation of the imposed effects of ultrasonic radiation. With the assumption of a linear trend of displacement, we obtained an average displacement rate of 1.5% (of image) per minute for non-ultrasound case. In other words, in every minute 1.5% of the pores were occupied by water. When ultrasound comes into play, the average rate goes up to

around 3.5% per minute. The ultrasonic source is located on the right side of the model and the flow in this direction could be enhanced. In other words, water could preferentially flow on this direction due to vibrating force generated by ultrasound.

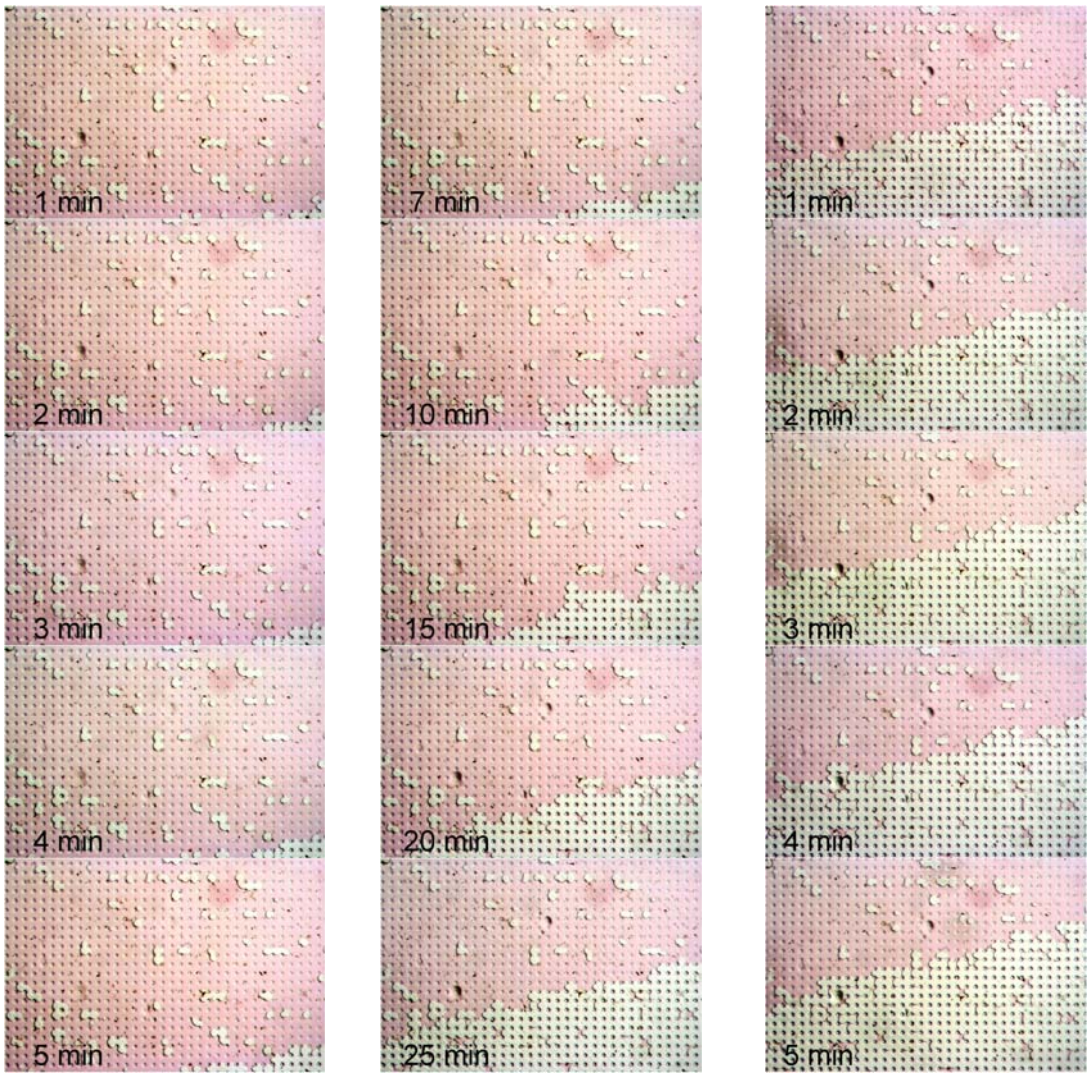

(a) (b) (c)

Fig. 5-6: Experiment at the rate of 0.03 ml/hr: (a), (b) without ultrasonic radiation and (c) continuing the same experiment with ultrasonic exposure (lighter color (white) corresponds to water – displacing phase).

Different part of the models was also pictured during 0.03 ml/hr experiment. The images are shown in **Fig. 5-7**. Those images were acquired after switching the ultrasonic source on. One observes a steady progress of water displacement and more compact cluster is obtained under ultrasonic waves.

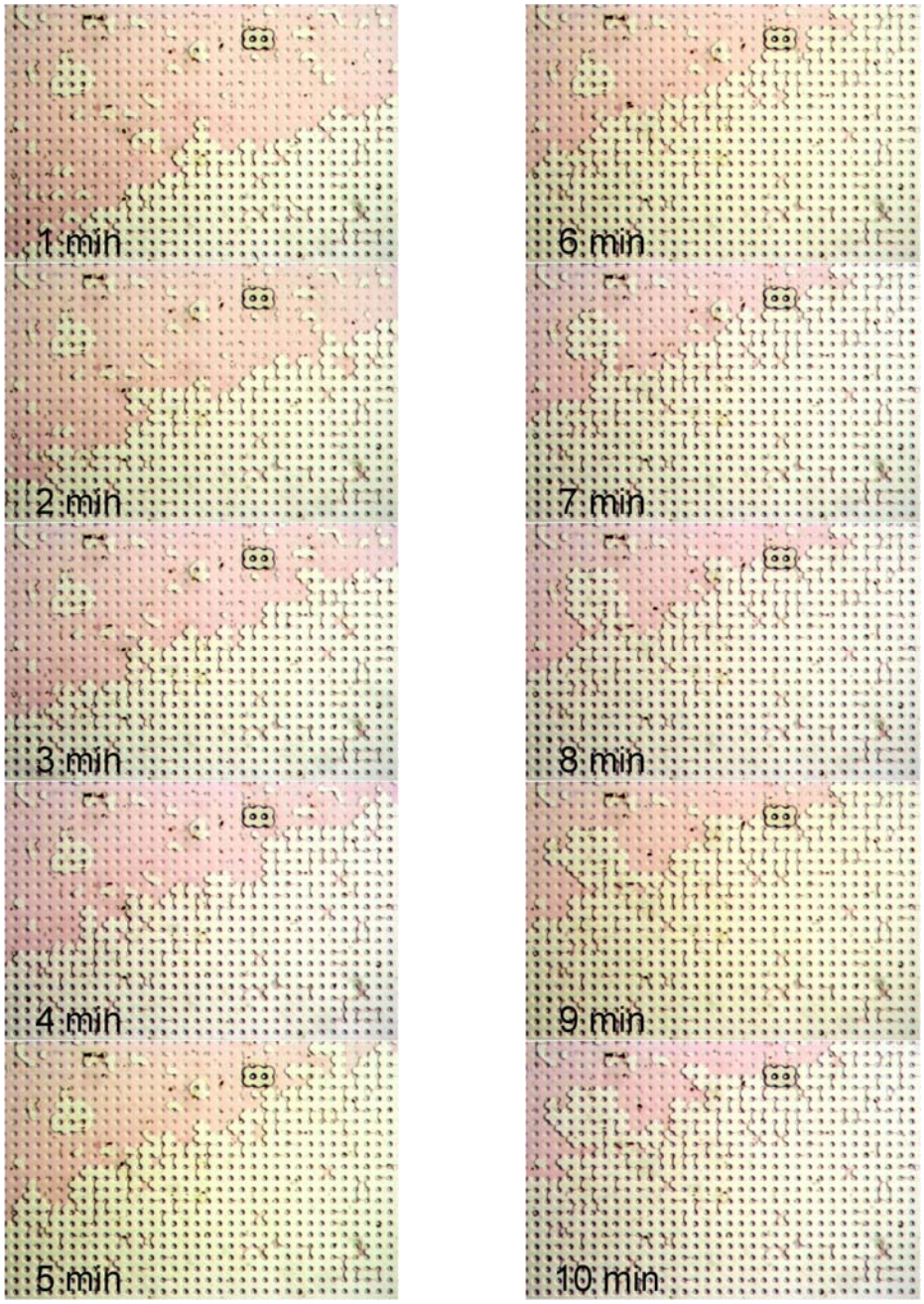

Fig. 5-7: Ultrasonic experiment with rate of 0.03 ml/hr.

To observe the effect of injection rate, another experiment was run at the rate of 0.10 ml/hr. Again, we started without ultrasonic energy and then switched to ultrasonic at certain stage. **Fig. 5-8** shows snapshots of non-ultrasonic and ultrasonic cases.

At the higher rate, the non-ultrasonic case shows a steady progress of the front (**Fig. 5-8 (a)**). Applying the same calculus to obtain the average rate of progress, we observed that the displacement rate decreased from 5% per minute for the non-ultrasonic case to 1.5% per minute for the ultrasonic one. In other words, the ultrasonic effect is negative at higher rates. One also observes branching in certain direction (towards the top part of the model shown in **Fig. 5-8(b)**). This is in line with our results form 5-spot sand pack models in previous chapter and also observations in the Hele-Shaw experiments reported by Hamida and Babadagli (2005c, 2007a, 2008b).

Two separate parts independent of each other were also pictured with and without ultrasonic energy during the same experiment. **Fig. 5-9** shows the non-ultrasonic case. One observes a good sweep resulting in a compact cluster. Looking at another part of the model after switching the ultrasonic energy, one observes that less compact but more branched displacement pattern (**Fig. 5-8 (b)**). The sweep is not as good as the non-ultrasonic case and finger type branches are quite obvious.

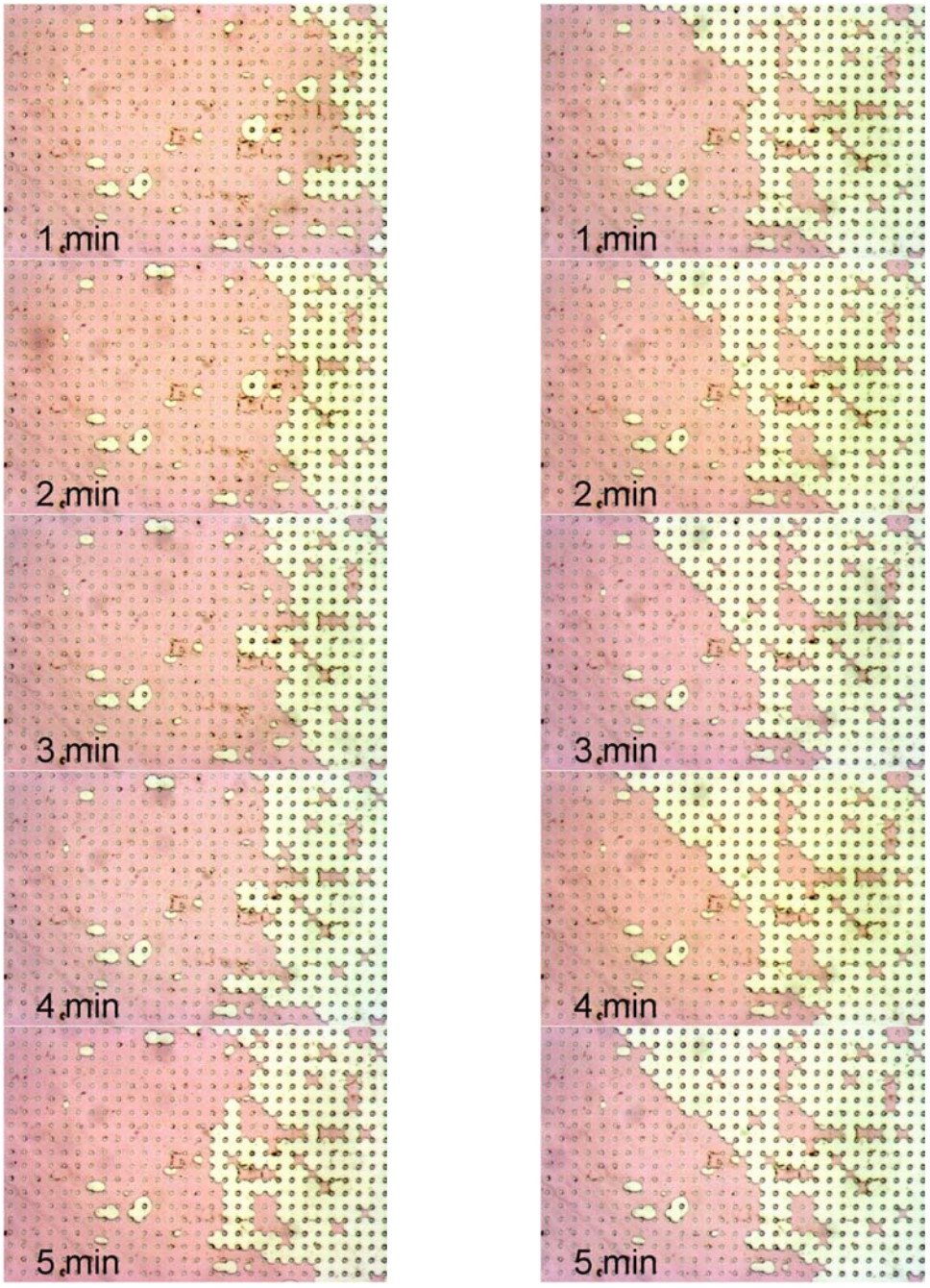

(a) (b)

Fig. 5-8: Experiment with rate of 0.10 ml/hr (a) without ultrasonic radiation, and (b) with ultrasonic exposure.

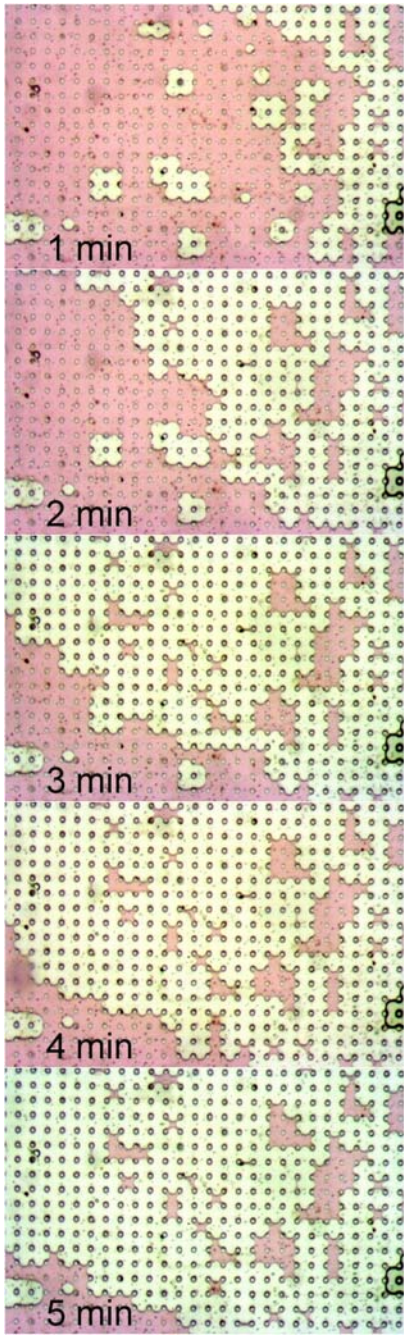

Fig. 5-9: NUS case, rate=0.1ml/hr.

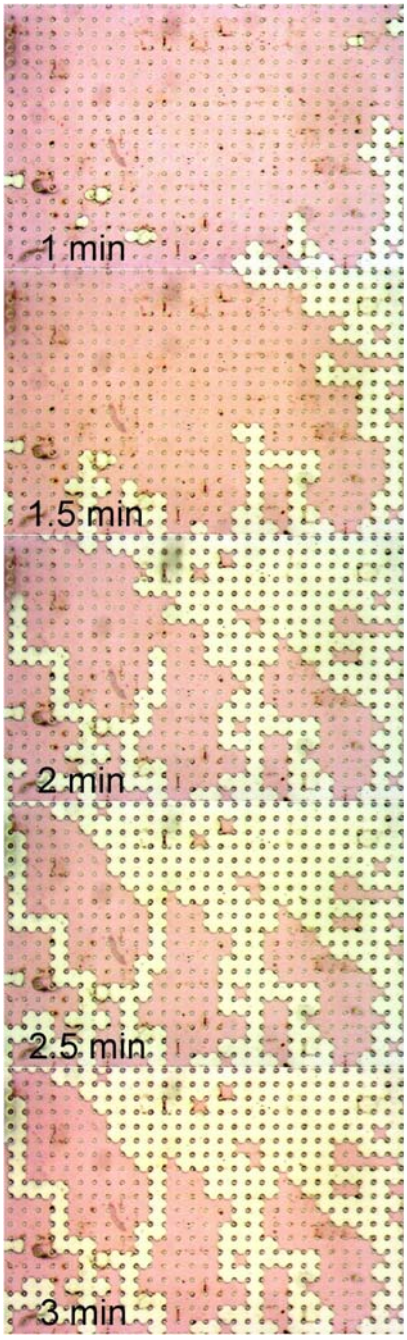

Fig. 5-10: US case, rate=0.1ml/hr.

As observed here and also in the sand pack visualization experiments, the effectiveness of acoustic energy on immiscible displacement is dependent on injection rate. A more general evaluation can be done using the capillary number. Hamida (2006) related the cluster (displacement pattern) characteristics (fractal dimension) to the capillary number. The capillary number is a dimensionless number representing the ratio of viscous forces to capillary forces and is defined by **Eq. 5-1**:

$$N_{ca} = \frac{v\mu}{\sigma \cos\theta} \qquad 5\text{-}1$$

where v is displacing fluid velocity, μ is displacing fluid viscosity, σ is interfacial tension (IFT) between displacing and displaced phases and θ is the contact angle. Commonly (also in our experiments), the displacing fluid is water and the displaced fluid is oil. Hence, **Eq.5-1** can be re-written as follows:

$$N_{ca} = \frac{v\mu_w}{\sigma_{ow} \cos\theta} \qquad 5\text{-}2$$

The residual oil saturation is dependent on the capillary number, as well as wettability characteristics and pore structure of the porous medium. When capillary number increases, residual oil saturation decreases. (Klins 1984; Green and Willhite 1998). When the rate is slow, the capillary forces such as the wettablity and IFT dominate the process.

Back to our experiments, in non-ultrasonic case (or normal case without external influence imposing on the system), the capillary number is directly related to injection rate. Thus, at higher rates, i.e. higher capillary number; the less residual oil will be remained in the system after displacement. For the ultrasonic cases, at low injection rates, the acoustic energy reduces the interfacial tension and thus increases the capillary number and makes a better sweep than the identical case without ultrasonic radiation.

5.4 Conclusions

We performed a few experiments in a homogeneous micro-model with and without ultrasonic energy at two different rates. For the lower injection rate, a positive effect of ultrasonic energy creating a better sweep and displacement was observed. At the higher rate, the presence of ultrasonic energy appeared to be less effective either by keeping the pattern unchanged (around the ports far from the ultrasonic source) or making it be more branched towards the production end yielding eventually a poorer sweep (around the ports closer to the ultrasonic source).

However giving a decisive theory needs more experiments in a wider range of injection rates, various wettabilities, and different designs of pore characteristics (heterogeneous micro-models).

CHAPTER 6

PENETRATION OF ULTRASONIC WAVES IN DIFFERENT MEDIA

Upon obtaining very promising results out of lab-scale experimental works, the question arouse on the feasibility of the process at field scale. To use the ultrasonic radiation as a well stimulation method, first the propagation of such waves in porous media should be investigated. The main problem of commercialization of such a process is the limited penetration radius of acoustic waves through porous media. Wave's attenuation in a medium containing rock and fluid is high and limits the potential application to near well bore zone. In addition to medium properties, the attenuation also depends on wave source specifications such as intensity, frequency, polarization, and so on.

Biot (1956a, 1956b) developed a theory for propagation of elastic waves in porous medium saturated by compressible viscous fluid. Biot's theory predicts that the penetration depth for ultrasonic waves at frequency of 20 kHz is 2 to 10 cm. Because the attenuation is proportional to the square of frequency, low frequency waves are more applicable to penetrate to the reservoir in longer distances (Hamida and Babadagli 2008b). If a periodic signal with frequency (f) is distorted, in a frequency domain, it will be a composition of main frequency and its harmonics with higher

frequencies which are integer multiples of (f). However, the harmonics are usually smaller in amplitude as their frequency increases and the dominant frequency (with the greatest amplitude) is normally the first harmonic with frequency (f) (Smith 1997).

Therefore, during the penetration of low frequency elastic waves through porous medium, the wave shape might be distorted due to energy loss and attenuation. This creates harmonics with higher frequencies, hence we may expect to have waves in order of ultrasonic frequencies as the low frequency seismic waves penetrate deeper in the reservoir. However, they might be negligible in intensity comparing to main harmonic and also due to their higher frequencies they attenuate faster.

In order to examine the penetration rate of ultrasonic waves, we designed a set-up to measure the attenuation and also the effect of distance from the source on imbibition performance.

6-1 Penetration Experiments Setup and Procedure

We tested ultrasonic waves in air, water and a slurry mixture of sand and water to understand how the properties of waves change while it radiates and travels through the surrounding medium. For the experiments in air, we used Prowave ceramic transducers, which were tuned at a center frequency of 40 kHz (that means their sensitivity is the best at this frequency) and will be decreasing by going away from the center frequency. Hence, for the experiments in air, we connected a transmitter of this kind to the function generator which was creating a signal of 10 V amplitude at 40 kHz frequency. An oscilloscope was used to measure the received wave, which was converted to electrical signal by the ultrasonic receiver.

For water and slurry medium experiments, we used the setup shown in **Fig.6-1**. Sonicator® 3000 ultrasonic processor generates the waves and the intensity of the waves was measured at three different distances from the source using the same ceramic receivers connected to the oscilloscope. Three imbibition cells containing oil-wet cores saturated with heavy oil with viscosity of 500cp were located at certain distances from the source as shown in **Fig.6-1**.

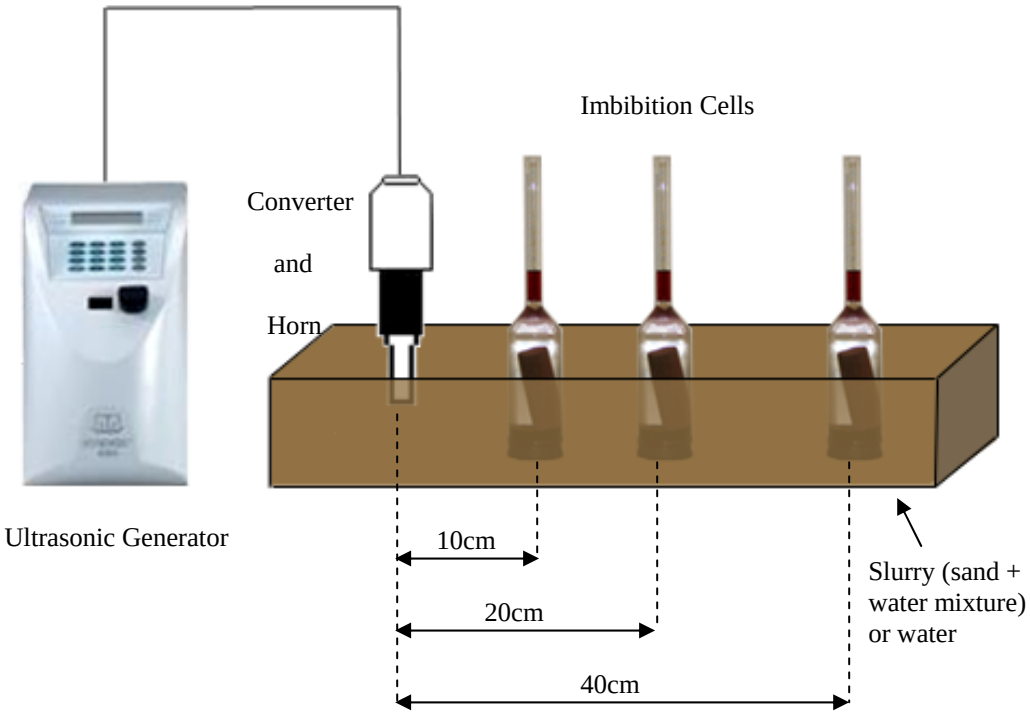

Fig.6-1: Penetration experiments setup for slurry and water medium.

6.2 Results

6.2.1 Imbibition Recovery

We chose oil wet imbibition experiments because the effect of ultrasonic was more critical on them as discussed in Chapter 3. The production curves are shown in **Fig. 6-2**. Due to their oil wet nature of the sample, the production needs quite a long time to start. As seen, until around 20,000 minutes, there was no production in all three experiments inside sand mixture while for water cases; it had a small amount of production. Closer cells to the source yielded faster and higher recoveries.

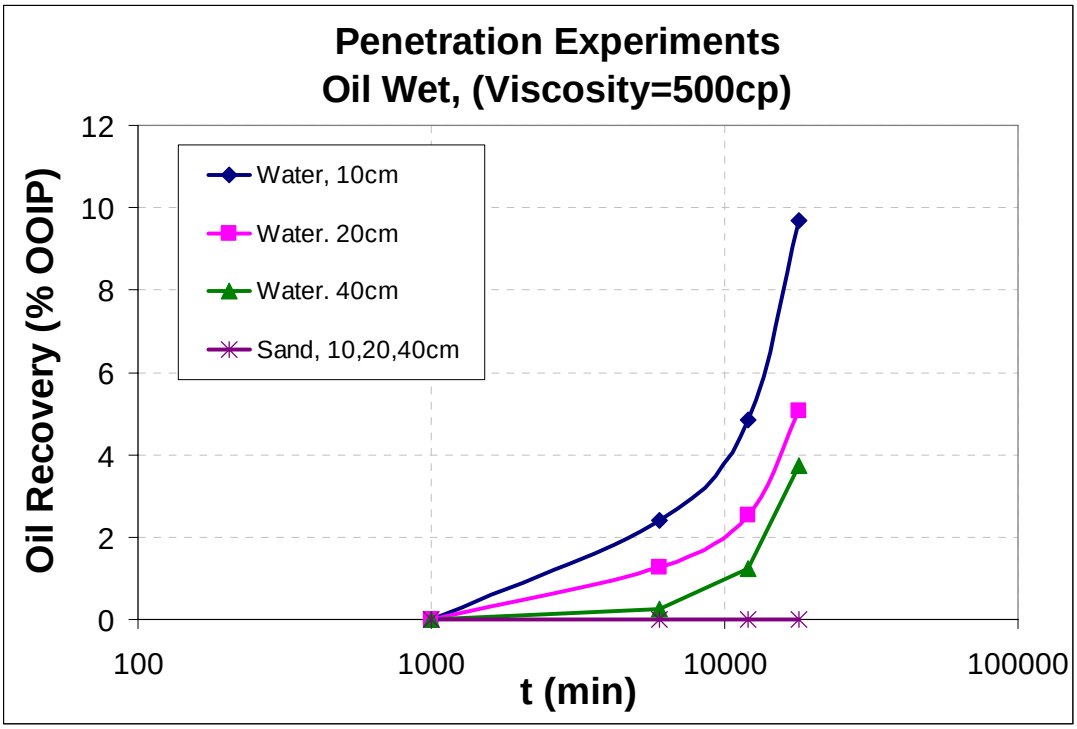

Fig. 6-2: Recovery curves for penetration experiments in water and slurry.

6.2.2 Wave Propagation

The wave properties as it propagates through each medium were also measured. In air, we used ceramic ultrasonic transducers set at 40 kHz. Function generator sends a sinusoidal electrical signal to transmitter and it converts the electrical signal to ultrasonic waves. On the other side, receiver converts the received ultrasonic wave to an electrical signal which can be detected by oscilloscope. The wave shapes in receiver in three different distances of 10 cm, 20 cm and 40 cm are shown in **Figs. 6-3 to 6-5** as they appear on oscilloscope screen. At the distance of 10 cm, a signal with amplitude of 1 V and frequency of 39.997 kHz was detected. (**Fig. 6-3**). At 20 cm distance, the amplitude decreased to 500 mV and frequency was read as 39.995 kHz. (**Fig. 6-4**). This wave will have an amplitude of almost 200 mV and frequency of 30.870 kHz when reaches the distance of 40 cm. (**Fig. 6-5**)

Comparing these three measurements gives us an idea about attenuation of ultrasonic waves radiating in air. From 10 cm to 20 cm, the wave amplitude decreased to almost half. As the power is proportional to the square of amplitude, at the latter place the wave power is a quarter of power at the former place. Coming to the third point at 40 cm, the wave amplitude is about 200 mV which shows a decrease in the power at around one fifth of the previous point (20 cm). For comparisons, we can use the concept of decibel (dB) which is a dimensionless logarithmic unit stating the ratio of two quantities of the same nature. For the wave intensity, the sound intensity level is defined by **Eq.6-1**:

$$L_{dB} = 10 \log \frac{I_1}{I_0} \qquad 6\text{-}1$$

where I_1 is the sound intensity, which is defined as the sound power divided by the surface area of a sphere with radius of the distance of each point to the source. I_0 is a reference intensity usually defined as 10^{-12} W/m^2. However, when we compare the two points to each other, the difference in intensity level is defined as:

$$L_{dB2} - L_{dB1} = 10 \log \frac{I_2}{I_0} - 10 \log \frac{I_1}{I_0} = 10 \log \frac{I_2}{I_1} \qquad 6\text{-}2$$

In our experiment in air, when intensity at the second point is the quarter of the first point, the intensity level decreased by 6 dB and from the second point to the third; this difference is about 7 dB.

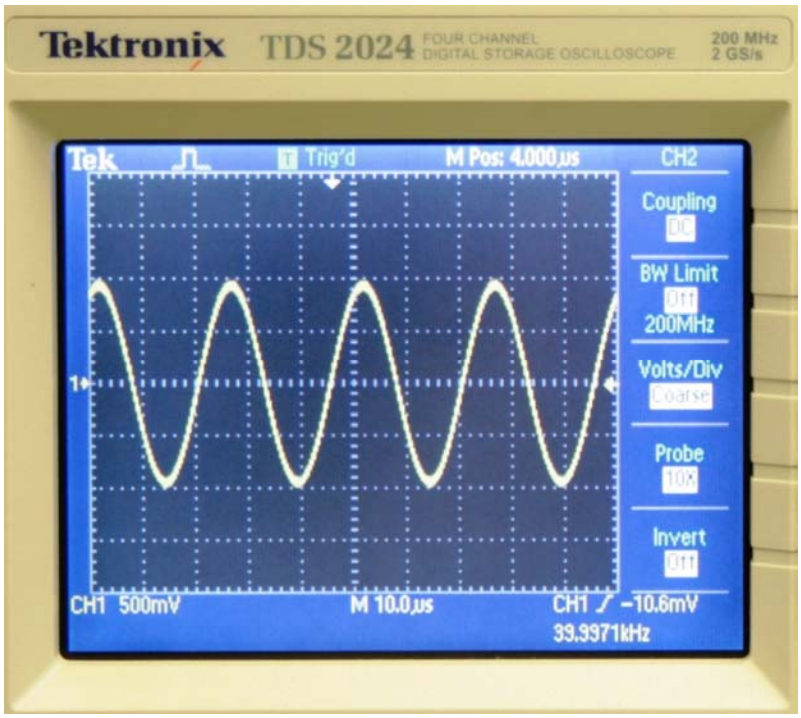

Fig.6-3: Received signal in air at a distance of 10cm.

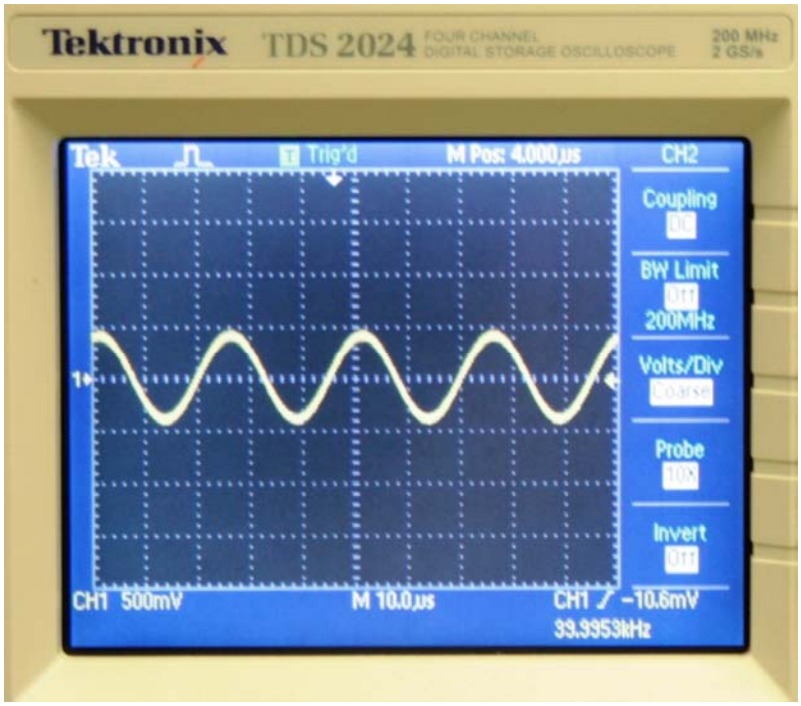

Fig.6-4: Received signal in air at a distance of 20cm.

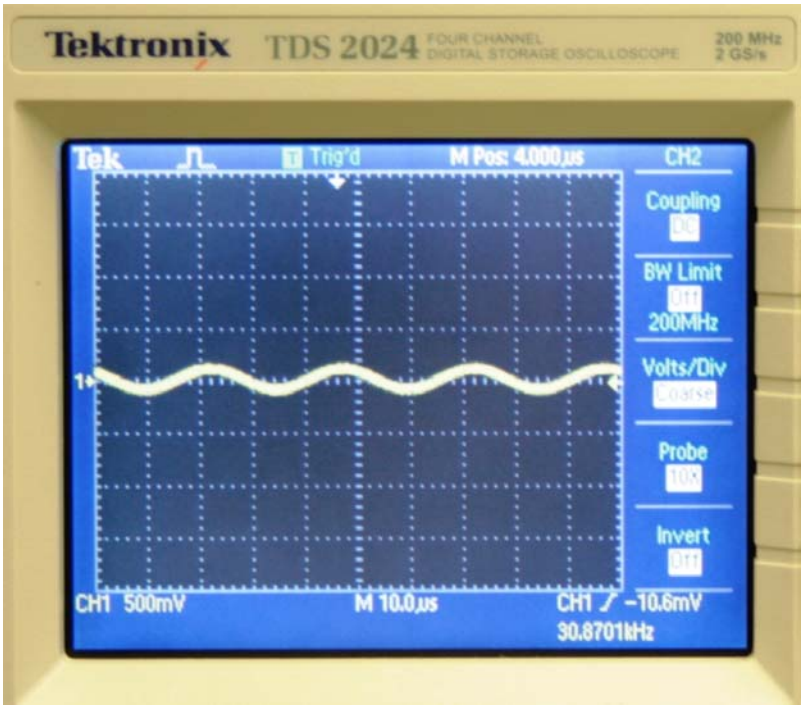

Fig.6-5: Received signal in air at a distance of 40cm.

For the experiments in water bath, we used Sonicator® 3000 ultrasonic generator to obtain higher power. We also measured the wave properties inside the bath using the same ceramic receivers. **Figs. 6-6 to 6-8** show the received signal under water at the distances of 10 cm, 20 cm and 40 cm, respectively.

In this case, the wave shapes are not as "clean" as the air experiments. This could be due to different source specification; different propagation medium and using the transducer at a frequency far form its center frequency. As seen in **Figs. 6-6 to 6-8**, one may observe noise in the wave but still its general form can be recognized. For the 10 cm case (**Fig. 6-6**), the signal has an average amplitude of almost 4 V and a frequency of 20.26 kHz. At 20 cm distance, the amplitude decreases to 2 V and

frequency is 20.08 kHz (**Fig. 6-7**). When the wave reached 40 cm distance from the source, its average amplitude was 1 V and frequency was as low as 18.79 kHz (**Fig.6-8**).

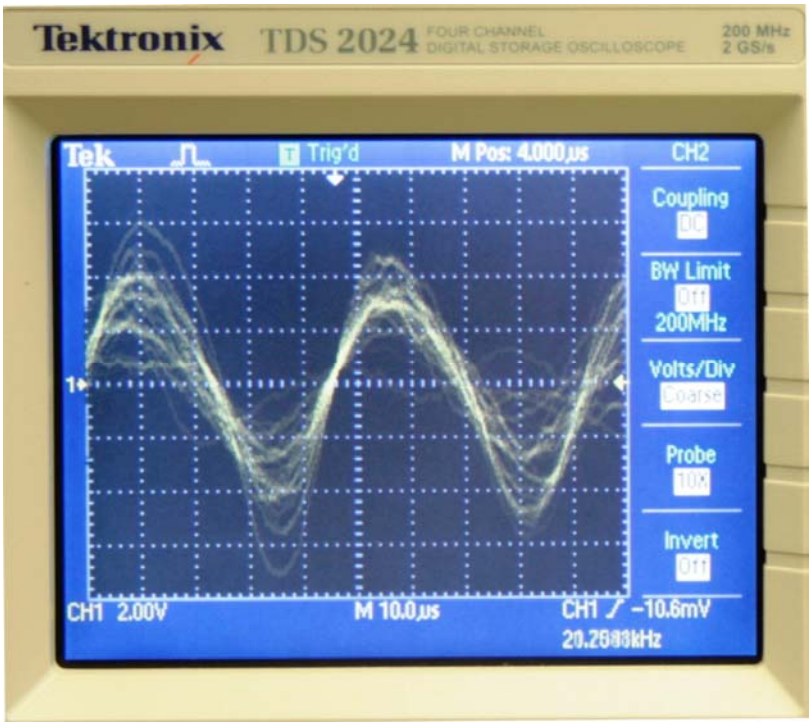

Fig.6-6: Received signal in water at a distance of 10cm.

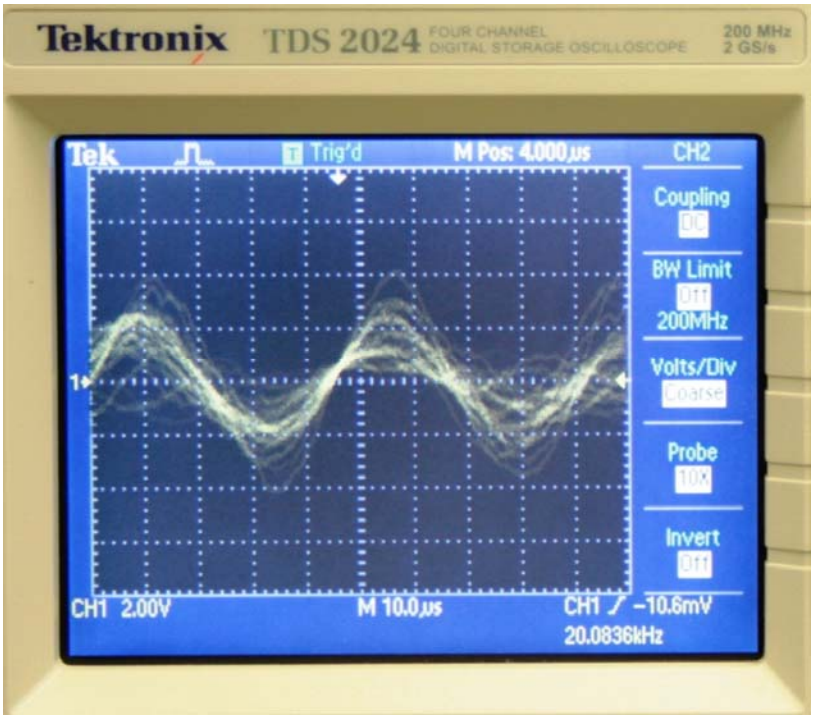

Fig.6-7: Received signal in water at a distance of 20cm.

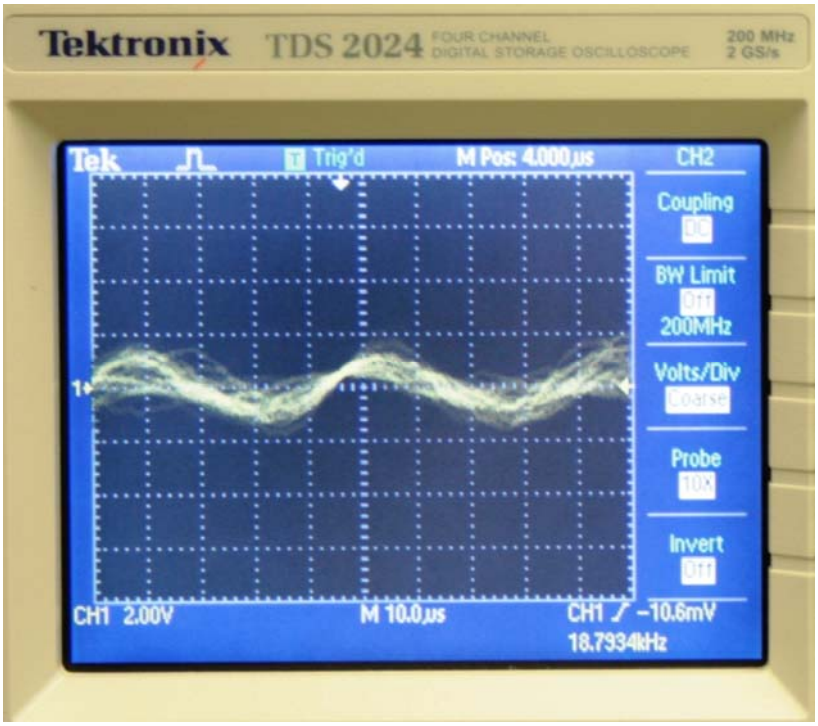

Fig.6-8: Received signal in water at a distance of 40cm.

The situation inside the slurry was completely different. Measuring the wave did not give any information. The acquired wave shape is shown in **Fig. 6-9**. What was received was almost a noise and the receiver could not detect any specific frequency in its range.

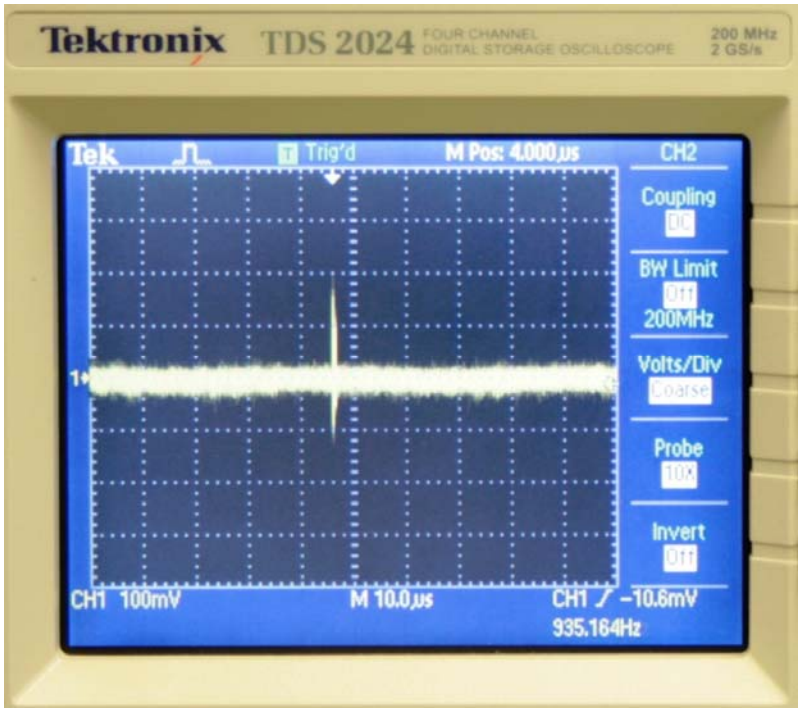

Fig.6-9: Received signal in slurry (sand+water).

A schematic diagram of all penetration experiments is shown in **Fig. 6-10**.

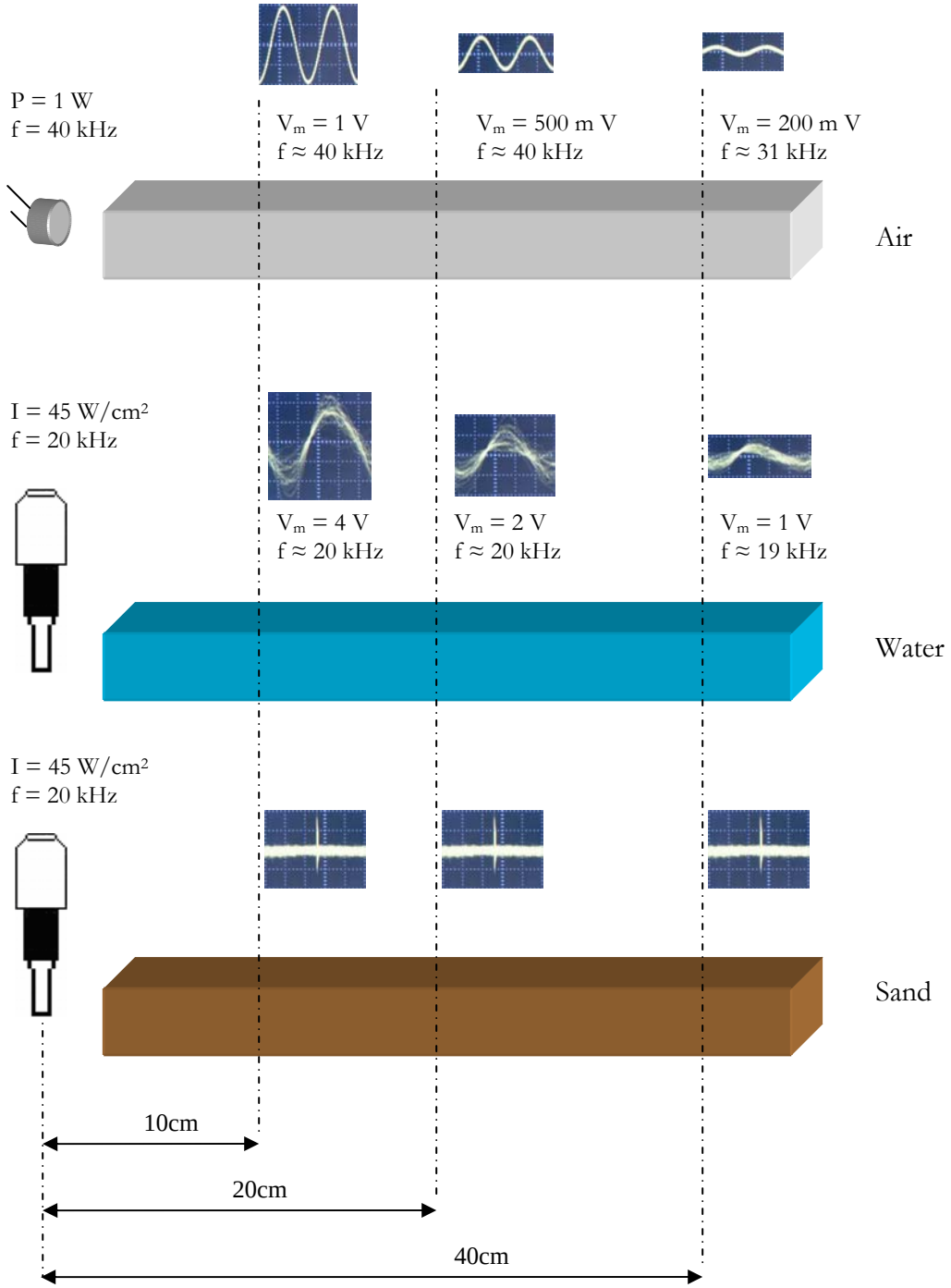

Fig.6-10: Penetration experiments diagram (P:Power, I:Intensity, f:Frequency).

6.3 Conclusions

Running a series of imbibition experiments inside water and slurry (sand+water) at different distances from the ultrasonic source and also measuring the wave shape and properties at these distances using ultrasonic transducer connected to oscilloscope, we observed that water behaves similar to air. Around the source (up to 20 cm in our experiments), the reduction in intensity was as expected which was based on normal intensity relation to distance from the source, i.e. it decrease proportional to $1/r^2$ and frequency change is certainly negligible. Beyond this distance (e.g. at 40 cm), attenuation in the medium showed changes particularly in the frequency of propagating wave. Inside the slurry, attenuation was much higher so that we did not acquire any wave shape in the receiver even close to the source. This might depend on source frequency and power and also sensitivity of transducer, but based on our observations, we can state that the wave loss in the slurry medium was much higher than in air and water cases.

CHAPTER 7

CONCLUSIONS

7.1 Accomplishments

Different sets of experiments were performed to investigate the effects of ultrasonic radiation on immiscible displacement of oil by water in porous media and on the rate and amount of oil recovery by spontaneous (capillary) imbibition process. The experimental program includes four sets of experiments. In each series, different rock/fluid/flow parameters were targeted and their change under ultrasonic waves and the ultimate effect of this change on the process and oil recovery were clarified.

7.1.1 Core experiments

In the core experiments, the spontaneous (capillary) imbibition/drainage of brine into oil saturated Berea sandstone cores was considered. Several parameters such as wettability, oil viscosity, initial water saturation, and the frequency and intensity of ultrasonic waves were tested.

These experiments showed that increasing ultrasonic radiation results in more recovery by capillary imbibition. The effect of ultrasonic energy on improved recovery is less pronounced for samples with higher viscosity oil. In oil wet cases, the effect of ultrasonic radiation on recovery is much more significant than the water-wet case. The

presence of initial water saturation in oil wet experiments facilitates oil recovery under ultrasound most likely due to the peristaltic movement of non-wetting water phase.

7.1.2 Visual Experiments – 2-D Sand Pack Models

To acquire a visual sense of how oil is displaced by water under ultrasonic waves, 2-D sand pack experiments were performed. Different conditions such as wettability, oil viscosity, initial water saturation, and injection rates were tested.

More compact clusters with shorter and thicker fingers were obtained under ultrasonic radiation in water-wet models. In the presence of ultrasonic field in the water-wet/light oil case, only water was produced after breakthrough implying that water has short-circuited between injection and production ports while in oil-wet samples more oil was produced after breakthrough when ultrasound was applied.

For the oil wet cases, no cluster was formed as in the water-wet cases. In the former, light mineral oil formed side branches especially through the edges. This was not observed in the identical models saturated with higher oil viscosities and less widened clusters developed towards the outlet were formed. But, the cluster was not as compact as it was in the water-wet cases.

Initial water saturation in oil wet models helped the injected water go faster to the outlet direction rather than branching out and spreading towards the edges.

5-spot model experiments showed that, at higher rates of injection, ultrasonic energy deformed the uniform pattern which would have formed without acoustic waves. At low rates, however, water swept more efficiently with ultrasonic energy. This clearly indicates that the effect of ultrasonic energy is more pronounced as the rate

was lowered, i.e., the capillary forces are more dominant compared to the viscous forces. This also explains why capillary imbibition recoveries were higher when ultrasonic energy was applied.

7.1.3 Visual Experiments – Micro-models

To investigate the immiscible displacement at pore scale, a homogenous nanotechnology-based micro-model was built and experiments were performed on the model by displacing kerosene by water at different injection rates.

For a lower injection rate, we observed a positive effect of ultrasonic waves making a better sweep, while for the higher rate, the presence of ultrasonic appeared to be less effective causing faster movement of the front as fingers. This is in line with the observations made at core scale through 2-D sand pack models.

7.1.4 Penetration Test

Imbibition experiments were run at specific distances from the ultrasonic source and measurements for ultrasonic wave shapes, frequency, and intensity using a ceramic ultrasonic transducer which converts the received ultrasonic waves to electrical signal were conducted.

No significant change in the frequency up to 20 cm off the source in air and water was observed. Beyond this distance the frequency started to decrease. The intensity also decreased gradually as getting far from the source.

The oil recovery by capillary imbibition systematically decreased as the distance from the sources was increased. The slurry mixture of sand and water showed a high

resistance to ultrasonic wave propagation. Imbibition experiments showed no recovery in slurry mixture regardless the distance implying that ultrasonic effect was not felt at all.

7.2 Future Work

Different frequencies and intensities of the ultrasonic energy can be tested, i.e., a combination of high frequency/high intensity or low frequency/high intensity waves for capillary imbibition experiments. Another application is to test the intermittent use of ultrasonic waves instead of continuous to optimize the process in terms of cost.

There has been a very limited micro-model study in the literature. In this work, we tested only the effect of injection rate to identify the relative effects on the capillary and viscous forces. Micro-model investigations using homogeneous and heterogeneous models with different medium properties such as wettability are recommendable. Micro-model investigations are essential because they to provide a good insight into pore scale interactions between fluids and also between fluid and rock under acoustic energy.

Wave penetration studies are mostly theoretical and more physical tests using different ultrasonic sources and more powerful transducers can be performed for various medium properties. More realistic well and reservoir models can also be employed for penetration tests.

REFERENCES

AARTS, A. C. T. and G. OOMS (1998). "Net Flow of Compressible Viscous Liquids Induced By Traveling Waves in Porous Media." Journal of Engineering Mathematics **34**(4): 435-450.

AARTS, A. C. T., et al. (1999). "Enhancement of Liquid Flow through a Porous Medium by Ultrasonic Radiation." SPE Journal **4**(4): 321-327.

ABAD-GUERRA, B. P. (1976). "Methods for Restoring Productivity to Gas Wells in the Clinton sand of Ohio: A Laboratory and Field Experiment." Pennsylvania State University. **Ph.D. thesis**

BERESNEV, I. A. and P. A. JOHNSON (1994). "Elastic-Wave Stimulation of Oil Production - a Review of Methods and Results." Geophysics **59**(6): 1000-1017.

BERESNEV. I.A. et al. (2005). "The Mechanism of Recovery of Residual Oil by Elastic Waves and Vibrations." SEG Expanded Abstracts 24, 1386-1390; DOI:10.1190/1.2147946

BIOT, M. A. (1956a). "Theory of Propagation of Elastic Waves in a Fluid-Saturated Porous Solid .1. Low-Frequency Range." Journal of the Acoustical Society of America **28**(2): 168-178.

BIOT, M. A. (1956b). "Theory of Propagation of Elastic Waves in a Fluid-Saturated Porous Solid .2. Higher Frequency Range." Journal of the Acoustical Society of America **28**(2): 179-191.

BIOT, M. A. (1962). "Mechanics of Deformation and Acoustic Propagation in Porous Media." Journal of Applied Physics **33**(4): 1482.

BJERKNES, V. F. K. (1906). "Fields of Force." New York, Columbia University Press.

BJORNDALEN, N. and M. R. ISLAM (2004). "The Effect of Microwave and Ultrasonic Irradiation on Crude Oil during Production with a Horizontal Well." Journal of Petroleum Science and Engineering **43**(3-4): 139-150.

BLAKE, F. G. (1949). "Bjerknes Forces in Stationary Sound Fields." Journal of the Acoustical Society of America **21**(5): 551-551.

BUCKINGHAM, M. J. (1997). "Theory of Acoustic Attenuation, Dispersion, and Pulse Propagation in Unconsolidated Granular Materials Including Marine Sediments." Journal of the Acoustical Society of America **102**(5): 2579-2596.

BUCKINGHAM, M. J. (1999). "Theory of Compressional and Transverse Wave Propagation in Consolidated Porous Media." Journal of the Acoustical Society of America **106**(2): 575-581.

BUCKINGHAM, M. J. (2005). "Compressional and Shear Wave Properties of Marine Sediments: Comparisons between Theory and Data." Journal of the Acoustical Society of America **117**(1): 137-152.

CHEN, W. I. (1969). "Influence of Ultrasonic Energy upon the Rate of Flow of Liquids through Porous Media." Chemical Engineering, West Virginia University. **Ph.D. thesis:** 141.

CHERSKIY, N. V., et al. (1977). "The Effect of Ultrasound on Permeability of Rocks to Water." Transactions (Doklady) of the U.S.S.R. Academy of Sciences. Earth science sections. **232**: 201-204.

DEZHKUNOV, N. V. and T. G. LEIGHTON (2004). "Study into Correlation between the Ultrasonic Capillary Effect and Sonoluminescence." Journal of Engineering Physics and Thermophysics **77**(1): 53-61.

DUHON, R. D. and J. M. CAMPBELL (1965). "The Effect of Ultrasonic Energy on Flow through Porous Media." SPE 1316, 2nd Annual Eastern Regional Meeting of SPE/AIME, Charleston, WV.

DUNIN, S. and V. N. NIKOLAEVSKII (2005). "Nonlinear Waves In Porous Media Saturated With Live Oil." Acoustical Physics **51**(1): S61-S66 (1).

DUNN, K. and T. F. YEN (2001). "A Plausible Reaction Pathway of Asphaltene under Ultrasound." Fuel Processing Technology **73**(1): 59-71.

DUSSEAULT, M., et al. (2000). "Pressure Pulsing: The Ups And Downs of Starting a New Technology." Journal of Canadian Petroleum Technology **39**(4): 13.

FAIRBANKS, H. V. and W. I. CHEN (1971). "Ultrasonic Acceleration of Liquid Flow through Porous Media." Chemical Engineering Progress Symposium Series. **67**: 105.

FRENKEL, J. (1944). "On The Theory of Seismic and Seismoelectric Phenomena in a Moist Soil." Journal of Physics **111**(5): 230-241.

GADIEV, S. M. (1977). "Use of Vibrations in Oil Production (Ispol'zovaniye Vibratsii v Dobyche Nefti)." Moscow, Nedra Press.

GANIEV, R. F., et al. (1989). "Wave Mechanism for the Acceleration of a Liquid Flowing in Capillaries and Porous Media." Soviet Physics - Doklady. **34**: 267-283.

GOLLAPUDI, U. K., et al. (1994). "Ultrasonic Treatment for Removal of Asphaltene Deposits during Petroleum Production." SPE 27377, 1994 SPE Int. Symposium on Formation Damage Control, Lafayette, LA.

GRAHAM, D. R. (1997). "Steady and Oscillatory Flow through Model Porous Media." University of Illinois. **M.Sc. thesis**

GRAHAM, D. R. (1999). "Acoustic Stimulation of Multiphase Flow In Porous Media." University of Illinois. **Ph.D. thesis**

GRAHAM, D. R. and J. J. L. HIGDON (2000a). "Oscillatory Flow of Droplets in Capillary Tubes. Part 1. Straight Tubes." Journal of Fluid Mechanics **425**: 31-53.

GRAHAM, D. R. and J. J. L. HIGDON (2000b). "Oscillatory Flow of Droplets in Capillary Tubes. Part 2. Constricted Tubes." Journal of Fluid Mechanics **425**: 55-77.

GREEN, D.W. and G.P. WILLHITE (1998) "Enhanced Oil Recovery." Society of Petroleum Engineering, Richardson, TX.

GUNAL, O.G. and M.R. ISLAM, (2000). "Alteration of Asphaltic Crude Rheology with Electromagnetic and Ultrasonic Irradiation." Journal of Petroleum Science and Engineering, **26**: 263-272.

HAMIDA, T. (2006). "Effect of Ultrasonic Waves on Immiscible and Miscible Displacement in Porous Media." M.Sc. Thesis, University of Alberta, Edmonton, AB.

HAMIDA, T. and T. BABADAGLI, (2005a) "Effect of Ultrasonic Waves on the Capillary Imbibition Recovery of Oil." SPE 92124, presented at the 2005 Asia Pacific Oil & Gas Conference and Exhibition, Jakarta, Indonesia, April 5-7, 2005

HAMIDA, T. and T. BABADAGLI, (2005b) "Capillary Interaction of Different Oleic and Aqueous Phases between Matrix and Fracture under Ultrasonic Waves." SPE 94105, presented at the SPE Europec/EAGE Annual Conference, Madrid, Spain, June 13-16, 2005

HAMIDA, T. and T. BABADAGLI, (2005c) "Effects of Ultrasonic Waves on Immiscible and Miscible Displacement in Porous Media." SPE 95327, presented at the 2005 SPE Annual Technical Conference and Exhibition, Dallas, Texas, Oct. 9-12, 2005

HAMIDA, T. and T. BABADAGLI, (2006) "Investigations on Capillary and Viscous Displacement under Ultrasonic Waves." Journal of Canadian Petroleum Technology, **45** (2): 16-19, Feb. 2006.

HAMIDA, T. and T. BABADAGLI, (2007a) "Fluid-fluid Interaction during Miscible and Immiscible Displacement under Ultrasonic Waves." The European Physical Journal B, **60**, 447–462, DOI: 10.1140/epjb/e2008-00005-5

HAMIDA, T. and T. BABADAGLI, (2007b) "Immiscible Displacement of Oil by Water in Consolidated Porous Media Due To Capillary Imbibition under Ultrasonic Waves." Journal of the Acoustical Society of America **122**(3): 1539–1555, DOI: 10.1121/1.2756190

HAMIDA, T. and T. BABADAGLI, (2007c) "Analysis of Capillary Interaction and Oil Recovery under Ultrasonic Waves." Transport in Porous Media (2007) **70**: 231–255, DOI 10.1007/s11242-006-9097-9

HAMIDA, T. and T. BABADAGLI, (2008a) "Effects of Ultrasonic Waves on the Interfacial Forces Between Oil and Water." Ultrasonics Sonochemistry **15** (2008): 274–278.

HAMIDA, T. and T. BABADAGLI, (2008b) "Displacement of Oil by Different Interfacial Tension Fluids under Ultrasonic Waves." Colloids and Surfaces A: Physicochemical and Engineering Aspects **316** (2008): 176–189.

HILPERT, M., et al. (2000). "Capillarity-Induced Resonance of Oil Blobs in Capillary Tubes and Porous Media." Geophysics **65**(3): 874-883.

JOHNSTON, H. K., II. (1971). "Polymer Viscosity Control by the Use of Ultrasonics." Chemical Engineering Progress Symposium Series **67**, 39-45.

KARPERIEN, A. (2005). "FracLac V.2." NSW, Australia, Charles Stuart University.

KLINS, M. (1984), "Carbon Dioxide Flooding." International Human Resources Development Corporation, Boston, MA.

KOSTROV, S. and W. WOODEN (2005). "In Situ Seismic Stimulation Shows Promise For Revitalizing Mature Fields." Oil & Gas Journal **103**(15): 43-49.

KUZNETSOV, O. L., and S. A., Efimova, (1983). "Application of Ultrasound in Oil Industry (Primeneniye Ultrazvuka V Neftianoy Promyshlennosti)" Nedra Press (in Russian).

KUZNETSOV, O. L., et al. (1998). "Improved Oil Recovery by Application of Vibro-Energy to Waterflooded Sandstones." Journal of Petroleum Science and Engineering **19**(3-4): 191-200.

KUZNETSOV, O. L., et al. (2002). "Seismic Techniques of Enhanced Oil Recovery: Experimental and Field Results." Energy Sources **24**(9): 877-889.

LI, W. Q., et al. (2005). "Vibration-induced Mobilization of Trapped Oil Ganglia in Porous Media: Experimental Validation of a Capillary-Physics Mechanism." Journal of Colloid and Interface Science **289**(1): 193-199.

LIEBOVITCH, L. S. and T. TOTH (1989). "A Fast Algorithm to Determine Fractal Dimensions by Box Counting." Physics Letters A **141** (8-9): 386-390.

LIN, J. R. and T. F. YEN (1993). "An Upgrading Process through Cavitation and Surfactant." Energy & Fuels **7**(1): 111-118.

MALYKH, N., Petrov V. and G. Sankin (2003). "On Sonocapillary Effect" Proceedings of the 5-th World Congress on Ultrasonics, Paris. 2003. P. 1343-1346

METTIN, R., et al. (1997). "Bjerknes Forces between Small Cavitation Bubbles in a Strong Acoustic Field." Physical Review E **56**(3): 2924-2931.

MORIN, N. (2001). "Hands-on Demonstration of Basic Processing." NanoFab, University of Alberta, Edmonton, AB.

MORRIS, B. P. (1974). "Sonic Stimulation of Marginal Wells." Drilling and Production Institute Selected Papers, Paper 9.

NERETIN, V. D. and V. A. YUDIN (1981). "Results of Experimental Study of the Influence of Acoustic Treatment on Percolation Processes in Saturated Porous Media." Topics in Nonlinear Geophysics (Voprosi nelineinoy geofisiki): All Union Research Institute of Nuclear Geophysics and Geochemistry: 132-137.

NIKOLAEVSKII, V. N. (1989). "Mechanism of Vibroaction for Oil Recovery from Reservoirs and Dominant Frequencies." Doklady Akademii Nauk SSSR **307**(3): 570-575.

NIKOLAEVSKII, V. N. (1992). "Rock Vibration and Finite Oil Recovery." Fluid Dynamics **27**(5): 689-696.

NIKOLAEVSKII, V. N. and G. S. STEPANOVA (2005). "Nonlinear Seismics and the Acoustic Action on the Oil Recovery from an Oil Pool." Acoustical Physics **51**: S131-S139.

NIKOLAEVSKIY, V. N., et al. (1996). "Residual Oil Reservoir Recovery With Seismic Vibrations." SPE Production & Facilities **11**(2): 89-94.

NORRIS, A. N. (1989). "Stoneley-Wave Attenuation and Dispersion in Permeable Formations." Geophysics **54**(3): 330-341.

NOSOV, V. A. (1965). "Soviet Progress in Applied Ultrasonics, Vol. 2: Ultrasonics in the Chemical Industry." Consultants Bureau, New York.

POESIO, P. and G. OOMS (2004). "Formation and Ultrasonic Removal of Fouling Particle Structures in a Natural Porous Material." Journal of Petroleum Science and Engineering **45**(3-4): 159-178.

POESIO, P., et al. (2002). "An Investigation of the Influence of Acoustic waves On the Liquid Flow through a Porous Material." Journal of the Acoustical Society of America **111** (5), Pt.1, May 2002: 2019-2025

POESIO, P., et al. (2004). "Removal of Small Particles from a Porous Material by Ultrasonic Irradiation." Transport in Porous Media **54**(3): 239-264.

POGOSYAN, A. B., et al. (1989). "Separation of Hydrocarbon Fluid and Water in an Elastic Wavefield Acting on a Porous Reservoir Medium." Transactions (Doklady) of the USSR Academy of Sciences, Earth Science Sections, 307, 575-577.

RASBAND, W. S. (1997-2005). "ImageJ." Maryland, USA, U.S. National Institute of Health.

ROBERTS, P.M., I.B. ESIPOV and E.L. MAJER, (2003). "Elastic Wave Stimulation of Oil Reservoirs: Promising EOR Technology?" The Leading Edge, **22** (5): 448+450+452-453, May 2003.

ROZINA, E.Y., (2003). "Effect of Pulsed Ultrasonic Field on the Filling of a Capillary with a Liquid." Colloid Journal 64 (3) 359.

ROZINA, E.Y. and Y.P. ROSIN, (2003). "About the Nature of the Sound Capillary Pressure." Presented at the XIII Session of the Russian Acoustical Society, Moscow, August 25–29, 2003.

SADEGHI, K. M., et al. (1994). "Sonochemical Treatment of Fossil-Fuels." Energy Sources **16**(3): 439-449.

SADEGHI, K. M., et al. (1992). "A New Process for Tar Sand Recovery." Chemical Engineering Communications **117**: 191-203.

SADEGHI, K. M., et al. (1990). "Novel Extraction of Tar Sands by Sonication with the Aid of Insitu Surfactants." Energy & Fuels **4**(5): 604-608.

SCHOEPPEL, R. J. and A. W. HOWARD (1966). "Effect of Ultrasonic Irradiation on Coalescence and Separation of Crude Oil-Water Emulsions." SPE 1507, 41st Annual Fall Meeting of the SPE/AIME, Dallas, TX.

SHAW RESOURCE SERVICES, Inc., (1992). "Sona-Tool Test Information. Sonic Well Stimulation Research Pushed 1970." Independent Petroleum Monthly, 40.

SIMKIN, E. M. (1993). "A possible Mechanism of Vibroseismic Action on an Oil-bearing Bed." Journal of Engineering Physics and Thermophysics **64**(4): 355-359.

SIMKIN, E. M., et al. (1990). "Creation and Industrial Realization of the Technology of Controllable Acoustic Treatment for Mineral Production Stimulation in Wells (A Report)." Krylov Research Institute of Oil and Gas (VNII) (in Russian).

SIMKIN, E. M. and M. L. SURGUCHEV (1991). "Advanced Vibroseismic Technique for Water Flooded Reservoir Stimulation, Mechanism and Field Tests Results." The 6th European IOR Symposium, Stavanger, Norway.

SIMONOV, B. F., et al. (2000). "Vibro-seismic Stimulation of Oil Bearing Formations from the Surface." Neftyanoe Khozyaistvo(5): 41-46.

SMITH, S.W. (1997) "The Scientist and Engineer's Guide to Digital Signal Processing." California Technical Publishing, San Diego, CA

SPANOS, T., et al. (2003). "Pressure Pulsing At the Reservoir Scale: A New IOR Approach." Journal of Canadian Petroleum Technology **42**(2): 16-28.

TAI, K. (2005) "NanoFab Glass Microfluidic Device Fabrication Manual." NanoFab, University of Alberta, Edmonton, AB.

TAMURA, S., et al. (2005). "Liquid Adhesion to an Ultrasonically Vibrating End Surface." Journal of Applied Physics **98**(6): 063524-063524-6.

VENKITARAMAN, A., et al. (1995). "Ultrasonic Removal of near-Wellbore Damage Caused by Fines and Mud Solids." SPE Drilling & Completion **10**(3): 193-197.

WESTERMARK, R.V., J.F. BRETT, and D.R. MALONEY, (2001) "Enhanced Oil Recovery with Downhole Vibration Stimulation." SPE 67303, presented at the SPE Production and Operations Symposium, Oklahoma City, Oklahoma, March 24-27, 2001.

WONG, S. W., et al. (2003). "Near Wellbore Stimulation by Acoustic Waves." SPE 82198, 2003 SPE European Formation Damage Conference, The Hague, Netherlands.

WONG, S. W., et al. (2004). "High-power/High-frequency Acoustic Stimulation: A Novel and Effective Wellbore Stimulation Technology." SPE Production & Facilities **19**(4): 183-188.

YEN, T. F. and K. DUNN (1999). "Conversion of a Refinery Asphaltene under Ultrasound." Abstracts of Papers of the American Chemical Society **217**: U233-U233.

ZHU, T., H. XUTAO and P. VAJJHA, (2005) "Downhole Harmonic Vibration Oil-Displacement System: A New IOR Tool." SPE 94001, presented at the 2005 SPE Western Regional Meeting, Irvine, CA, March 30- April 1, 2005.

ZIMMERMANN, C. and M. STERN (1994). "Analytical Solutions for Harmonic Wave Propagation in Poroelastic Media." Journal of Engineering Mechanics. **120**(10): 2154.